

Synthesis and Deposition of Functional Nano-Materials on Natural Fibres

Von der Fakultät für Mathematik, Informatik und Naturwissenschaften
der RWTH Aachen University
zur Erlangung des akademischen Grades eines
Doktors der Naturwissenschaften genehmigte Dissertation

vorgelegt von
M.Sc
Ahmed Gomaa Abd ALLAH Hassabo
aus Dameitta, Ägypten

Berichter: Univ. Prof. Dr. rer. nat. Martin Möller
Univ. Prof. Dr. rer. nat. Andrij Pich

Tag der mündlichen Prüfung: 06.06.2011

Diese Dissertation ist auf den Internetseiten der Hochschulbibliothek online verfügbar.

Synthesis and Deposition of Functional Nano-Materials on Natural Fibres

From the Faculty of Mathematics, Computer Science and Natural Sciences
of the Rheinisch-Westfälischen Technische Hochschule Aachen
RWTH-Aachen University
to obtain the academic degree of
Doctor of Natural Science (Dr. rer.nat.)

Approved thesis
Submitted by
M.Sc. Organic Chemistry
Ahmed Gomaa Abd ALLAH Hassabo
From Egypt
born in Dameitta 10.03.1979

Advisor: Univ. Prof. Dr. rer. nat. Martin Möller
Univ. Prof. Dr. rer. nat. Andrij Pich

Tag der mündlichen Prüfung: June 06.2011

Diese Dissertation ist auf den Internetseiten der Hochschulebibliothek online verfügbar.

Aachen University of Technology (RWTH)
Institute of Technical and Macromolecular Chemistry (DWI/ITMC)
GERMANY

The undersigned certify that they have read, and recommend to the Aachen University of Technology (RWTH) for acceptance, a thesis entitled:

**Synthesis and Deposition of Functional Nano-Materials on
Natural Fibres**

Submitted by **Ahmed Gomaa Abd ALLAH Hassabo** in total fulfilment of the requirements of the degree of Doctor Philosophy of Science

Approved by thesis committee:

Certified and Approved by (Advisor):

Univ. Prof. Dr. rer. nat. Martin Möller
Aachen University of Technology (RWTH-Aachen)
Institute of Technical and Macromolecular Chemistry (DWI/ITMC)

Certified and Approved by (Advisor):

Univ. Prof. Dr. rer. nat. Andrij Pich
Aachen University of Technology (RWTH-Aachen)
Institute of Technical and Macromolecular Chemistry (DWI/ITMC)

Accepted by (Further examiner):

Univ. Prof. Dr. rer. nat. Walter Richtering
Aachen University of Technology (RWTH-Aachen)
Institute of Physical Chemistry (IPC)

Accepted by (Chairman):

Univ. Prof. Dr. rer. nat. Paul Kögerler
Aachen University of Technology (RWTH-Aachen)
Institute of Inorganic Chemistry (IAC)

Date: June 06.2011

AUTHOR'S DECLARATION

I hereby declare that I am the sole author of this thesis. All the experiments in this thesis constitute work carried out by the candidate unless otherwise stated. The thesis's tables, figures, bibliography and appendices, and complies with the stipulations set out for the degree of Doctor of Philosophy by the RWTH-Aachen University of Technology (RWTH-Aachen).

I further authorize RWTH-Aachen University of Technology (RWTH-Aachen) to reproduce this thesis by photocopying or by other means, in total or in part, at the request of other institutions or individuals for the purpose of scholarly research.

Title of Thesis/Dissertation:

Synthesis and Deposition of Functional Nano-Materials on Natural Fibres

Signature

Author Hassabo, Ahmed Gomaa Abd Allah

DWI/ITMC, RWTH-Aachen University

THESIS ABSTRACT

This Thesis deals with the modification of natural fibres properties by applying a functional coating to the fibre. Natural fibres, i.e. cotton and wool, have been chosen as fibrous material giving contribute to the fact that they cannot be modified in bulk, like synthetic fibres where additives can be added in the melt before spinning. The focus of the modification has been directed towards thermo-regulating properties, textile gloss and improved dyeing. Common to all three tasks is the necessity to develop a binder for permanent application of the functional entity. This has been achieved via polymeric binders, namely polyethylene imine (PEI) and polyacrylates. The phase-change resins were applied for thermo-regulating, micro-gel based soft colloids were used for gloss modification and dendrite polymer dyes were used for dyeing. The prepared polymer were characterised using NMR, IR, SEM, DSC. Treated fibres were characterised according to the required end-use.

Summing up the fibre surface properties can be controllable improved by selecting the appropriate polymer structure and by adjusting the corresponding treatment parameters.

THESIS KURZFASSUNG

Diese Arbeit beschäftigt sich mit der Modifizierung von NaturfaserEigenschaften durch Anlegen einer funktionalen Beschichtung auf der Faser. Natürliche Fasern wie Baumwolle und Wolle, sind als Faserstoffe ausgewählt worden, durch die Tatsache, dass sie nicht im bulk verändert werden können, wie synthetische Fasern, wo Zusatzstoffe vor dem Spinnen in der Schmelze zugesetzt werden können. Der Schwerpunkt der Modifizierung wurde auf thermo-regulierenden Eigenschaften gerichtet, Textil Glanz und verbessertes Färben. Gemeinsam ist allen drei Aufgaben die Notwendigkeit, ein Bindemittel für die permanente Anwendung der funktionellen Einheit zu entwickeln. Dies wurde durch polymere Bindemittel, nämlich Polyethylenimin (PEI) und Polyacrylate erreicht Die Phase-Change-Materialien für Thermo-Regulierung angewendet, Mikro-Gel basierte Soft Kolloide wurden für Glanz Modifikation verwendet und Dendriten Polymer Farbstoffe wurden zum Färben verwendet. Die hergestellten Polymere wurden durch NMR, IR, SEM, DSC gekennzeichnet. Behandelte Fasern wurden in Übereinstimmung mit End-Anwendung durch gekennzeichnet.

Zusammenfassend können die Faseroberflächeneigenschaften durch die Auswahl der geeigneten Polymerstruktur und durch die Anpassung der entsprechenden Behandlungsparameter kontrolliert verbessert werden.

ACKNOWLEDGMENTS

First, I thank ALLAH for all his blessings. Any success earned by this research deservedly belongs to almighty "Allah" *Thanks ALLAH*.

A grateful acknowledgement to the **Egyptian Government (Egyptian ministry of higher education and scientific research, Missions Department)** to which granted the scholarship to pursue the PhD degree at **RWTH-Aachen University** and the German language course, and also for giving life to this challenging PhD project. It offered me the possibility to cooperate with **DWI an der RWTH** and to gain life-time experiences while I stayed in Aachen to study at RWTH-Aachen University, also, for the financial support.

Perhaps the most significant contribution was by **Prof. Dr. Martin Möller**, Head of the Institute of Textile Chemistry and Macromolecular Chemistry (DWI/ITMC), RWTH-Aachen University. His unflagging efforts to improve readability, assistance with writing, and his suggestions concerning content were an incalculable asset. Therefore, I affectionately dedicated my research to his amazing patience and tolerance.

I equally thank **Prof. Dr. Crisan Popescu**, at (DWI/ITMC), who introduced various aspects of organic chemistry to me, a very exciting subject that never got my attention before. I have learned a great deal from him about how to express the concepts in a clear and logical manner, and made a major contribution refining this work, so he deserves a special deep heart thanks.

Co-operation and technical assistance from my fellow-colleagues at (DWI/ITMC) who helped me to make this work possible are gratefully acknowledged. Special thanks to my colleagues **Nicolae Goga**, **Christine Schmitz** and **Marcus Nobis** for their help and support. This work is a testimony to their professionalism and technical excellence. In addition, I cannot forget **Angela Huschens** from DWI secretarial board, which she helps me a lot during my studying.

Also I want to thank my wife **Amina**, and my children, **Adam**, **Areej** and **Akram** for showing me "the meaning of life". Thank you **Amina** for your understanding and for all the constant support and encouragement, for your deep love, confidence and serenity making me believe in this day. I also want to thank you for being a superb mother, assisting and caring for my children when I had to be away. Also, thank you for your pure smile, tender hugs, softhearted and for showing me the beauty of life...and...the eternity of night.

Ahmed G. Hassabo

June 2011

We complain ...

Because Allah has made thorns under the roses ...

It would be better for us to thank him ...

Because ALLAH has made the roses over the thorns!!

I suffered a lot ...

When I found myself barefoot...

But I thanked ALLAH a lot...

When I found another that has no feet!!

DEDICATION

GRATEFULLY DEDICATED

TO MY WIFE "AMINA",

MY CHILDREN "ADAM", "AREEJ" AND "AKRAM"

WHOSE ENCOURAGEMENTS INSPIRED ME!

**FINALLY, I AM GRATEFUL TO THE SOUL OF MY FATHER MR GOMAA ABD ALLAH,
WHO I MISS HIS BODY BUT NOT HIS MIND.**

TABLE OF CONTENTS

Author's Declaration	vi
Thesis Abstract.....	vii
Thesis Kurzfassung.....	vii
Acknowledgments	ix
Dedication.....	xiii
Table of Contents	xv
List of Tables.....	xix
List of Figures	xx
List of Schemes.....	xxiii
List of Equations	xxiv
List of Abbreviations and Symbols.....	xxv
A - Chemical Abbreviations	xxv
B - Symbols Abbreviations	xxvi
C - General Abbreviations	xxvii
1. Introduction	1
1.1. Natural Fibres	1
1.1.1. Cellulosic Fibres	1
1.1.1.1. Chemical Structure of Cellulose	1
1.1.1.2. Physical Structure of Cellulose	3
1.1.2. Protein Fibres	4
1.1.2.1. Chemical Structure of α -Helix.....	5
1.1.2.1.1. Cuticle.....	5
1.1.2.1.2. Cortex	5
1.1.2.1.3. Cortical cell.....	6
1.1.2.1.4. Macrofibril.....	6
1.1.2.1.5. Matrix	6
1.1.2.1.6. Microfibril	6
1.1.2.1.7. Twisted molecular chain and helical coil	6
1.1.2.2. Physical Structure of α -Helix	6
1.2. Functionalising the Fibre Surfaces	7
A - Structure of the fibre surface.....	8
B - Charge of the fibre surface.....	9
1.2.1. Phase Change Materials for Thermoregulation	10
1.2.1.1. PCMs Classification and Requirements	11
1.2.1.1.1. Inorganic PCM materials	11
1.2.1.1.2. Organic PCM materials.....	12
1.2.1.2. Definition and Determination of Specific Heat.....	12
1.2.2. Dyeing and Lustre Properties of Textile Materials.....	15
1.2.2.1. Thermo-Sensitive Microgels to Improving Textile Gloss	17

1.2.2.2. Functionalised PEI (Polyethylene Imine) to Improving Textile	18
2. Organic PCM Materials based on Paraffin Compounds for Textiles	20
2.1. Introduction	20
2.2. Experimental.....	21
2.2.1. Materials.....	21
2.2.2. Methods	21
2.2.2.1. Preparation of HDI Derivatives	21
2.2.2.1.1. HDI_1 derivative	21
2.2.2.1.2. HDI_2 derivative	22
2.2.2.2. Preparation of PCMs Compounds	22
2.2.2.3. Coating of Wool and Cotton Fibres/Fabrics with PCM Compound.....	23
2.2.3. Measurements	24
2.2.3.1. Differential Scanning Calorimetry (DSC)	24
2.2.3.2. Scanning Electron Microscope (SEM)	24
2.3. Result and Discussion	24
2.3.1. Optimising the Reaction Condition.....	26
2.3.1.1. Effect of Temperature	27
2.3.1.2. Effect of Time	28
2.3.1.3. Effect of Polymer: Paraffin Molar Ratio	30
2.3.1.4. Effect of Paraffin Types	34
2.3.2. Textile Application	38
2.4. Conclusions	40
3. Organic PCM/Polybehenyl Acrylate Composites for Textile Usage	41
3.1. Introduction	41
3.2. Experimental.....	41
3.2.1. Materials.....	41
3.2.2. Methods	42
3.2.2.1. Preparation of PCM/Polymer Composite based on Poly Behenyl Acrylate	42
3.2.2.1.1. Solid – solvent polymerization	42
3.2.2.1.2. In-situ Solid–Solid polymerization of behenyl acrylate in presence of PCM compounds.....	44
3.2.3. Measurements	44
3.2.3.1. Differential Scanning Calorimetry (DSC)	44
3.2.3.2. NMR Measurements.....	44
3.2.3.3. Size Exclusion Chromatography Analysis (SEC)	44
3.2.3.4. Scanning Electron Microscope (SEM)	45
3.2.3.5. PCM Heat Transfer Measure	45
3.3. Result and Discussion	46
3.3.1. Characterization of the Poly(behenyl acrylate)	46
3.3.2. Characterization of the PCM/polymer composite	46
3.3.2.1. Comparison between PCM/polymer composites based on homo-polymer and co-polymer of BA	52

3.3.2.2. Study the effect of the poly(behenyl acrylate) concentration on different PCM/polymer composites	53
3.3.2.3. Effect of heat on the behaviour of PCM/polymer composite	53
3.3.2.4. Stability of PCM-polymer composite at storing.....	54
3.3.3. Applying the PCM/polymer composite on clothing insulation materials.....	55
3.4. Conclusions.....	58
4. Inorganic Encapsulation of Inorganic PCM for Textile Usage.....	59
4.1. Introduction.....	59
4.2. Experimental	61
4.2.1. Materials	61
4.2.2. Methods	61
4.2.2.1. Preparation of PCM-Silica Capsules.....	61
4.2.2.1.1. Preparation of hydrophobic silica particles	61
4.2.2.1.2. Preparation of inorganic PCM capsules	61
4.2.2.2. Preparation Film from PCM-Silica Capsules and Polypropylene.....	62
4.2.2.3. Coating of Wool and Cotton Fibres/Fabrics with PCM Compound	62
4.2.3. Measurements	63
4.2.3.1. Differential Scanning Calorimetry (DSC).....	63
4.2.3.2. Scanning Electron Microscopy (SEM).....	63
4.2.3.3. Mechanical Properties.....	63
4.3. Result and Discussion	64
4.3.1. Encapsulation into Silica Particles	64
4.3.2. Textile Application.....	65
4.3.3. Polypropylene Film with PCM-Silica Capsules	66
4.4. Conclusions.....	67
5. Polyvinylcaprolactam-Co-Polymer Microgels to Handle Gloss Properties of Natural Fibres	69
5.1. Introduction.....	69
5.2. Experimental	69
5.2.1. Materials	69
5.2.2. Methods	70
5.2.2.1. Synthesis of Amphoteric, Anionic and Neutral Microgels.....	70
5.2.2.2. Fibre Treatment	71
5.2.3. Measurements	71
5.2.3.1. Liquid state NMR Measurements	71
5.2.3.2. Scanning Electron Microscope (SEM).....	71
5.2.3.3. Gloss measurement	72
5.3. Result and Discussion	72
5.3.1. Microgel Synthesis.....	72
5.3.1.1. Chemical Composition of Microgels	73
5.3.1.2. Microgel Morphology.....	75
5.3.2. Microgel Deposition of Fibres.....	76
5.3.3. Gloss Measurement.....	77

5.4. Conclusions	82
6. Deposition of Functionalized Polyethylenimine-Dye onto Cotton and Wool Fibres..	83
6.1. Introduction	83
6.2. Experimental.....	84
6.2.1. Materials.....	84
6.2.2. Methods	85
6.2.2.1. Synthesis of Quaternary Ammonium Salt (QI).....	85
6.2.2.2. Synthesis of the Reactive Dye stuff (RD).....	87
6.2.2.3. Synthesis of Functionalized Polyethylenimine-Dye	88
6.2.2.4. The Pre-treatment of the Fibres	89
6.2.2.5. Deposition onto Cotton and Wool Surfaces.....	89
6.2.3. Measurements	89
6.2.3.1. NMR Measurements.....	89
6.2.3.2. Adsorption and Isothermal Studies	89
6.2.3.3. Colour Measurements.....	90
6.3. Results and Discussion	91
6.3.1. Synthesis of Reactive Dye stuff (RD)	91
6.3.2. Synthesis of Modified Poly(ethyleneimine)s	91
6.3.3. Adsorption of FPEI Compounds onto Fibres	94
6.3.3.1. Effect of pH.....	94
6.3.3.2. Effect of Salt	94
6.3.4. Isothermal Studies	96
6.3.5. Kinetic Study	99
6.3.6. Colour Strength.....	101
6.4. Conclusions	102
7. Summary.....	103
8. Zusammenfassung	106
9. Reference.....	110
Curriculum Vita	123
List of Publications.....	125
A - Publications Arising from This Thesis.....	125
B - Other Publications.....	125
C - Oral Lectures.....	126
D - Posters.....	126

LIST OF TABLES

Table 1: Values of coefficients A to H for synthetic sapphire (Al_2O_3) ⁽⁴⁴⁾	14
Table 2: Effect of reaction temperature on Tp and ΔH of second heating for PCM compounds prepared from polymers with n-octadecane	27
Table 3: Effect of reaction time on Tp and ΔH of second heating for PCM compounds prepared from polymers with n-octadecane	30
Table 4: Effect of molar ratio on Tp and ΔH of second heating for PCM compounds prepared from polymers with octadecane	33
Table 5: Peak temperature and enthalpy of second heating for different paraffin compounds .	34
Table 6: Peak temperature and enthalpy of second heating for different polymer compounds.	34
Table 7: Effect of different paraffin type on enthalpy, onset, peak temperature and duration index of second heating for PCM polymer composites	37
Table 8: DSC and DI results of coated fabric with PCM polymer composites	38
Table 9: Homopolymerization of BA: starting materials and results. ¹⁾	43
Table 10: Copolymerization of BA with HEA: starting materials and results. ¹⁾	43
Table 11: DSC data for PBA/ $\text{C}_{17}\text{H}_{35}\text{COOCH}_3$ and PBA/ $\text{C}_{18}\text{H}_{37}\text{OH}$ composites	51
Table 12: DSC data for PBA_I and PBA/HEA_I and their composites with $\text{C}_{17}\text{H}_{35}\text{COOCH}_3$.	52
Table 13: The melting temperature and the heat of phase transition for several inorganic salt hydrates.....	59
Table 14: Properties of PCM capsules from hydrated inorganic salts with silica particles.....	64
Table 15: DSC data for PCM materials from hydrated inorganic salts with silica particles	64
Table 16: DSC and DI results of coated fabric with inorganic PCM polymer composites	65
Table 17: Ingredients used for the synthesis of different microgels	71
Table 18: The conditions for fibre treatment with different microgels.....	71
Table 19: Composition of modified poly(ethyleneimine)s (FPEI)	88
Table 20: Comparison between the parameters of adsorption isotherm models	99
Table 21: FPEI concentration desorbed from the fibres after 1800 sec treatment	99
Table 22: The values of the kinetic parameters as obtained from the experimental data.....	101
Table 23: Colour strength of cotton and wool fibre treated with FPEIs compounds before and after washing with and without salt adding during the treatment at pH 7.....	102

LIST OF FIGURES

Figure 1: Chemical structure of cellulose	2
Figure 2: Schematic structure of a mature cotton fibre, identifying its six parts ⁽¹²⁾	3
Figure 3: Exploded diagram showing the microstructure of wool fibre ^(26, 27)	5
Figure 4: Possible bonds between different wool protein chains	7
Figure 5: Titration curve for wool fibre with HCl and KOH ⁽⁴²⁾	10
Figure 6: Different way of the light beam impinges on a surface	17
Figure 7: Chemical structure of PCM's polymers	21
Figure 8: Enthalpy and peak temperature of second heating for PCM compounds from n-octadecan and different polymer compounds at different reaction temperature ...	28
Figure 9: Enthalpy and peak temperature of second heating for PCM compounds from n-octadecane and different polymer compounds at different reaction time	29
Figure 10: Comparison of DSC recorded data for the polymer-n-octadecane crystals (symbols) and those of pure n-octadecane (dotted line)	31
Figure 11: Duration index for the PCM-polymer composites from n-octadecane with different polymer compound with different molar ratio	32
Figure 12: Enthalpy and temperature of second heating for PCM compounds with different paraffin type	35
Figure 13: Duration index values for PCM compounds with different paraffin compounds....	36
Figure 14: DSC curves of coated cotton and wool fabrics with HDI derivatives (cooling and 2 nd heating)	39
Figure 15: Scanning electron micrograph for coated cotton with HDI_2 derivative a) after treatment b) after heating at 50°C for 15 min	40
Figure 16: Scanning electron micrograph for coated wool with HDI_2 derivative a) after treatment b) after heating at 50°C for 15 min	40
Figure 17: The experimental setup: a) thermometer applied on the face of the phase change material and b) the device with the side instruments for control of heat flow and recording temperature	45
Figure 18: ¹ H NMR spectra of behenyl acrylate and its polymer	46
Figure 19: ¹³ C NMR spectra of behenyl acrylate and its polymer	46
Figure 20: IR spectra of behenyl acrylate and its polymer.....	47
Figure 21: IR spectra of PBA/C ₁₇ H ₃₅ COOCH ₃ and PBA/C ₁₈ H ₃₇ OH composites	48

Figure 22: Raman spectra of PBA/C ₁₇ H ₃₅ COOCH ₃ and PBA/C ₁₈ H ₃₇ OH composites.....	48
Figure 23: ¹ H NMR theoretical shifts for behenyl acrylate, poly(behenyl acrylate), methyl octadecanoate and n-Octadecanol	49
Figure 24: ¹ H NMR experimental shifts for PBA/C ₁₇ H ₃₅ COOCH ₃ and PBA/C ₁₈ H ₃₇ OH composites	49
Figure 25: ¹³ C NMR theoretical shifts for behenyl acrylate, poly(behenyl acrylate), methyl octadecanoate and n-Octadecanol	50
Figure 26: ¹³ C NMR experimental shifts for PBA/C ₁₇ H ₃₅ COOCH ₃ and PBA/C ₁₈ H ₃₇ OH composites	50
Figure 27: DSC spectra for PBA/C ₁₇ H ₃₅ COOCH ₃ and PBA/C ₁₈ H ₃₇ OH composites.....	51
Figure 28: SEM micrograph for organic PCM material retained in PBA matrix.....	51
Figure 29: Specific heat for PBA_I and PBA/HEA_I and their composites with C ₁₇ H ₃₅ COOCH ₃	52
Figure 30: Enthalpy values of phase change process for the PCM/polymer composites	53
Figure 31: Temperature values of phase change process for the PCM/polymer composites	53
Figure 32: Behaviour of PBA/C ₁₇ H ₃₅ COOCH ₃ composite during heating with 10°C/min.....	54
Figure 33: DSC graphs of PCM/polymer composites stored at room temperature for PBA/C ₁₇ H ₃₅ COOCH ₃ and PBA/C ₁₈ H ₃₇ OH composites	54
Figure 34: Storing stability at room temperature of PBA/C ₁₇ H ₃₅ COOCH ₃ and PBA/C ₁₈ H ₃₇ OH composites in terms of temperature and enthalpy of melting	55
Figure 35: Three-layer sandwich model of an insulator with PCM	56
Figure 36: The temperature programme used for measuring the insulator property of a PCM/polymer composite.....	57
Figure 37: The temperature recorded on the two sides of the PCM/polymer composite	57
Figure 38: The difference temperature for a constant heat flow	57
Figure 39: Molecular structure of poly(ethoxysiloxane) (PAOS).....	60
Figure 40: X-plore extruder for the production of polymer films.....	62
Figure 41: The DSC plots of silica capsules containing Na ₂ SO ₄ .10H ₂ O (A) and HN ₂ PO ₄ .12H ₂ O (B)	64
Figure 42: Inorganic PCM (Na ₂ HPO ₄ .12H ₂ O) encapsulated in silica particles	65
Figure 43: Inorganic PCM (Na ₂ SO ₄ .10H ₂ O) encapsulated in silica particles.....	65

Figure 44: DSC plots of films of PP and PP with PCM capsules from $\text{Na}_2\text{SO}_4 \cdot 10\text{H}_2\text{O}$, $\text{HNa}_2\text{PO}_4 \cdot 12\text{H}_2\text{O}$	66
Figure 45: Cross-section of poly propylene film with 5% PCM capsules.....	67
Figure 46: Different material structures used in preparation of microgel compounds	70
Figure 47: SEM image of VCL/IADME/VIm (MG_1) microgel.....	75
Figure 48: SEM image of VCL/IADME (MG_2) microgels	75
Figure 49: SEM image of VCL/AAEM (MG_3) microgels.....	75
Figure 50: SEM image of treated cotton fibres using microgels MG1 and MG2.....	78
Figure 51: SEM image of treated wool fibres using microgels MG1 and MG3.....	79
Figure 52: The light surface for cotton and wool fibres.....	80
Figure 53: Gloss index values of treated cotton fibre with various microgels	81
Figure 54: Gloss index values of treated wool fibre with various microgels	81
Figure 55: Chemical structure of PEI and C. I. Basic Red 51	84
Figure 56: UV-VIS absorption spectra of reactive dyestuff in THF ($c = 0.02 \text{ g/L}$)	91
Figure 57: ^1H NMR spectrum of modified PEI in $\text{DMSO}-d_6$ (FPEI_1)	92
Figure 58: Water solutions of FPEIs at 0.2 g/L	93
Figure 59: UV-VIS spectra of FPEIs in water at concentration of dyestuff 0.02 g/L	93
Figure 60: The amount of FPEI before and after washing adsorbed onto cotton and wool fibres at $\lambda = 498$ at different pH treatment medium.....	95
Figure 61: The amount of FPEI before and after washing adsorbed onto cotton and wool fibres at $\lambda = 498$ with and without salt added to treatment medium	96
Figure 62: Colour intensity (ΔE) for cotton and wool fibres before and after washing without salt in the treatment medium.....	97
Figure 63: Concentration-time curve for cotton and wool fibres before and after washing without salt in the treatment medium.....	100

LIST OF SCHEMES

Scheme 1: Scheme of host polymer with side chains and retains PCM material	16
Scheme 2: Scheme for preparation of the HDI_1	23
Scheme 3: Scheme for preparation of the HDI_2	25
Scheme 4: Scheme of hexamethylene diisocyanate uretdione and alkan (C ₁₈ H ₃₈)	26
Scheme 5: General scheme of the heat transfer measurement of a PCM	45
Scheme 6: Schematic illustration of the preparation of the inorganic PCM capsules based on silica nanoparticles ⁽¹²³⁾	60
Scheme 7: Preparation scheme of amphoteric microgel MG_1	73
Scheme 8: Preparation scheme of anionic microgel MG_2	73
Scheme 9: Preparation scheme of neutral microgel MG_3	73
Scheme 10: Hydrolysis effect of MG_1 microgel in different pH medium	76
Scheme 11: Scheme to preparation of 2-oxo-1,3-dioxolan-4-yl)methyl phenyl carbonate	85
Scheme 12: Scheme of the second step to prepare the quaternary ammonium salt (QI)	86
Scheme 13: Scheme to prepare the reactive dyestuff (RD)	87
Scheme 14: Structure of functionalized polyethylenimine-dye (FPEI)	88

LIST OF EQUATIONS

Equation 1: $H \propto \Delta T \Rightarrow H \propto (T_f - T_i)$	12
Equation 2: $H = C (T_f - T_i)$	12
Equation 3: $H = m C_p \Delta T$	13
Equation 4: $H = m L_p$	13
Equation 5: $C_{P \text{ Sample}} = \frac{H_{\text{Sample}}}{H_{\text{Alu min a}}} \times \frac{m_{\text{Alu min a}}}{m_{\text{Sample}}} \times C_{P \text{ Alu min a}}$	13
Equation 6: $C_p(T) = A + BT + CT^2 + DT^3 + ET^4 + FT^5 + GT^6 + HT^7$	13
Equation 7: $DI = \frac{\Delta H \times \rho}{\Delta T}$	14
Equation 8: $R = \frac{\Delta T \times A}{H}$	14
Equation 9: $K/S = \frac{(1-R)^2}{2R} - \frac{(1-R_o)^2}{2R_o}$	90
Equation 10: $q_e = \frac{q_m C_e K_L}{1 + C_e K_L}$	98
Equation 11: $\frac{1}{q_e} = \frac{1}{q_m} + \left(\frac{1}{q_m K_L} \right) \left(\frac{1}{C_e} \right)$	98
Equation 12: $q_e = K_F C_e^{1/n}$	98
Equation 13: $\ln q_e = \ln K_F + \frac{1}{n} \ln C_e$	98
Equation 14: $\frac{dq}{dt} = k_1 (q_e - q_t)^n$	100
Equation 15: $\ln(q_e - q_t) = \ln(q_e) - k_1 t$ for n=1 (first order reaction)	100
Equation 16: $q_e^{1-n} - (q_e - q_e)^{1-n} / (1-n) = k_1 t$ for n≠1	100

LIST OF ABBREVIATIONS AND SYMBOLS

A - CHEMICAL ABBREVIATIONS

Abbreviation	Description
AAEM	Acetoacetoxyethyl methacrylate
AIBN	2,2'-azobisisobutyronitrile
AICN	1,1'-Azobis(cyclo-hexanecarbonitrile
AMPA	2,2'-azobis(2-methylpropionamidine) dihydrochloride
BA	Behenyl acrylate
BIS	N,N'-methylene bis(acrylamide)
Blocbuilder® initiator	N-tert-butyl-N-(1'-diethylphosphono-2,2'-dimethylpropyl)-O-(2-carboxyl-prop-2-yl)
BPO	Benzoyl peroxide
D₂O	Deionized water
DABCO	1,4-diazobicyclo[2.2.2]octane
DMF	N,N-dimethylformamid
DMSO	N,N-dimethylsulfoxide
FPEI	Functionalised poly(ethyleneimine)s
HDI	Hexamethylene diisocyanate uretdione
HEA	2-hydroxyethyl acrylate
IADME	Itaconic acid dimethyl ester
MODS	Trimethoxy (octadecyl)silane
PAOS	Poly(ethoxysiloxane)
PBA	Polybehenyl acrylate
PDDEG	Poly(dodecyl ethylene glycol)
PDEG	Poly(decyl ethylene glycol)
PDMS	Polydimethyl siloxane
PEI	Poly(ethyleneimine)
PLA	Polylauryl acrylate
PMMA	Poly(methyl methacrylate)
PP	Polypropylene
PVCL	Poly(N-vinylcaprolactam)
QI	3-(((2-oxo-1.3-dioxolan-4-yl)methoxy)carbonylamino) propan-1-N,N,N-trimethyl ammonium iodide
RD	((E)-(2-oxo-1.3-dioxolan-4-yl)methyl 3-((4-((2-chloro-4-nitrophenyl) diazenyl)phenyl)(methyl) amino)propylcarbamate
SG-1	Free nitroxide N-tert-butyl-N-(1'-diethylphosphono-2,2'-dimethylpropyl)-nitroxide
TEOS	Tetraethyl orthosilicate
THF	Tetrahydrofuran
VCL	N-vinylcaprolactam
VIm	Vinylimidazole

B - SYMBOLS ABBREVIATIONS

Abbreviation	Description
ΔE	Colour Intensity
ΔH	Enthalpy of fusion
ΔT	Change in temperature
A	Area of the PCM material
\AA	Angstrom
C	Heat capacity
C_e	Equilibrium FPEI concentration in solution (mg/L)
C_p	Specific heat
DI	Duration Index
H	Heat
K/S	Colour Strength, (K: absorption coefficient and S: scattering coefficient)
k_1	Kinetic rate constant of pseudo first order
K_F	Freundlich adsorption constant (L/mg)
K_L	Langmuir adsorption constant (L/mg)
λ	Wavelength (nm)
L_p	Latent heat
M	Mass of the material
n	Heterogeneity factor for freundlich adsorption
q_e	Equilibrium FPEI concentration on the fibre (mg/g)
q_m	Maximum capacity of the fibre (mg/g)
q_t	Amount of dye adsorbed (mg/g) at time t
R	Total resistance to dry heat transfer
R_c	Reflectance of coloured sample
R_o	Reflectance of uncoloured (white) sample
ρ	PCM density
T	Temperature
T_f	Final temperature
T_F	Temperature of face of the PCM material
T_i	Initial temperature
T_o	Melting onset temperature
T_p	Melting peak temperature
T_R	Temperature of rear of the PCM material

C - GENERAL ABBREVIATIONS

Abbreviation	Description
clo	clothing insulation
DSC	Differential Scanning calorimetric
GPC	Gel permeation chromatography
L.R	Liquor ratio
M.wt	Molecular weight
M_f	Molecular formula
μm	micrometer
nm	nanometre
PCM	Phase change material
pI	Isoelectric point
rpm	Rotation per minute
RT	Room temperature
SEC	Size Exclusion Chromatography Analyses
SEM	Scanning electron microscopy
UV-vis	Ultraviolet-visible
w_t	Weight

1. Introduction

In the world's hot and temperate zones, the fibres used were usually cellulosic or vegetable-based: cotton, linen, jute, ramie and hessian. All these fibres are vegetable in origin and have a common chemistry. Cellulosic fibres grow readily in hot climates, and the resultant garments were designed appropriately for wear in hot weather. In colder regions, nomadic tribesmen combed their animal flocks as they moulted each spring, and spent the long winter nights spinning and weaving the soft, woolly fibres into garments that would keep them warm and dry throughout the cold winter season ahead.

The contemporary consumer is able to choose from a wide array of fibres, which may be classified as follows ⁽¹⁻⁴⁾:

- **Cellulosic fibres:** natural fibres of vegetable origin, like cotton, linen, jute, ramie, hessian and sisal.
- **Protein fibres:** natural fibres of animal origin, like wool (Sheep), alpaca (Alpaca), mohair (Goats), cashmere (Goats), angora (Rabbit), camel (Camel), vicuna (Vicuna) and silk (Silkworm).
- **Man-made fibres:** fibres produced by man. For many years textile technologists endeavoured to produce fibres with similar characteristics to natural ones. Now they are attempting not to imitate natural fibres, but to create fibres with characteristics which are distinct from these. Synthetic fibres now are playing a major role in the textile industry, due partly to the great variety of moderately priced fabrics which can be made from them.

1.1. Natural Fibres

1.1.1. Cellulosic Fibres

1.1.1.1. Chemical Structure of Cellulose

Cellulose is an important structure material in the plant kingdom.⁽⁴⁾ It is the main construction material of the plant cell walls that are made out of it. ⁽⁵⁾ Native cellulose occurs in plant such as cotton (in the seed and hair) and ramie which contain a highly pure cellulose, as lignocelluloses in bast fibers such as flax, hemp, jute (in the stems and leaves) and wood where it occurs in combination with lignin, homocellulose. ⁽⁶⁾

Haworth (1929) has proposed that the structural formula of sugars be written in a roughly three-dimensional prescriptive manner, which when applied to cellulose yield the formula in **Figure 1**. Furthermore, it is a polysaccharide made up of β -D (+) glucose residues. These molecules condensed and linked together linearly by means of 1-4, β - glucosidic bonds. ⁽⁷⁻⁹⁾

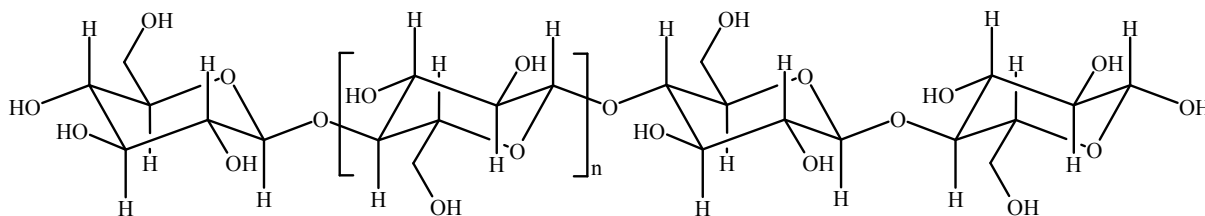


Figure 1: Chemical structure of cellulose

Each repeating anhydroglucose unit has three reactive hydroxyl groups, so they are polyhydroxyl alcohols. ^(8, 10) Two of these groups in the position 2 and 3 are secondary hydroxyl groups, whereas the last one in the position 6 is a primary hydroxyl group. ⁽¹¹⁾ Cellulose molecules have the opportunity of forming many hydrogen bonds with its primary hydroxyl groups because it is more reactive than secondary hydroxyl group. ^(5, 7) In addition, the primary hydroxyl group is more acidity than the secondary. ⁽¹¹⁾

Steric hindrance is an important consideration, particularly in the case of bulky reacting species; position 6 is least sterically hindered. ⁽⁵⁾ Whenever the distance between the various oxygen and hydrogen atoms in the cellulose molecule reaches 3Å or less, they interact with each other to form intermolecular hydrogen bonding. ⁽⁸⁾

As it is noticeable from the **Figure 2** ⁽¹²⁾, cotton fibre consists of primary and secondary layers, while lumen is present in the centre. Primary layer holds up to 30% cellulose and non-cellulosic materials. This cellulose is of lower molecular weight with the degree of polymerization (DP) between 2,000 and 6,000. Secondary wall is rich in cellulose of higher weight with DP of 14,000. ⁽¹³⁾

More detailed the cotton fibre has the following composition:

- a) Cellulose: 88-96%. It is the main component of the cotton fibre and secondary wall posses highest percentage of the total cellulose
- b) Pectin's: 0.9 -1.2%. These are made of ploygalacturonic acid, and its magnesium salts, methylester, xylose. They are present mainly in primary wall.
- c) Proteins: 1.1-1.9%. These are made of protoplasm rest in lumen and aspartic, glutamic acid and praline. The primary wall contains 0.2-0.3% nitrogen.

- d) Waxes: 0.3-1.00%. they are composed of higher monovalent alcohol-tractional, palmitic, oleic acid, glycerine. Its melting point is 77°C. They are found on surface of cotton and in primary wall.
- e) Organic acids: 0.5-1.00%. These are salts of citric and L-maleic acid
- f) Mineral salts: 0.7-1.6%. These are hypochlorites, sulphates, phosphates, oxides of silicon, calcium, potassium, magnesium
- g) Sugar: 0.3% made of glucose, galactose, fructose, pentose.
- h) Toxine: 0.9%. Endotoxine, evolved from bacterial cells (0.017-100 g per bale of mass 218 kgs)
- i) Vitamins and pigment (flavones compound).

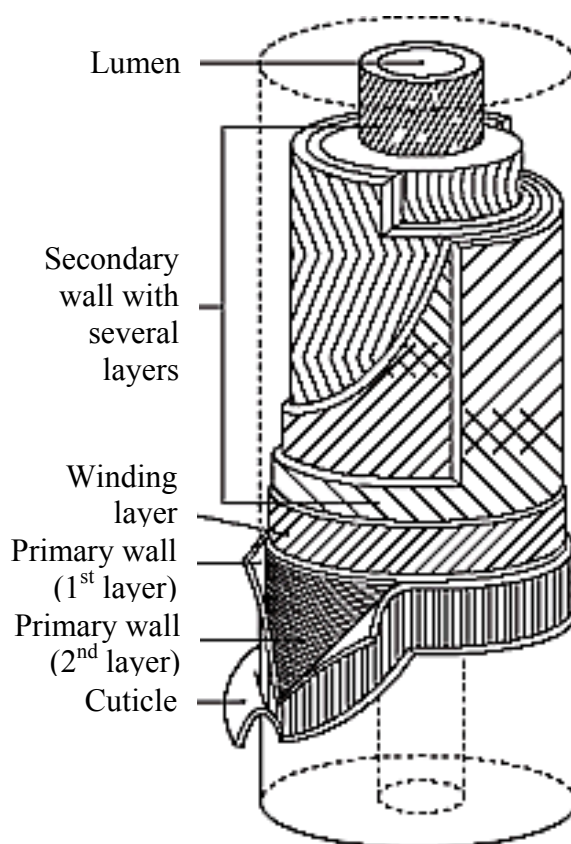


Figure 2: Schematic structure of a mature cotton fibre, identifying its six parts ⁽¹²⁾

1.1.1.2. Physical Structure of Cellulose

Cellulose has the capability of forming many hydrogen bonds along the length of the polymer chain with its three-hydroxyl groups.

These bonds, combined with the other (principally the Van der Waals attraction), bind together, and it is ranging perfect geometrical packing of crystal lattice (crystalline region) to random condition (amorphous region). ⁽⁷⁾

Reactivity and accessibility have been used to describe the easiness with which cellulose can react. More properly, reactivity of cellulose is the ability of the chain molecules to react with other molecules, whereas accessibility of cellulose defines the ease by which the functional groups of the chain molecule can be reached by the reactant molecule.⁽¹⁴⁾

1.1.2. Protein Fibres

Keratin fibres, like wool or human hair, can be considered as natural composite materials, where keratinous protein is the main basic constituents.⁽¹⁵⁾ Wool is high-quality protein fibre and is widely used as a high-quality textile material.⁽¹⁶⁾ It is well known that surface characteristic of fibres play an important role in the functional and aesthetic properties of the fabrics, and many surface modifications by chemical treatments are able to improve textile properties^(17, 18)

Wool, one of the oldest textile fibres known, is a remarkable renewable resource with exceptional properties - cool in summer, warm in winter and in a variety of weights suitable for both apparel and interior fibre applications⁽¹⁹⁾.

A raw wool fibre contains 25-70% by mass of impurities. These consist of wool grease, perspiration products (suint), dirt and vegetable matter such as burrs and seeds^(20, 21). Wool consists principally of keratin^(22, 23). Keratin fibres are not chemically homogeneous; they consist of a complex mixture of widely different polypeptides⁽²⁰⁾. Despite the classification of wool as a keratin, clean wool in fact contains only approximately 82% of the keratinous proteins, which are characterized by a high concentration of cystine. Approximately 17% of wool is composed of proteins which have been termed nonkeratinous, because of their relatively low cystine content⁽²⁰⁾.

Wool and other keratin fibres consist of two major morphological parts: the cuticle layer (usually referred as scale layer of wool) which is composed of overlapping cells that surround the cortex (inner part of the fibre)^(24, 25). The cortex comprises spindle-shaped cortex cells that are separated from each other by a cell-membrane complex (**Figure 3**^(26, 27)), which consists of non-keratinous proteins and lipids^(20, 28-31). The scaly structure of wool is responsible, to a great extent, for the tendency of wool to felt and shrink^(24, 32)

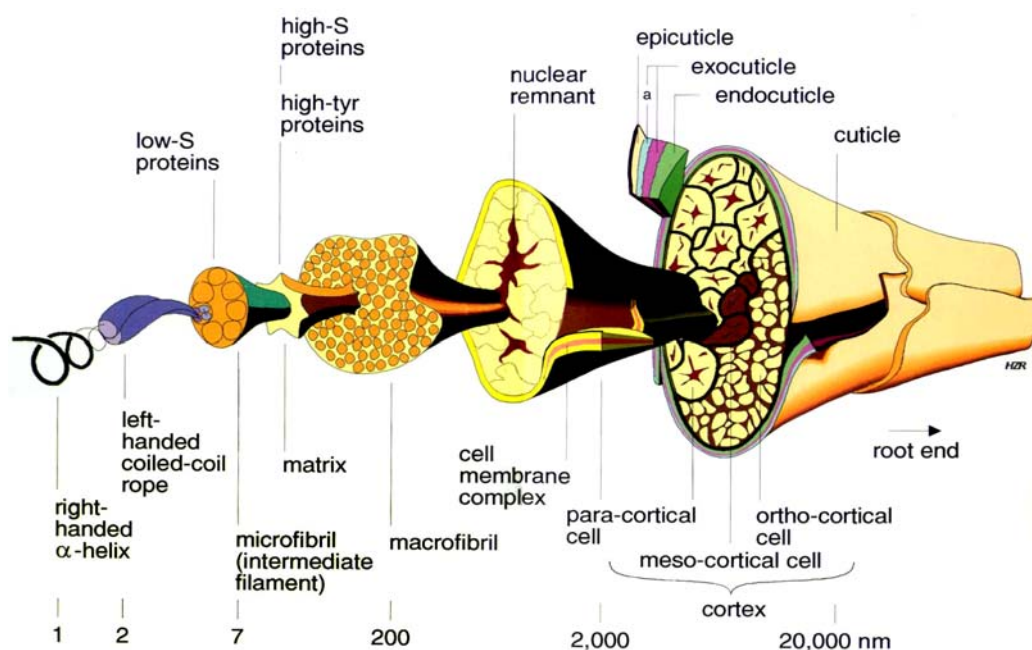


Figure 3: Exploded diagram showing the microstructure of wool fibre ^(26, 27)

1.1.2.1. Chemical Structure of α -Helix

A significant proportion of the polypeptide chains in wool are believed to be in the form of α -helix. ⁽²²⁾ The individual peptide chains in wool are held together by various types of covalent cross-links and non-covalent interactions (**Figure 4**). In addition to their occurrence between separate polypeptide chains (inter-chain), bonds can also occur between different parts of the same chain (intra-chain). With respect to the properties and performance of wool, however, inter-chains bonds are the most important of the two types ⁽²⁰⁾.

1.1.2.1.1. Cuticle

On the outside of the wool fibre is a protective layer of scales called cuticle cells. The scales have a waxy coating chemically bound to the surface. This stops water penetrating the fibre but allows absorption of water vapour. This makes wool water-repellent and resistant to water-based stains.

1.1.2.1.2. Cortex

The cortex – the internal cells - makes up 90% of the fibre. There are 2 main types of cortical cells – ortho-cortical and para-cortical. Each has a different chemical composition. The cells expand differently when they absorb moisture, making the fibre to bend. This creates the crimp in wool.

1.1.2.1.3. Cortical cell

The cortical cells are surrounded and held together by a cell membrane complex, acting similarly to mortar holding bricks together in a wall. The cell membrane complex allows easy uptake of dye molecules.

1.1.2.1.4. Macrofibril

Inside the cortical cells are long filaments called macrofibrils hold together by intermacrofibrillar matrix. The macrofibrils are made up of bundles of even finer filaments, called microfibrils or intermediate filaments, which are surrounded by an intermicrofibrillar matrix (intermediate filament associated proteins).

1.1.2.1.5. Matrix

The matrix consists of high sulphur proteins. Due to the large amount of amino-acids, wool can absorb up to 30% of its weight in water and can also retain large amounts of dye. The chemical composition is also responsible for wool's fire-resistance and anti-static properties.

1.1.2.1.6. Microfibril

Within the matrix area, there are embedded smaller units called microfibrils. The microfibrils in the matrix are rather like the steel rods embedded in reinforced concrete to give strength and flexibility. The microfibrils contain pairs of twisted molecular chains.

1.1.2.1.7. Twisted molecular chain and helical coil

Within the twisted molecular chains are protein chains that are coiled in a helical shape much like a spring. Hydrogen bonds and intermolecular disulphide bonds stiffen this structure. The helical coil – the smallest part of the fibre – gives wool its flexibility; elasticity and resilience, which helps wool fabric keep its shape and remain wrinkle-free in use (see **Figure 3 and Figure 4**).

1.1.2.2. Physical Structure of α -Helix

The amino acids in α helix are arranged in a right-handed helical structure where each amino acid residue corresponds to a 100° turn in the helix (i.e., the helix has 3.6 residues per turn), and a translation of 1.5 Å (0.15 nm) along the helical axis. The pitch of the alpha-helix (the

vertical distance between one consecutive turn of the helix) is 5.4 Å (0.54 nm) which is the product of 1.5 and 3.6. What is most important is that the N-H group of an amino acid forms a hydrogen bond with the C=O group of the amino acid four residues earlier; this repeated ($i + 4$ \Rightarrow i) hydrogen bonding is the most prominent characteristic of α -helix.

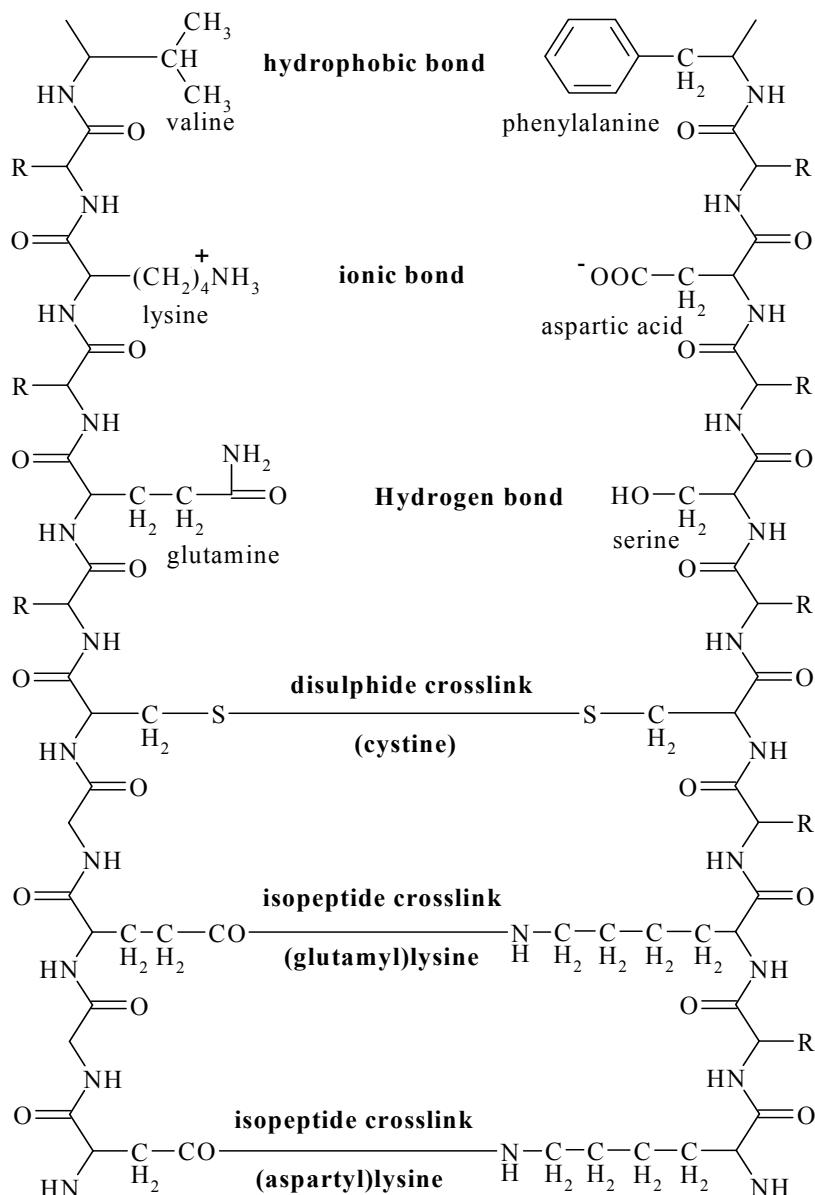


Figure 4: Possible bonds between different wool protein chains

1.2. Functionalising the Fibre Surfaces

‘Smart’ or ‘Functional’ materials usually form part of a ‘Smart System’ that has the capability to sense its environment and the effects thereof and, if truly smart, to respond to that external stimulus via an active control mechanism. Smart materials and systems occupy a ‘technology niche’ which also includes the areas of sensors and actuators ^(33, 34).

During the last ten years the traditional textile industry, that during the decades has favoured quality, has changed its strategy to support the innovation and the creation of new products and functionalities. This inversion of situation has allowed the consolidation of the emergence of two areas: “Technical Textiles” and “Smart Textiles and Interactive Fabrics (SFIT)”.

The important parameters to functionalise the fibre surfaces are the structure and charges of these surfaces. So, to improve these surfaces we must know first these parameters to handle the best material for each surface and develop it according to its surface structure and charge.

A - Structure of the fibre surface

The surface structure of the cotton is coated with a layer of fatty-waxy and pectin substances. The cotton fibre is mainly composed of α -cellulose, which is 88-96.5 % of the total mass of the fibre. The secondary wall of cotton fibre is of pure cellulose, whereas non-cellulosic material is present on the outer layers or inside the lumen of the fibre. ^(35, 36) The chemical composition of cotton varies with the variation in varieties of cotton, environment where it is cultivated and maturity level of the fibres. With the increase in maturity level there is an increase in the cellulosic percentage ⁽³⁷⁾.

Cotton is composed of cellulosic and non-cellulosic material. Presence of all organic and inorganic matter varies a lot depending upon many factors. However, majority of the non-cellulosic materials are taken away in the scouring process, which makes it absorbent so that it may pick and absorb dyes. All the same, this wax helps ginning, and spinning by providing a smooth surface, which attributes a little friction. It is also crucial to note that after scouring and bleaching most of the impurities are vanished and the fabric becomes pure cellulosic material. Nevertheless, it may still have insignificant percentage of added-impurities, which becomes part of the fibre during processing or impurities, which are not completely taken away.

The outer layer in wool fibre called cuticle cells (or scales), which overlap like tiles on a roof, make wool unique amongst textile fibres. The complex physical structure of cuticle cells is shown in **Figure 3**. An important function of cuticle cells is to anchor wool fibres in the skin of sheep. The exposed edge of each cuticle cell points from the fibre root towards the tip. This gives rise to a larger surface frictional value when a fibre is drawn in the against-scale direction than in the with-scale direction. The frictional difference helps to expel dirt and other contaminants from the fleece, but it is also responsible for wool's property of felting when agitated in water. This characteristic, which is not shared by any other textile fibre, enables fabrics with very dense structures to be produced, such as blankets, felts and overcoat

materials. When felting is regarded as undesirable (for example in knitted garments that will be machine-washed), processes are available to remove the frictional difference and make wool shrink resistant. The fibre surface is also largely responsible for the natural softness of wool and its property as one of the smoothest textile fibres.

Even after the natural wool grease has been removed by scouring with a detergent, wool fibres are relatively difficult to wet compared with other textile materials. This natural water repellency makes wool fabrics 'shower-proof' and able to resist water based stains. This property is the result of a waxy, hydrocarbon coating that is chemically bound to the surface of each scale. The coating survives processes such as dyeing and can only be removed by a severe chemical treatment.

For delivering the clean fibres to industry the greasy goes through scouring. This consists of washing the raw fibres with about 1% surfactant in a continuous 5–6 bowls line for removing the grease, suint, sand and dirt from the fibres.

B - Charge of the fibre surface

According to the chemical structure for cotton which shown in **Figure 1**, the cotton surface has negative charge due to the primary and secondary hydroxyl groups, and these charges increase at high pH (around 8 or 9). Therefore, the best treatment medium for the cotton surface is at pH 8.

On the other side the chemical structure of the wool as one can observe in **Figure 4** hosts both negative (formed by carboxyl group of amino acid) and positive (formed by amine group of amino acid) charges. pH of the treatment medium play an effective role for selecting the charge on the wool surface.

The isoelectric point, **pI**, is the pH of an aqueous solution of wool at which the molecules on average have no net charge. In other words, the negatively charged groups exactly balance the positively charged groups. The titration curve of wool, shown in **Figure 5**, indicates that at a pH lower than 3.61, both the carboxylate and amine functions are protonated (become COOH and NH_3^+), so the wool molecule has a net positive charge. At a pH greater than 10.91, the amine exists as a neutral base and the carboxyl as its conjugate base, so the wool has a net negative charge. This behavior is general for simple (bifunctional) amino acids. ⁽³⁸⁻⁴²⁾

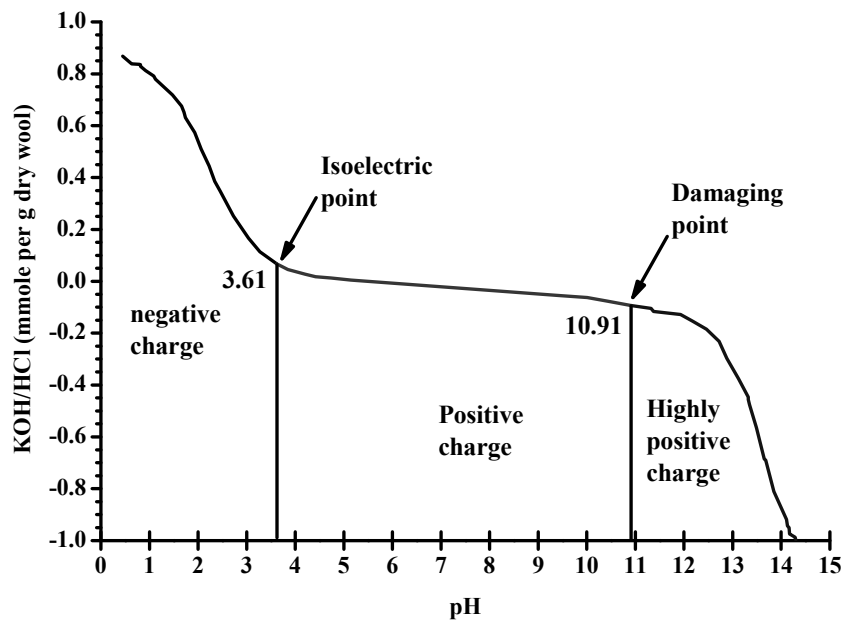


Figure 5: Titration curve for wool fibre with HCl and KOH ⁽⁴²⁾

1.2.1. Phase Change Materials for Thermoregulation

In textile industry, protection from extreme environmental conditions is a crucial requirement. Clothing that protects us from, extreme cold, intensive heat, open fire, high voltage; propelled bullets, toxic chemicals, nuclear radiations, biological toxins, etc are some of the illustrations. One of the best ways to functionalise the fibres surface is the deposition of some intelligent molecules on/in the fibre surface in order to gain a new property.

Phase Change Material (PCM) was born through the challenge of combating the severe temperature variations in space. In 1991, Colorado-based Outlast Technologies, Inc. achieved an exclusive license to the PCM technology with a vision to revolutionize outdoor wear. After prototype development and concept introduction to the textile industry, Outlast launched its first commercial product in 1997 in gloves and footwear.

Any material absorbs heat during heating process while its temperature is rising constantly. The heat stored in the material is released into the environment through a reverse cooling process. During the cooling process, the material temperature decreases continuously. A normal textile material absorbs about one kilo joule of heat per kilogram while its temperature rises by one degree Celsius. ^(33, 34)

The phase-change materials (PCM) are used to store latent heat. The storage of latent heat or thermal regulation is based on the transition of the (PCM) from a phase to another. When such

a material is heated to its melting point, it absorbs heat during the change of phase from solid to liquid state and releases heat when changes back from liquid to solid state.

Comparing the heat absorption during the melting process of a phase change material (PCM) with those in a normal heating process, a much higher amount of heat is absorbed if a PCM melts. A paraffin-PCM, for example, absorbs approximately 200 kilo-joules per kilogram when it undergoes a melting process. If a textile would absorb the same amount of heat its temperature would raise by 200 K. The high amount of heat absorbed by the paraffin in the melting process is released into the surrounding area in a cooling process starting at the PCM's crystallisation temperature. After comparing the heat storage capacities of textiles and PCM, it is obvious that by applying paraffin-PCM to textiles their heat storage capacities can be substantially enhanced ⁽³³⁾.

During the melting process, the temperature of the PCM remains constant. The same is true for the crystallisation process. The high heat transfer during the phase change process without temperature change makes PCM an area of interest for the heat storage.

The paraffins are either in solid or liquid state. In order to prevent the paraffin's leakage while in the liquid state, it is enclosed in small spheres with diameters of only a few micrometers. These microscopic spheres containing PCM are called PCM-microcapsules. The microencapsulated paraffin is either permanently locked like in acrylic fibres and in polyurethane foams, or coated onto the surface of a textile structure.

1.2.1.1. PCMs Classification and Requirements

PCM compounds should have some properties such as non-flammability, non-toxic, non-corrosive, chemically stable, high latent heat of fusion, high thermal conductivity, low changes in volume during phase change, and low PCM and containment cost.

1.2.1.1.1. Inorganic PCM materials

High latent heat of fusion, good thermal conductivity, no flammability and cheapness are the main advantages of inorganic materials. Nevertheless, they cause corrosion to most metals, phase decomposition and suffer from loss of hydrate. Incongruent melting and supercooling are the biggest problem with their exploitation. During melting and freezing, there are precipitations of other phases, which do not take part in next process of charging and discharging. Impurities can have a strong influence on the curves. The best examples of inorganic PCMs materials are a) calcium salts (calcium chloride hexahydrate ($\text{CaCl}_2 \cdot 6\text{H}_2\text{O}$),

etc), b) barium salts (barium carbonate BaCO_3 , etc) and c) sodium salts (sodium sulphate decahydrate ($\text{Na}_2\text{SO}_4 \cdot 10\text{H}_2\text{O}$), sodium carbonate decahydrate ($\text{Na}_2\text{CO}_3 \cdot 10\text{H}_2\text{O}$), etc).

1.2.1.1.2. Organic PCM materials

Low thermal conductivity, big volume changes during phase change, flammability are the main disadvantages of organic PCM materials. In addition, high latent heat of fusion, chemically stable, little or no supercooling, cheap, non-corrosive, non-toxic are the main advantages of these PCM materials.

The best examples of organic PCMs materials are a) paraffin wax (Decane, Dodecane, Tetradecane, Hexadecane, Octadecane, etc), b) polyethylenglycol, c) high-density polyethylene, d) stearic acid ($\text{C}_{18}\text{H}_{36}\text{O}_2$), palmitic acid ($\text{C}_{16}\text{H}_{32}\text{O}_2$), etc.

1.2.1.2. Definition and Determination of Specific Heat

Phase change materials (PCM) are used to achieve latent heat storage. The storage of latent heat or thermal regulation is based on the transition of a material (PCM) between phases. When a phase change material is heated to its melting point, it absorbs heat during the change of phase from a solid to a liquid state.

The heat is described as being *sensible heat* when it contributes to the change of temperature of the heated material. When heat is transferred to an object, the temperature of the object is increases. When heat is removed from an object, the temperature of the object decreases⁽⁴³⁾. The relationship between the heat (H) that is transferred and the change in temperature (ΔT) is

$$H \propto \Delta T \Rightarrow H \propto (T_f - T_i) \quad \text{Equation 1}$$

The proportionality constant in this equation is called the heat capacity (C). The heat capacity is the amount of heat required to raise the temperature of an object or substance one degree. The temperature change is the difference between the final temperature (T_f) and the initial temperature (T_i).

$$H = C (T_f - T_i) \quad \text{Equation 2}$$

The heat capacity C of a substance is the amount of heat required to change its temperature by one degree, and has units of energy per degree. The heat capacity is therefore an extensive variable since a large quantity of matter will have a proportionally large heat capacity.

A more useful quantity is the specific heat C_p (also called specific heat capacity), which is the amount of heat required to change the temperature of one unit of mass of a substance by one degree. Specific heat is therefore an intensive variable and has units of energy per mass per degree⁽⁴³⁾. This heat may be calculated from the following equation:

$$H = m C_p \Delta T \quad \text{Equation 3}$$

where C_p is the specific heat of the material, m is the mass of the material and ΔT is the change of temperature produced by the heat to that material.

Latent heat is the heat, which is not sensed by temperature change, but by the change of the state of the material (change of phase). During the process of change of phase, the temperature of the material does not change. The latent heat is calculated from the equation:

$$H = m L_p \quad \text{Equation 4}$$

where L_p is the specific latent heat of the phase change materials (melting, or crystallisation, vaporization, or condensation, etc).

Specific heat for an unknown material can be calculated with standard specific heat values of synthetic sapphire (alumina, Al_2O_3) by the following equation:

$$C_{p \text{ Sample}} = \frac{H_{\text{Sample}}}{H_{\text{Alu min a}}} \times \frac{m_{\text{Alu min a}}}{m_{\text{Sample}}} \times C_{p \text{ Alu min a}} \quad \text{Equation 5}$$

which C_p is the specific heat ($\text{J}\cdot\text{K}^{-1}\cdot\text{g}^{-1}$), m is the mass of material and H is the heat flow (mW). Synthetic sapphire (Al_2O_3) is used as a calibrant for heat capacity determination. The specific heat values C_p ($\text{J}\cdot\text{K}^{-1}\cdot\text{g}^{-1}$) at temperature T (in K) of this alumina can accurately calculated by the polynomial equation ⁽⁴⁴⁾:

$$C_p(T) = A + BT + CT^2 + DT^3 + ET^4 + FT^5 + GT^6 + HT^7 \quad \text{Equation 6}$$

The values of coefficients A to H for synthetic sapphire (Al_2O_3) are given for two temperature ranges was illustrated in **Table 1**. ⁽⁴⁴⁾

Table 1: Values of coefficients A to H for synthetic sapphire (Al₂O₃) ⁽⁴⁴⁾

	(T = 70 to 300 K) (T= -203.15 to 26.85°C)	(T = 290 to 2250 K) (T= 16.85 to 1976.85°C)
A	3.63245×10^{-2}	-5.81126×10^{-1}
B	-1.11472×10^{-3}	8.25981×10^{-3}
C	-5.38683×10^{-6}	-1.76767×10^{-5}
D	5.96137×10^{-7}	2.17663×10^{-8}
E	-4.92923×10^{-9}	-1.60541×10^{-11}
F	1.83001×10^{-11}	7.01732×10^{-15}
G	-3.36754×10^{-14}	-1.67621×10^{-18}
H	2.50251×10^{-17}	1.68486×10^{-22}

The PCMs are characterized by two thermodynamic parameters, namely the temperature at which the phase change (fusion/crystallization) occurs, and the enthalpy which accompany the change of phase, ΔH . For the engineering of insulation, there are also other indexes, which are defined for helping to choose a material for a specific use. For textile users such indexes are the duration index, DI ⁽⁴⁵⁾, and the total resistance to dry heat transfer, R ⁽⁴⁶⁾.

Duration index is a parameter characterising the material and the temperature at which it is aimed at functioning; the resistance to dry heat transfer is an index which is related also to the textile material on which PCM is applied.

The duration index, DI (J/cm³/K), which allows comparing how long a PCM will remain at a constant temperature during the phase change, is defined by ⁽⁴⁵⁾:

$$DI = \frac{\Delta H \times \rho}{\Delta T} \quad \text{Equation 7}$$

where ΔH is the enthalpy of PCM change of state, ρ is the PCM density and ΔT is the temperature difference between those of change of state and the temperature of interest (ambient, or body temperature).

The literature mentions the computerized thermal manikin used to simulate the heat loss from a human being to a cooler environment and able to measure the insulation value of the clothing systems ^(46, 47). The manikin provides the total resistance to dry heat transfer:

$$R = \frac{\Delta T \times A}{H} \quad \text{Equation 8}$$

provided by a material of area (A), having the temperature difference of the two sides of the material, $\Delta T = T_F - T_R$ (F , face, and R , rear, of the material) and through which passes a known heat flow, H . The value for textiles is given in “clo” ($\text{m}^2 \cdot ^\circ\text{C}/\text{W}$), $1 \text{ clo} = 0.155 \text{ m}^2 \cdot ^\circ\text{C}/\text{W}$, which is the unit for clothing insulation adopted from studies of hygienic comfort ^(46, 47). A 0 clo corresponds to a naked person and 1 clo corresponds to a person wearing a typical business suit.

The encapsulation of PCM is the most advantageous technique to merge the expected enriched heat performance with the other textile qualifications on the same product. ⁽⁴⁸⁾ The incorporation of PCMs into textiles in the form of a shell-core matrix brings many opportunities such as prevention of PCM dispersion in the structure, less evaporation and minimum interaction with the environment, increased heat transfer area, long shelf-life on a garment for normal fabric-care processes, and no adverse effect on the textile properties.

The encapsulated PCM materials are usually embedded in a thermally conductive medium. The characteristics of capsules, phase change material and conductive medium can be designed to provide the enhanced thermal management in a wide variety of applications.

An alternative way to deposit the organic PCM materials on textiles is to encapsulate them in another organic material which may prevent the flow of the melted PCM from the surface. One of the simplest ideas is to prepare composites of PCM/polymer in which the polymer has side chains, the gap between two chains being able to accommodate crystal of PCM. A **Scheme 1** shows such a host material with side chains and the retained PCM material.

The inorganic phase change materials are largely used for energy storage in various applications including building insulation. They have the important advantage of having high storage density (high enthalpy change at phase transition). On the other side they have the disadvantages of overcooling and corrosion, which impede on their use.

Inorganic PCM materials cannot be easily microencapsulated because inorganic salts are corrosive ^(48, 49). We considered the encapsulation in silica based capsules by using poly(ethoxysiloxane) (PAOS ^(49, 50)) to produce capsules with the core made of hydrated salt.

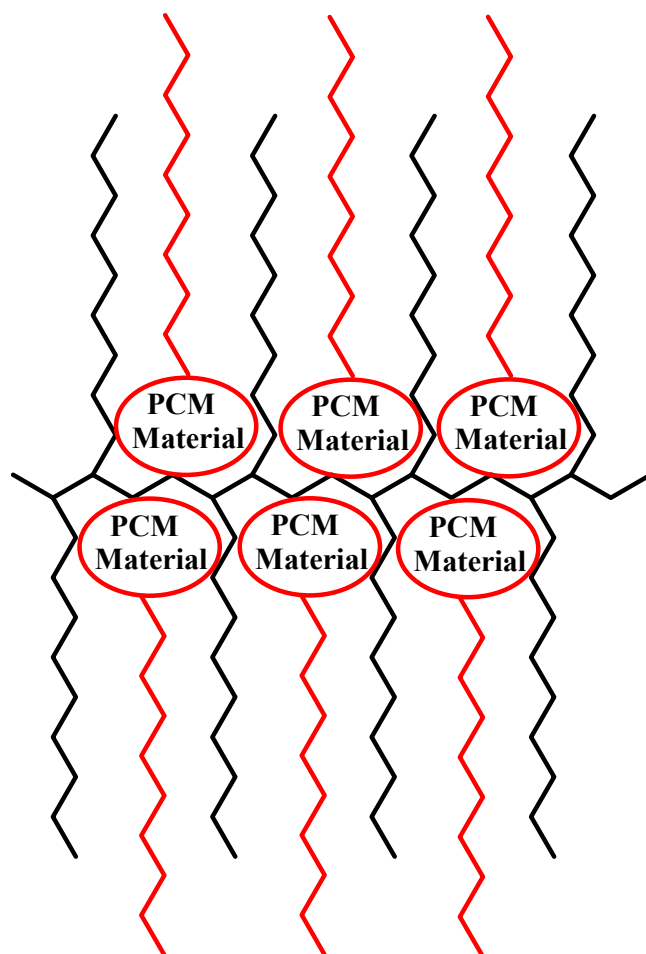
1.2.2. Dyeing and Lustre Properties of Textile Materials

The coating and infiltrating operations cover most of the dyeing and wet finishing processes. The colouring process renders most of the commercial value of a fabric. It is achieved either by coating (pigment printing) or by infiltrating (printing and dyeing) the fibres. ⁽⁵¹⁾

Dyeing is a traditional way to impart colour onto fibres. The liquid penetration onto cloth is a complicated phenomenon from both a scientific and physical standpoint ⁽⁵²⁾. Coloured compounds comprising pigments and dyes are used widely in textile, plastic, food, cosmetic, paper, printing, pharmaceutical and dyeing industries. Many of these are toxic or even carcinogenic. ⁽⁵³⁾ Different studies on the sorption of dyes by textile fibres have shown that the electro-kinetic potential and surface charge density of fibres can be influence largely by dyes ⁽⁵⁴⁻⁵⁷⁾.

In many industrial applications, the adsorption of cationic polymer onto surface occurs about 50 times faster than of the uncharged polymer ⁽⁵⁸⁾. This makes the adsorption kinetics of adsorption very important and consequently this fact has given support to a fair amount of research on adsorption kinetics ^(59, 60).

Lustre is an important aesthetic property of textile fabrics. ^(13, 61) The Textile Institute defined luster ⁽⁶²⁻⁶⁵⁾ as “The display of different intensities of light, reflected both specularly and diffusely from different parts of a surface exposed to the same incident light.”



Scheme 1: Scheme of host polymer with side chains and retains PCM material

If a light beam impinges on a surface, it may be: a) absorbed or b) lost as visible light, or c) scattered as the light absorbed and reemitted at the same wavelength but the direction of travel may be different, or d) reflected specularly as on a mirror surface, or e) diffusely in varying intensity as on a chalkboard surface, or as a combination of both (see **Figure 6**). Reflectance is dependent on the twist level of yarn, softeners ⁽⁶⁶⁾ etc. Also, the reflectance properties of the fabrics are highly angle dependent.

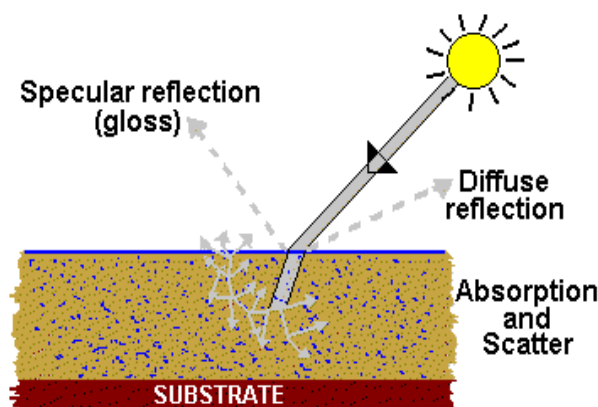


Figure 6: Different way of the light beam impinges on a surface

which **specular reflectance**: reflectance that exclude diffuse reflectance, as in a mirror, **diffuse reflectance**: reflectance that excludes specular (mirror) reflectance.

1.2.2.1. Thermo-Sensitive Microgels to Improving Textile Gloss

Microgels (describing the hydrogels with micro size) possess the unique properties of hydrogels particles. Hydrogels are three dimensionally cross-linked networks, which can not dissolve but swell in aqueous solution. Bulk hydrogels can not freely flow, although they have excellent swelling-de-swelling properties in aqueous solution. Hydrogels are usually prepared via free radical polymerization of the monomers, such as *N*-isopropylacrylamide (NIPAm), acrylamide (AAM), and acrylic acid (AAc), etc., in the presence of chemical cross-linkers, such as *N,N'*-methylene-bisacrylamide (BIS) in aqueous solution.⁽⁶⁷⁻⁷⁰⁾ Because of the good biocompatibility, excellent swelling-de-swelling properties, and stimuli-responsive behaviour, hydrogels have been extensively investigated for their potential applications as controlled drug release materials,^(67, 71-73) in tissue engineering,^(71, 74) and as biosensors.^(75, 76)

As compared to hydrogels, microgels also have the characteristics of the colloidal particles. The microgels can be easily dispersed in aqueous solution, which can be injected into any position needed. Hence, microgels have superiority over hydrogels as controlled drug release materials. Furthermore, the applications of hydrogels may also require a fast response to external stimuli. To achieve this, the reduction of the hydrogel size is prove a promising

approach because the response rate is inversely proportional to the square of the characteristic dimension of the hydrogel.⁽⁷⁷⁾

Microgels are usually prepared by emulsion copolymerization with or without the addition of surfactant, like sodium dodecyl sulfate (SDS) using NIPAm, AAm, and AAc as monomers or co-monomers and BIS as cross-linker.⁽⁷⁸⁻⁸²⁾ Depending on the monomers used, the resulting microgels may be sensitive to the external stimuli, such as temperature, pH value, and ionic strength of the aqueous solution.⁽⁷⁸⁻⁸²⁾

An important property of the microgels is to deposit onto the fibre surfaces. There are four types of microgel namely: anionic, cationic, neutral and amphoteric microgels. The first type, the anionic microgel can interact with the surfaces having positive charge like hair and wool fibres. These fibres have positive charge in acidic medium due to presence of amine groups which ionize to ($^+\text{NH}_3$) in acidic medium.⁽¹³⁾ This allows the microgel to interact with their surfaces.

The second type of microgel is the cationic one and this type can interact with the surfaces having negative charge like cotton fibre. This fibre has high negative charge in alkaline medium due to presence of hydroxyl group which ionize to (O^-) in alkaline medium.⁽¹³⁾ The negative charge allows the microgels to deposit much easier on the surface. The third type of microgel is the neutral microgel, which has no charge, and can deposit on any type of surfaces. The fourth type of microgel is the amphoteric one. It has positive charge in acidic medium and negative charge in alkaline medium and it can deposit on negative or positive surface according to the pH medium of the treatment bath.

1.2.2.2. Functionalised PEI (Polyethylene Imine) to Improving Textile

Cationic polymers are largely used in the treatment of cotton and wool fibres for improving their properties. It is known that these polymers are highly substantive to these fibres under mild conditions, because their surfaces bear a negative charge at pH above 3.6^(39, 40) on wool and 2.8 for cotton.⁽⁸³⁾

The use of the polyelectrolyte PEI in the fibre pre-treatment favours to a great extent the adsorption of a reactive dye onto fibres, and could be very interesting for textile industry because it produces a strong increase of antimicrobial activity⁽⁵⁴⁾.

The area of polyelectrolyte adsorption onto cellulosic and keratin fibres had been studied in detail for around 40 years, Wågberg *et al*, has answered two important questions, namely why

are the polyelectrolytes adsorbed on some surfaces, and where polyelectrolytes adsorbed on the fibres? ⁽⁵⁹⁾

The easiest way to describe the adsorption is as an interaction between the charges on the fibres and the polyelectrolytes. The electrostatic interaction between cationic groups of polymer and anionic charge existing on cotton and wool surface is responsible for the polymer coating

Since natural fibres are porous in nature it is obvious that the molecular mass of the polyelectrolyte will have a large impact on the adsorbed amount. It has also generally been found that when the molecular mass of the polymer decreases, there is an increase in adsorption since more surfaces will be available for the polymer with the lower molecular mass. This holds true for polyethyleneimine ⁽⁸⁴⁻⁸⁷⁾ and other cationic polymer (polyacrylamides ^(88, 89), poly (dimethyl diallyl ammonium chloride); polyDMDAAC ⁽⁶⁰⁾) and possibly also many other types of cationic water-soluble polyelectrolytes.

2. Organic PCM Materials based on Paraffin Compounds for Textiles

2.1. Introduction

Microencapsulation technology was utilised in the early 1980s by the US National Aeronautics and Space Administration (NASA) with the aim of managing the thermal barrier properties of garments, in particular for use in space suits. They encapsulated phase change materials (PCMs) (e.g. nonadecane) with the hope of reducing the impact of extreme variations in temperature encountered by astronauts during their missions in space ⁽⁹⁰⁾. Ultimately, the technology was not taken up within the space programme. However, the potential was recognized and PCM capsules are now used for various materials ⁽⁹¹⁻⁹³⁾, particularly outdoor wear garments (parkas, vests, thermals, snowsuits and trousers) and interior textiles (blankets, duvets, mattresses and pillowcases).

Besides being designed to combat cold, textiles containing PCMs help also to prevent overheating; their overall effect can be described as thermoregulation. The microcapsules have walls less than 1 μm thick and are typically 20 – 40 μm in diameter, with a PCM loading of 80 – 85 %. The small capsule size provides a relatively large surface area for heat transfer. Thus the rate at which the PCM reacts to an external temperature changes is very rapid. ⁽⁹⁴⁾

N-Alkanes are often used as thermal energy storage materials ^(95, 96); the melting and crystallization behaviour of n-alkanes has been widely studied. Although very high latent heat can be obtained, the bulk n-alkanes are not easy to handle in practical applications. Microencapsulation can help keeping liquids into solid form for which reason the process of microencapsulating phase change materials (Micro-PCMs) has attracted more attention recently.

Micro-PCMs have been studied as active or pumped coolants ⁽⁹⁷⁻⁹⁹⁾, solar and nuclear heat storage systems, ^(100, 101) and packed beds as heat exchangers. ⁽¹⁰²⁾ Micro-PCMs have also been used in the manufacture of thermo regulated fibres, ⁽¹⁰³⁾ fabrics, and foams. ⁽¹⁰⁴⁾ Yamagishi *et al* ⁽¹⁰⁵⁾ studied the melting and crystallization processes of microencapsulated n-tetradecane and n-dodecane with a melamine formaldehyde and gelatine shell and microcapsule diameters in the range of 5–1000 μm . The degree of super-cooling of microencapsulated n-tetradecane and microencapsulated n-dodecane increased when the diameter was lower than 100 μm .

By this work, six different types of paraffin waxes suitable for textile applications were encapsulated for being used as phase change materials on textiles. Various polymer structures were used as complex coacervates.

2.2. Experimental

2.2.1. Materials

Chemicals: Hexamethylene diisocyanate uretdione (**HDI-uretdione**), polylauryl acrylate (**PLA**), poly(decyl ethylene glycol) (**PDEG**), poly(dodecyl ethylene glycol) (**PDDEG**), dodecyl alcohol, dodecylamine.

Paraffin: *n*-decane, *n*-dodecane, *n*-tetradecane, *n*-hexadecane, *n*-octadecane, eicosane.

Solvents: toluene, hexane, diethyl ether, 1, 2-dichloroethane, *n*-pentane.

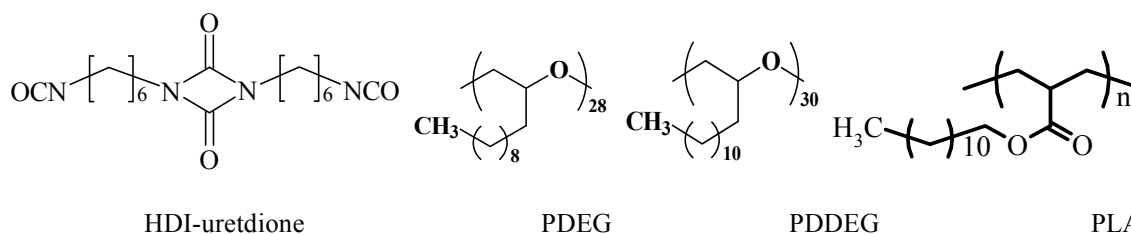


Figure 7: Chemical structure of PCM's polymers

2.2.2. Methods

2.2.2.1. Preparation of HDI Derivatives

2.2.2.1.1. HDI_1 derivative

The HDI derivatives was prepared as described by *Keul et al* ⁽¹⁰⁶⁾, and the scheme for preparation is illustrated in **Scheme 2**. A solution of dodecyl alcohol (2.44 g, 13.1 mmol) in toluene (5 mL) is stirred at room temperature under nitrogen. HDI (2 g, 5.94 mmol) is slowly added, and the resulting solution is then stirred for 24 h at 75°C. Cooling to room temperature leads to a white solid. The solvent is removed in vacuum (10^{-2} mbar), and the product is purified by washing with hexane and small amounts of diethyl ether. A white powder of diurethane uretdione (3.87 g, 92%) is obtained.

Diurethane uretdione (0.63 g, 0.888 mmol) is dissolved in 1, 2-dichloroethane (10 mL) under nitrogen and dodecylamine (0.182 g, 0.977 mmol) is added at 65°C. The resulting solution is stirred at 65°C for 24 h; cooling to room temperature, removal of solvent, and washing with *n*-

pentane leads to a white solid. The product is dried in vacuum (10^{-2} mbar) at room temperature. A white powder of (**HDI_1**) derivative (0.76 g, 96%) is obtained.

2.2.2.1.2. *HDI_2 derivative*

The preparation is illustrated in **Scheme 3** and it can be described as: Diurethane uretdione (2 g, 2.82 mmol) is dissolved in toluene (21 mL) under nitrogen and 6-amino-1-hexanol (0.4 g, 3.38 mmol) is slowly added at 60°C. The resulting solution is stirred at 60°C for 24 h, then cooled at room temperature, solvent is removed in vacuum, and the obtained compound is washed firstly with n-hexane and then with small amounts of diethyl ether, and dried in vacuum at 50°C. The white solid powder is hydroxyl functionalized compound (2.28 g, 98 %).

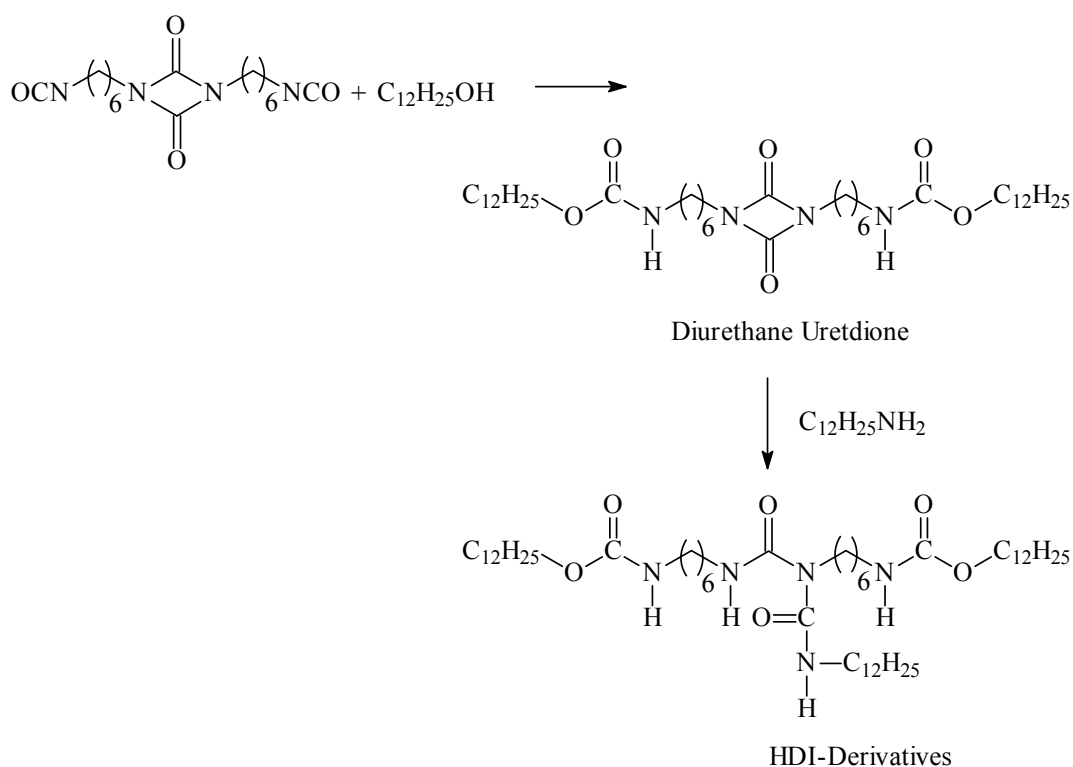
A solution of hydroxyl-functionalised compound (1 g, 1.21 mmol) in 1,2-dichloroethane (14 ml) is stirred at 70°C under nitrogen. HDI (0.2 g, 0.62 mmol) is slowly added, and the resulting solution is then stirred for one week at 70°C. The solution is cooled at room temperature, the solvent is removed under vacuum, and this leads to a white solid. For purification, the product is recrystallised from isopropyl alcohol. A white powder of pre-stage compound for HDI_2 (1.02 g, 85%) is obtained.

Pre-stage compound for HDI_2 (1 g, 0.5 mmol) is dissolved in 1,2-dichloroethane (10 ml) under nitrogen and dodecyl amine (0.1 g, 0.54 mmol) is slowly added at 80°C. The resulting solution is stirred at 65°C for 25 h. The solution is cooled to room temperature, then the solvent is removed under vacuum, and this yields to a white solid, HDI_2 which is washed with n-pentane (1.06 g, 96%). The dried product is used for further application.

2.2.2.2. **Preparation of PCMs Compounds**

The PCMs compounds are prepared by reacting different polymers (HDI-derivatives, polylauryl acrylate (**PLA**), poly(decyl ethylene glycol) (**PDEG**) and poly(dodecyl ethylene glycol) (**PDDEG**)) with various paraffin compounds ($C_{10} - C_{20}$) in different molar ratio (Polymer to Paraffin of 1: 1, 1: 2, 1: 4 and 2:1) at high temperature (80 – 140°C) for a time ranging from 10 to 16 h, and then measured by DSC.

Different paraffins, namely n-decane, n-dodecane, n-tetradecane, n-hexadecane, n-octadecane and n-nonadecane were chosen for encapsulating.



Scheme 2: Scheme for preparation of the HDI_1

2.2.2.3. Coating of Wool and Cotton Fibres/Fabrics with PCM Compound

A coating method was used to apply the prepared PCM materials from HDI derivatives on cotton and wool fibres. Coating material is a water soluble synthetic dispersion, commercially available for fabrics, polyurethane based, anionic, with 45–48% active content. Fixing agent comprising melamine resins with low formaldehyde content was used for cross linking, which was miscible in water, nonionic and of 8–9 pH value.

Recipes were prepared for 1:1 and 1:1.5 mixtures of the coating material and the PCM materials. Ten units coating material were stirred at 600 rpm for 5 min and then 10 or 15 units PCM material were mixed while increasing the stirring rate up to 1000 rpm for the next 15 min. 1.5% fixing agent was blended and stirring rate was halved for the last 2–3 min.

The fabrics were immersed into the coating dispersion solution at 40–50°C, coated fabric samples were fixed in a drying oven for 15 min and the temperature increased gradually from 60 to 80°C and then conditioned for the subsequent 24 h.

To determine the actual incorporation percentages of the PCM materials transferred to the sample, which depends also on the coating thickness, we weighed the coated and uncoated pieces of fabric.

2.2.3. Measurements

2.2.3.1. Differential Scanning Calorimetry (DSC)

Differential scanning calorimetry was carried out on a NETZSCH DSC 204 differential scanning calorimeter under nitrogen flow (20 mLmin^{-1}). Samples (5–10 mg weighed to 0.1 mg precision) were heated on a programme of heat-cool-heat from 0 to 100°C with a heating/cooling rate of $10 \text{ K}\cdot\text{min}^{-1}$ heating rate. Melting temperature and enthalpy are determined from the second heating run.

2.2.3.2. Scanning Electron Microscope (SEM)

Scanning Electron Microscopy HITASHI S-3000 microscope S, at 15-kV acceleration voltage, after gold coating was used to study the surface morphology and the cross section of the composite films.

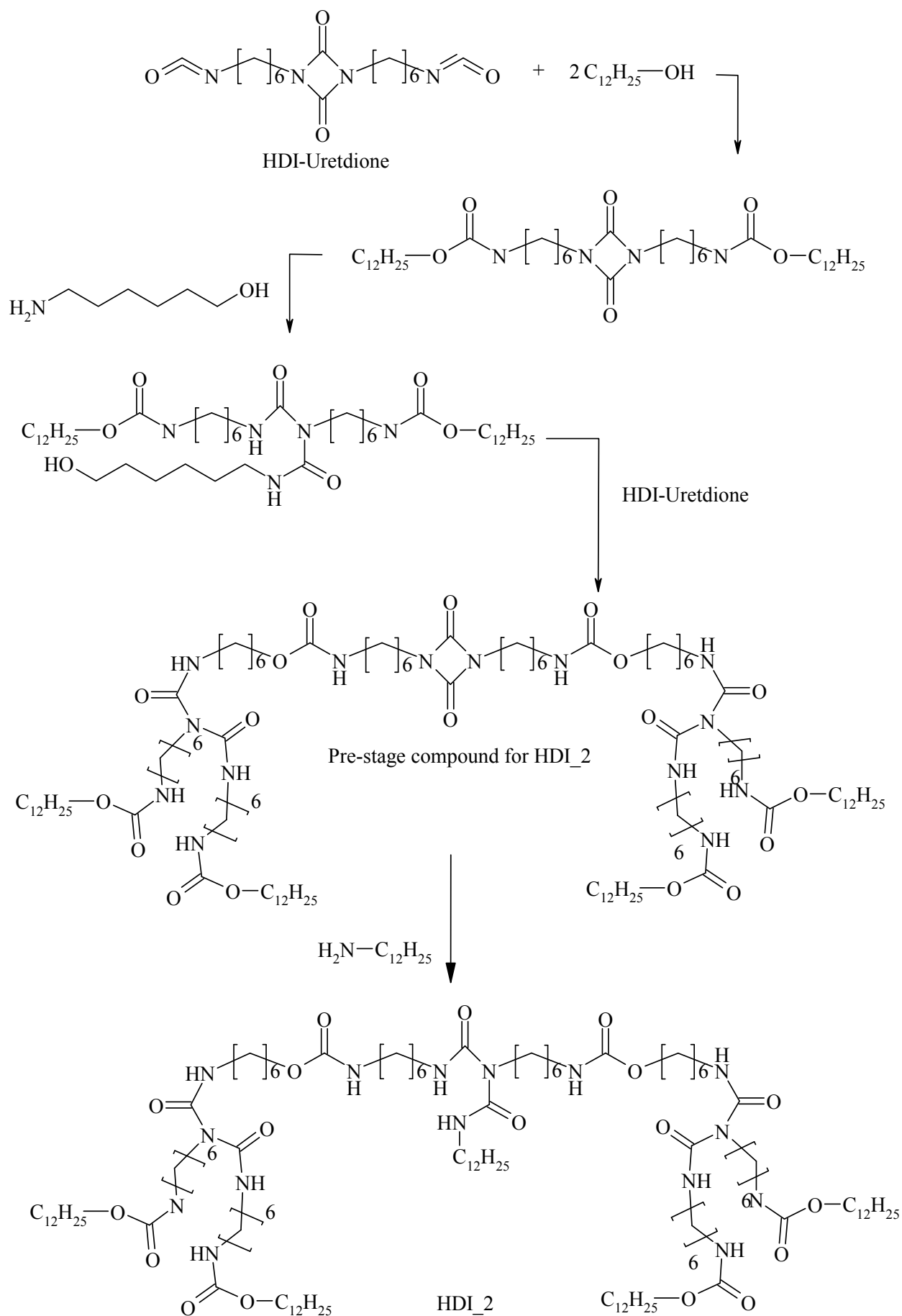
2.3. Result and Discussion

Polymer/Paraffin composite which merges paraffin thermal characteristics (melting point and melting enthalpy) with the polymer retaining network are successfully produced. The paraffin wax in the composites crystallises without damaging the polymer network. This methodology may be used with various polymers with the aim to produce PCM composites which need to have a melting transition occurring within the temperature range of interest ($30 - 40^\circ\text{C}$) and an enthalpy of at least 200 J/g , for being of interest.

Because the desired phase-change effect of the paraffin, more paraffin means larger amount of latent heat is stored/released during a cycle. On the other side, the paraffin content of the composite is limited by the amount of polymer which is required for arresting it.

An alternative way is to prepare composites of paraffin-polymer in which the polymer has side chains, and the gap between two chains is equal to the size of paraffin molecule. This may produce eutectic crystals with enhanced properties. A **Scheme 4** shows such a host material with side chains obtained from hexamethylene diisocyanate uretdione and an alkane ($\text{C}_{18}\text{H}_{38}$).

We expect that using such a compound for hosting paraffin molecules will result in improved paraffin/polymer composites, able to store better the heat than the usual mixtures do.



Scheme 3: Scheme for preparation of the HDI_2

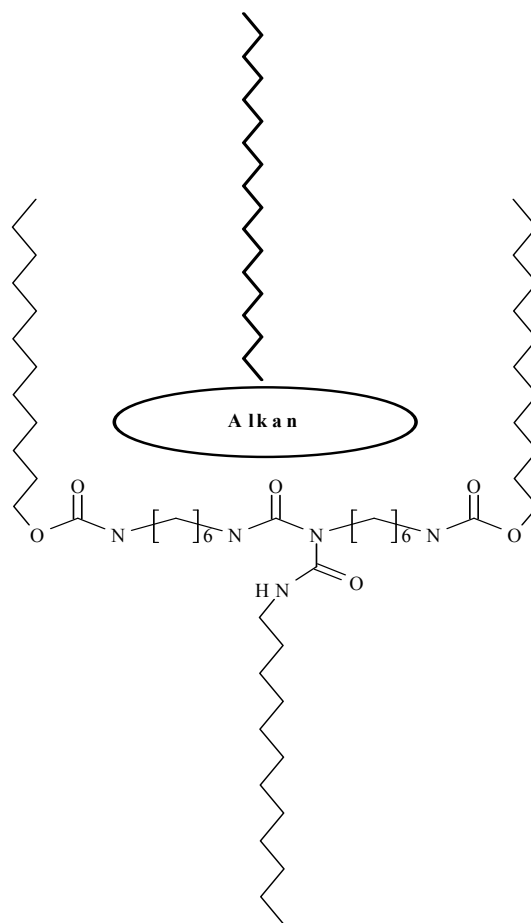
Following these considerations we have screened several polymers and paraffins for identifying the mixtures which store the largest amount of heat and have the phase change transition within the range of body temperature.

We considered five different polymers, namely: poly(dodecyl ethylene glycol) (PDDEG), poly(decyl ethylene glycol) (PDEG), hexamethylene diisocyanate uretdione derivatives (HDI_1 and HDI_2) and polylaurylacrylate (PLA) and six different paraffins, namely: *n*-decane, *n*-dodecane, *n*-tetradecane, *n*-hexadecane, *n*-octadecane, eicosane.

2.3.1. Optimising the Reaction Condition

For optimising the reaction condition in order to have PCM compound with high storage heat, all the polymers were reacted with one of the paraffin (*n*-octadecane), and reaction time and temperature were investigated in relation with the DSC results for the temperature and heat of the phase change process.

The molar ratio of polymer to paraffin compound, and type of paraffin compounds were also varied in order to find the optimum formulation to prepare suitable PCM compounds.



Scheme 4: Scheme of hexamethylene diisocyanate uretdione and alkan ($C_{18}H_{38}$)

2.3.1.1. Effect of Temperature

PCMs were produced by using different polymers (PLA, PDEG, PDDEG, HDI_1 and HDI_2) and n-octadecane with molar ratio of 1:2 at different temperatures (80–140 °C) for 14h. The DSC results obtained from second heating run of DSC for the prepared compounds are shown in **Table 2** and **Figure 8**. It is obvious that, the raising of the temperature of reaction from 80 to 100 °C is accompanied by a enhancement of melting temperature T_p (29.6, 30.2, 31.5, 31.8 and 32.8; PDEG, PDDEG, HDI_1, HDI_2 and PLA respectively), and enthalpy ΔH (159.1, 156.2, 177.4, 160.9 and 188.8; PDEG, PDDEG, HDI_1, PLA and HDI_2 respectively). The increase of the reaction temperature above 100°C does not bring any improvement to the melting temperature T_p and enthalpy ΔH for all PCM compounds. One concludes that the optimum temperature for reacting the paraffin with any of the investigated polymers is 100°C.

Table 2: Effect of reaction temperature on T_p and ΔH of second heating for PCM compounds prepared from polymers with n-octadecane

Polymer	Reaction Temp. °C	2 nd Heating		
		T_o (°C)	T_p (°C)	ΔH (J/g)
PDEG	80	22.3	26.3	83.5
	100	25.1	29.6	159.1
	120	24.8	29.3	148
	140	24.6	29	145.2
PDDEG	80	25.0	29.9	130
	100	25.3	30.2	156.2
	120	24.8	29.6	145
	140	24.4	29.1	144
HDI_1	80	26.4	30.2	156.4
	100	27.5	31.5	177.4
	120	27.0	30.9	174.3
	140	26.7	30.6	170.5
HDI_2	80	27.4	30.9	170.3
	100	28.2	31.8	188.8
	120	27.9	31.5	182.6
	140	27.7	31.2	181.2
Polylauryl acrylate [C ₁₅ H ₂₈ O ₂] _n	80	25.0	30.9	112.4
	100	26.5	32.8	160.9
	120	25.7	31.8	161.3
	140	25.8	31.9	161.5

Reaction Condition: Molar Ratio: 1:2; Time: 14h; Paraffin Type: *n*-Octadecane
 T_o : Onset Temperature, T_p : Peak Temperature, ΔH : Enthalpy

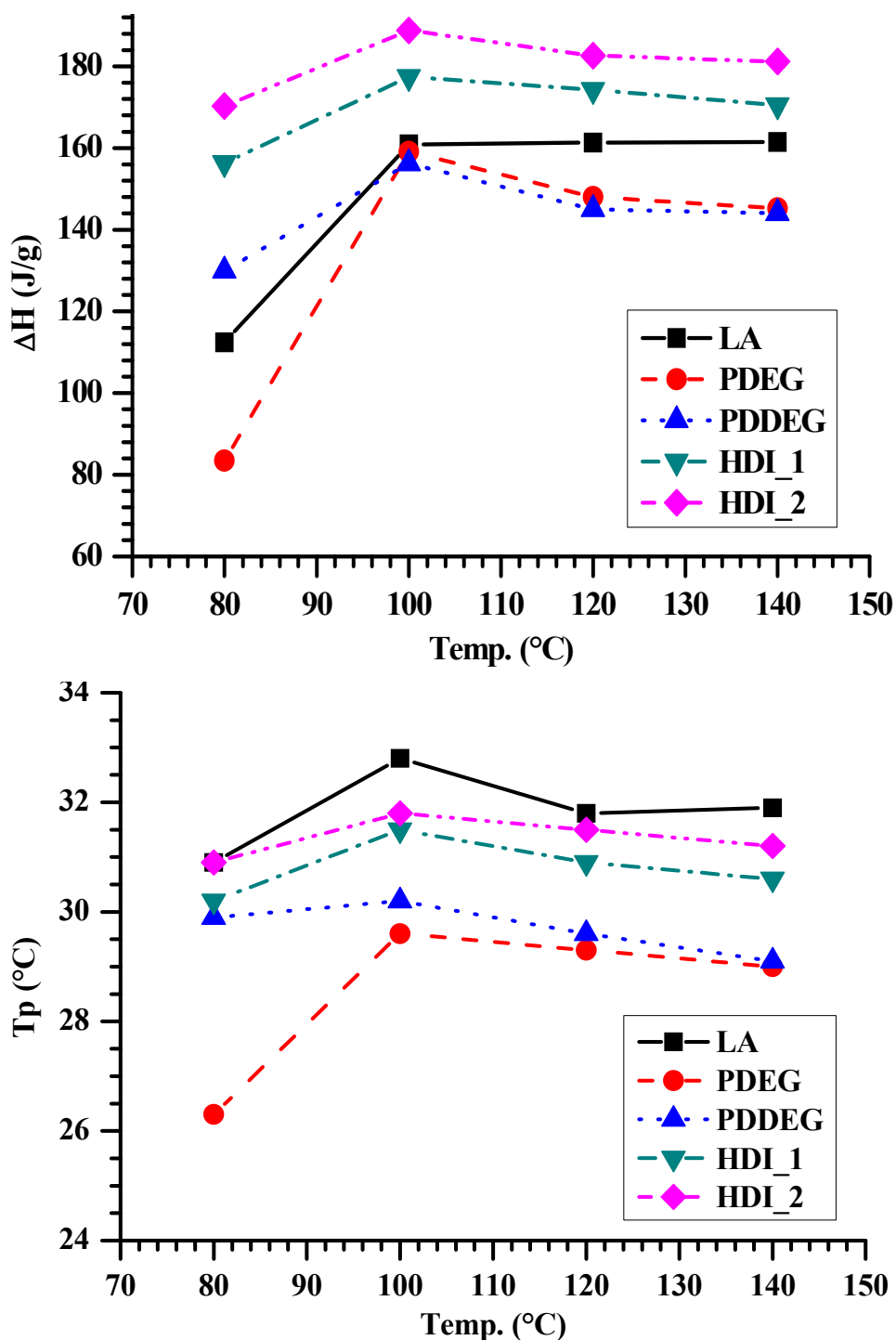


Figure 8: Enthalpy and peak temperature of second heating for PCM compounds from n-octadecan and different polymer compounds at different reaction temperature

2.3.1.2. Effect of Time

The effect of time of reaction on the preparation of PCMs compounds was investigated by carrying the reaction with different polymers (LA, PDEG, PDDEG, HDI_1 and HDI_2) mixed with n-octadecane with molar ratio of 1: 2 at 100°C for different reaction time (10 to 16 h). The DSC results from second heating run of DSC are shown in **Table 3** and **Figure 9**.

It appears that by using reaction times ranging from 10 to 16 h one may change significantly the melting temperature, T_p , and enthalpy, ΔH . One can conclude that the increase of the reaction time up to 14h leads to increase of both the melting temperature and the enthalpy; the values decrease again after 14 hours.

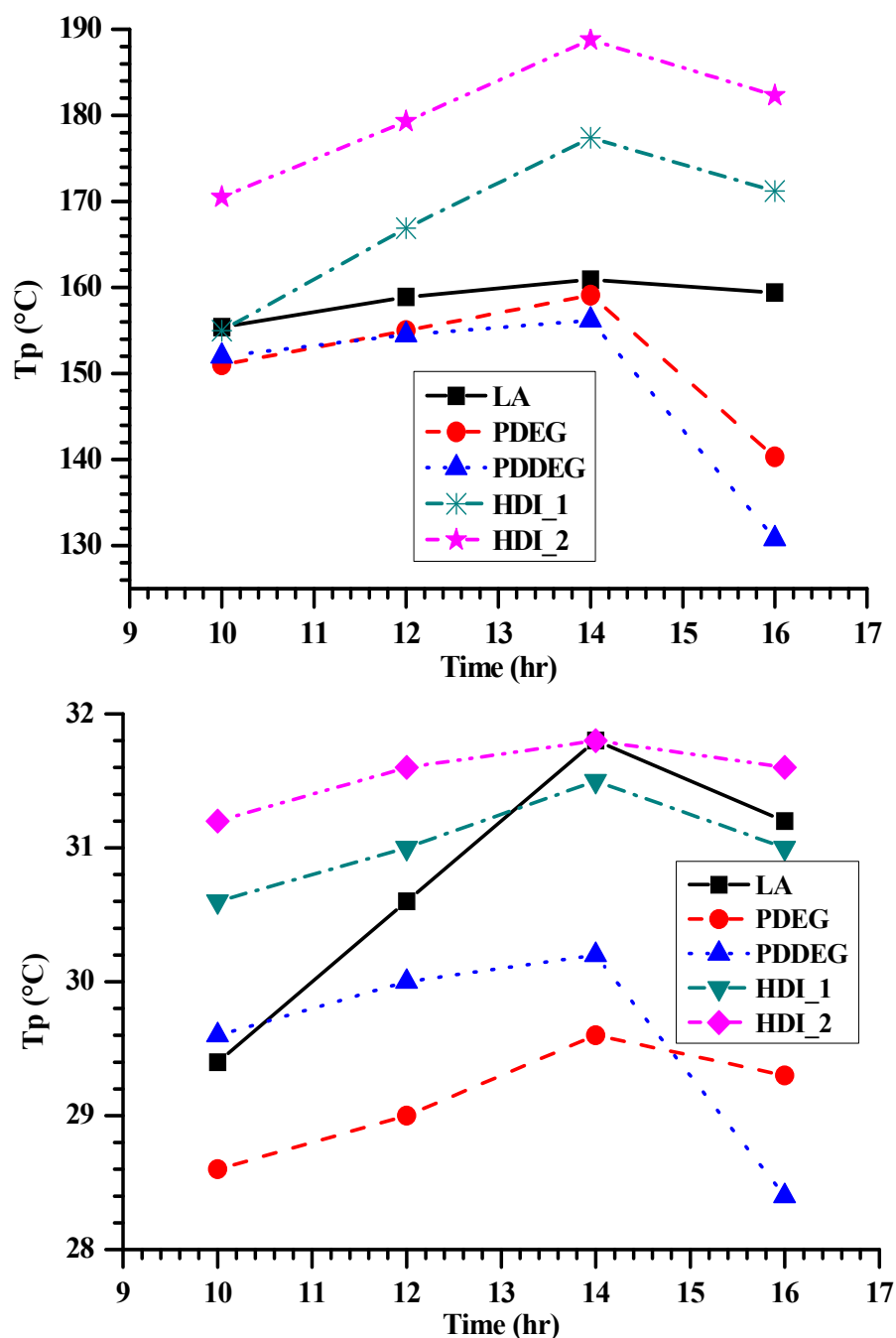


Figure 9: Enthalpy and peak temperature of second heating for PCM compounds from n-octadecane and different polymer compounds at different reaction time

Table 3: Effect of reaction time on T_p and ΔH of second heating for PCM compounds prepared from polymers with n-octadecane

Polymer	Reaction Time h	2 nd Heating		
		T_o (°C)	T_p (°C)	ΔH (J/g)
PDEG	10	24.3	28.6	151
	12	24.6	29	155
	14	25.1	29.6	159.1
	16	24.8	29.3	140.3
PDDEG	10	24.8	29.6	152
	12	25.1	30	154.5
	14	25.3	30.2	156.2
	16	23.8	28.4	130.8
HDI_1	10	26.7	30.6	155
	12	27.1	31	166.9
	14	27.5	31.5	177.4
	16	27.1	31	171.2
HDI_2	10	27.7	31.2	170.5
	12	28.0	31.6	179.3
	14	28.2	31.8	188.8
	16	28.0	31.6	182.3
Polylauryl acrylate [C ₁₅ H ₂₈ O ₂] _n	10	23.8	29.4	155.4
	12	24.7	30.6	158.9
	14	26.5	32.8	160.9
	16	25.8	31.9	159.4

Reaction Condition: Molar Ratio: 1:2; Temperature: 100°C; Paraffin Type: n-Octadecane

T_o : Onset Temperature,

T_p : Peak Temperature,

ΔH : Enthalpy

2.3.1.3. Effect of Polymer: Paraffin Molar Ratio

Further, we investigated whether the mixture of polymer with paraffin may reach an eutectic⁽¹⁰⁷⁾. N-octadecane (melting Temp.: 28°C, ΔH : 242.5 J/g⁽¹⁰⁸⁾) was used in four different molar ratios, calculated to the corresponding polymer (PDEG, PDDEG, HDI_1, HDI_2 and PLA), respectively 1:1, 1:2, 1:4 and 2:1 of polymer to paraffin. The DSC results from second heating for PCMs are shown in **Table 4** and **Figure 10**.

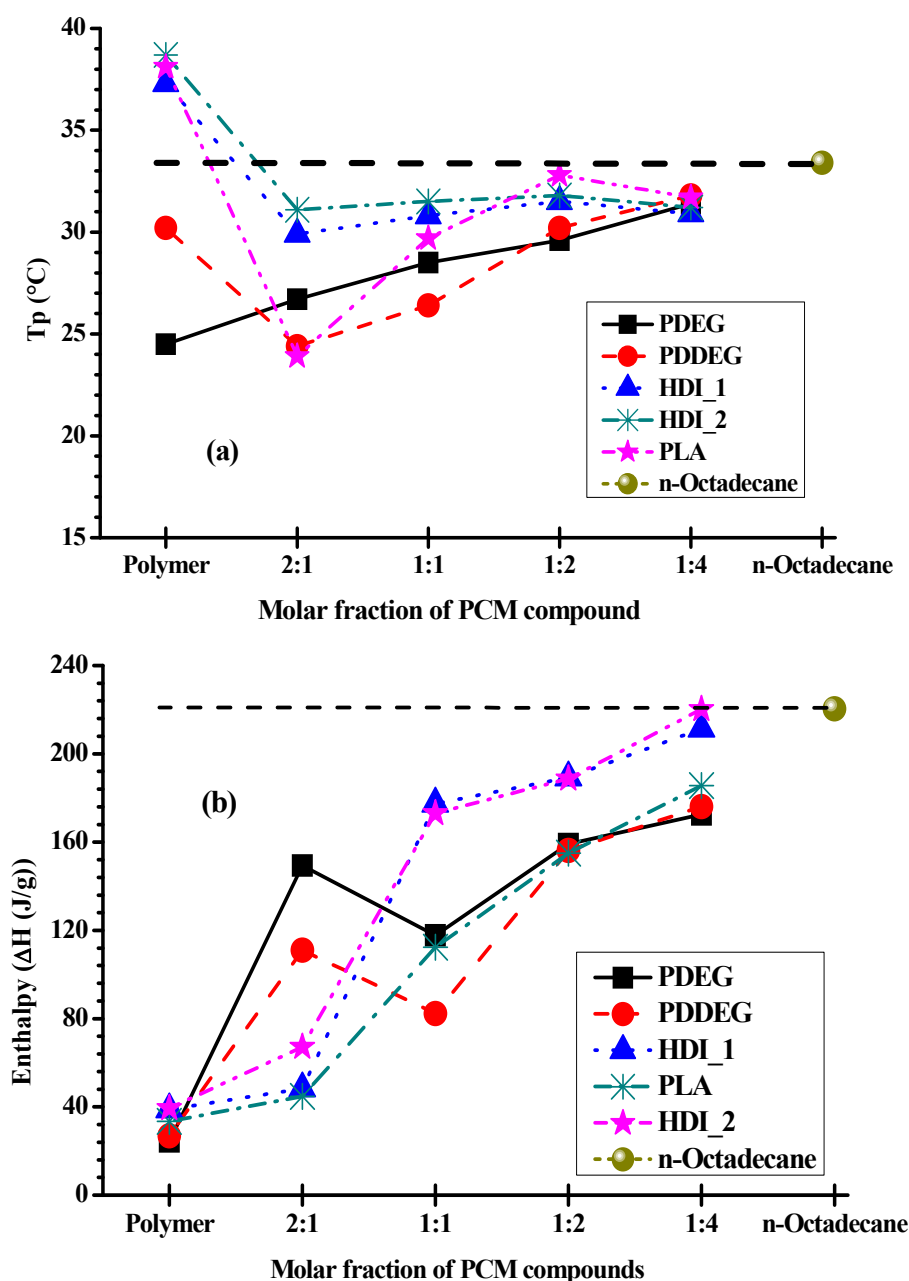


Figure 10: Comparison of DSC recorded data for the polymer-n-octadecane crystals (symbols) and those of pure n-octadecane (dotted line)

a) Temperature of melting for the polymer-paraffin mixtures; b) enthalpy of phase transition of the polymer-paraffin mixtures

One may notice that the DSC signal records, in most of the cases, a single endothermic effect at heating and a single exothermic effect at cooling, corresponding to the melt/crystallisation of the paraffin. In case of HDI_1 and HDI_2 there are several small endothermic events recorded at temperatures beyond the main peak, indicating the occurrence of several transitions. Since the effects are noticed at both the first and second heating cycle they correspond to reversible transitions and are probably due to side products formed during the process of obtaining the HDI derivatives.

One observes from the second heating run that, for PCM-polymer composites prepared from PDEG and PDDEG polymers the enthalpy (ΔH) decreases from the 33.3 % (2:1) till 50 % (1:1) molar ratio. By increasing the molar ratio till 80 % (1:4) the ΔH value increases and the melting temperature (T_p) increases too. On the other hand, for PCM-polymer composites prepared from PLA, HDI_1 and HDI_2 compounds the enthalpy (ΔH) and (T_p) goes from (2:1) to (1:2), and by increasing the percent of paraffin in the mixture till 80 % (1:4) the values of (T_p) and (ΔH) decrease.

Figure 10a shows that only the PCM-polymer composites produced from PDDEG and PLA seem having eutectic point, and eutectic composition.

As it appears, the temperatures of phase transition recorded for the mixtures (**Figure 10a**) is close to those of the pure paraffin in most of the cases. However the values recorded for the mixture with PDEG and PDDEG, respectively, seem to indicate the existence of a minimum, for ratio of monomer to paraffin of 2:1. On the other side, at such low molar fraction of paraffin in the mixture the heat of fusion is quite low, below 100 J/g, which makes the products less interesting for practical application (**Figure 10b**).

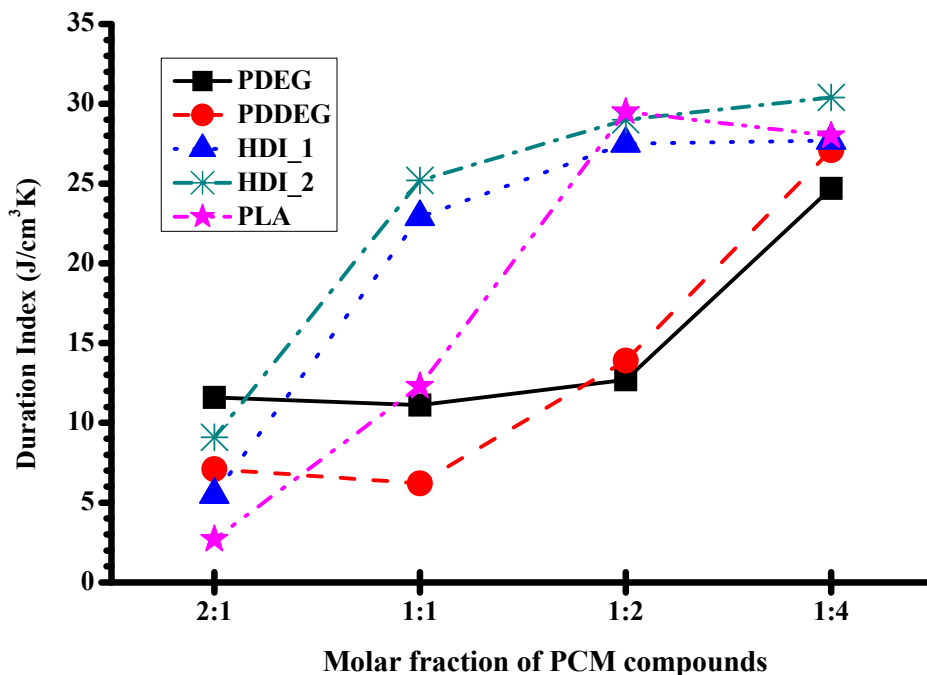


Figure 11: Duration index for the PCM-polymer composites from n-octadecane with different polymer compound with different molar ratio

Duration Index (DI): based on ΔT from melt point to body temperature (37°C) and average density of 0.8 g/cm³

The PCM-polymer composites are ranked in **Figure 11** from point of view of the Duration Index. The calculations are based on the insulating at body temperature of 37°C. The values of Duration Index show that out of the five polymers for making the composites with n-octadecane those which give the best material (having the highest Duration Index) are HDI_1 and HDI_2. Also one may notice that in all cases the mixtures in molar ratio 1:4 monomer to paraffin are the best ones, and those in molar ratio of 2:1 are the worst.

Table 4: Effect of molar ratio on T_p and ΔH of second heating for PCM compounds prepared from polymers with octadecane

Polymer	Molar Ratio	1 st Heating			1 st Cooling			2 nd Heating			DI * (J/cm ³ K)
		T_o (°C)	T_p (°C)	ΔH (J/g)	T_o (°C)	T_p (°C)	ΔH (J/g)	T_o (°C)	T_p (°C)	ΔH (J/g)	
PDEG	2: 1	21.6	26.1	120.9	19	23.0	146.8	22.1	26.7	149.4	8.0
	1: 1	23.3	28.4	120.9	17.3	21.1	112	23.4	28.5	117.8	6.9
	1: 2	27.8	29.9	165.4	18.1	19.5	137.4	25.1	27	159.1	10.7
	1: 4	26.3	31.2	177.6	24.3	28.8	177.8	26.5	31.4	172.6	13.2
PDDEG	2: 1	20.8	26.0	101	17	21.3	107.3	19.5	24.4	111.1	5.1
	1: 1	23.2	26.3	102.8	20.4	23.1	85.2	23.3	26.4	82.3	4.8
	1: 2	25.2	27.9	159.1	23	25.5	152.4	25.3	28	156.2	10.7
	1: 4	26.3	31.9	177.5	23.2	28.2	175.6	26.2	31.8	176.1	13.0
HDI_1	2: 1	26.9	28.8	66.9	22.5	24.1	61	27.9	29.9	48.4	4.3
	1: 1	27.9	31.6	178.3	22.2	25.1	167.8	27.2	30.8	177.4	14.9
	1: 2	27.2	31.2	186.2	21.6	24.7	176	27.5	31.5	189.3	15.9
	1: 4	27.5	31.1	215.7	24.9	28.2	187.1	27.3	30.9	211.4	13.7
HDI_2	2: 1	28.9	31.0	66.9	27.9	29.9	64.7	29.0	31.1	67.2	6.7
	1: 1	27.9	31.6	173.6	26.7	30.3	166.3	27.8	31.5	173.1	15.1
	1: 2	28.1	31.7	188.1	27.1	30.6	181.4	28.2	31.8	188.8	17.2
	1: 4	27.5	31.1	179.9	26.5	30.0	173.1	27.6	31.2	220.3	18.7
PLA [C ₁₅ H ₂₈ O ₂] _n	2: 1	14.6	23.9	45.7	15.7	25.7	41.9	14.6	23.9	44.8	1.6
	1: 1	27.7	32.0	120.4	23.6	27.3	106.2	25.7	29.7	112.4	8.0
	1: 2	26.5	32.8	156.3	22.1	27.4	140.6	26.5	32.8	155.1	11.8
	1: 4	28.1	33.1	195.3	24.7	29.1	175.9	26.9	31.7	185.6	14.7

*DI Duration Index: based on ΔT from melt point to body temperature (37°C) and average density of 0.8 g/cm³

Reaction Condition: Time: 14h; Temperature: 100°C; Paraffin: *n*-Octadecane; M.R: Polymer: Octadecane

T_o : Onset Temperature,

T_p : Peak Temperature,

ΔH : Enthalpy

2.3.1.4. Effect of Paraffin Types

The DSC results of different paraffin compounds used in this study are shown in **Table 5**, which obtained from second heating in DSC when heated from 0 to 100°C at 10°C min⁻¹. The data are closed to those in the literature. ⁽¹⁰⁹⁻¹¹¹⁾

Table 5: Peak temperature and enthalpy of second heating for different paraffin compounds

Paraffin Type	2 nd Heating	
	T _p (°C)	ΔH (J/g)
C₁₀ : <i>n</i>-decane	-16.7	11.69
C₁₂ : <i>n</i>-dodecane	-11.2	11.73
C₁₄ : <i>n</i>-tetradecane	8.8	77.9
C₁₆ : <i>n</i>-hexadecane	22.6	140.5
C₁₈ : <i>n</i>-octadecane	33.4	220.4
C₂₀ : <i>n</i>-eicosane	42.8	214.2

T_p: Peak Temperature, ΔH: Enthalpy

The polymers DSC results from second heating are given in **Table 6**. It is noticeable that the HDI_1, HDI_2, PLA and PDDEG are more stable thermally than that for PDEG. They may be, therefore, favoured for mixing with paraffins.

Table 6: Peak temperature and enthalpy of second heating for different polymer compounds

Polymer Compounds	2 nd Heating	
	T _p (°C)	ΔH (J/g)
HDI_1	37.3	38.92
HDI_2	38.7	39.43
PLA	38.1	33.52
PDEG	24.5	24.33
PDDEG	30.2	26.91

T_p: Peak Temperature, ΔH: Enthalpy

The DSC results from mixing paraffin compounds with different polymers (PDEG, PDDEG, HDI_1, HDI_2 and PLA) with molar ratio 1:2 at 100°C for 14h are shown in **Figure 12** and **Table 7**.

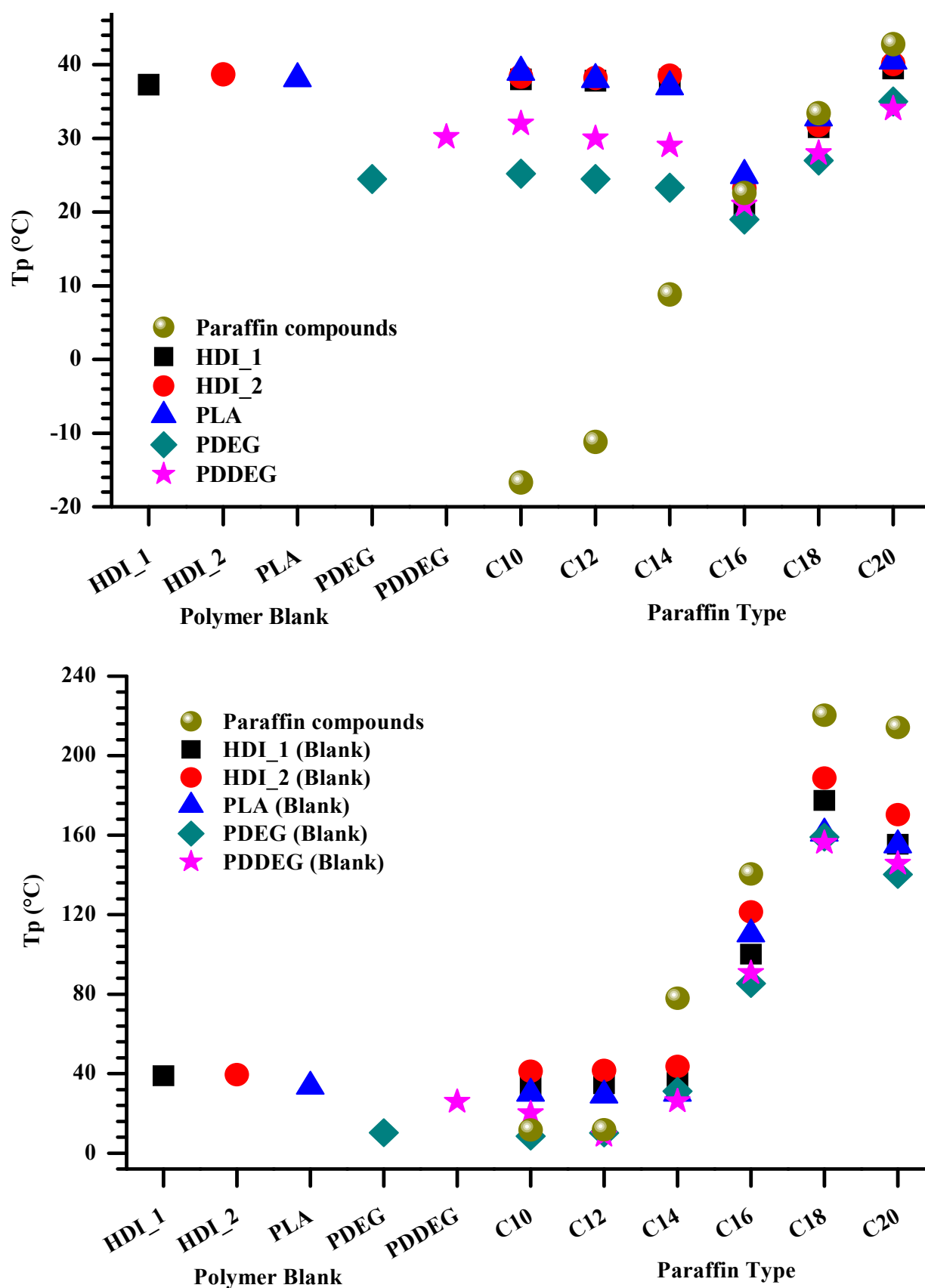


Figure 12: Enthalpy and temperature of second heating for PCM compounds with different paraffin type

Overall, the results in **Table 7** indicate, in line with literature, that the best paraffin in terms of temperature of phase transition and amount of heat stored/released are those with chains of more than 14 carbons, namely n-hexadecane, n-octadecane and n-eicosane⁽¹⁰⁸⁾. Evaluated from the point of view of duration index, the materials with fusion temperature around the target value (body temperature) lead to high DI values, as in **Figure 13**. The duration index indicates that, the best materials (having the largest DI) are HDI_2, HDI_1, PLA, PDEG and PDDEG mixed with n-eicosane (C20), followed by the mixture with n-octadecane (C18) and n-hexadecane (C16), respectively.

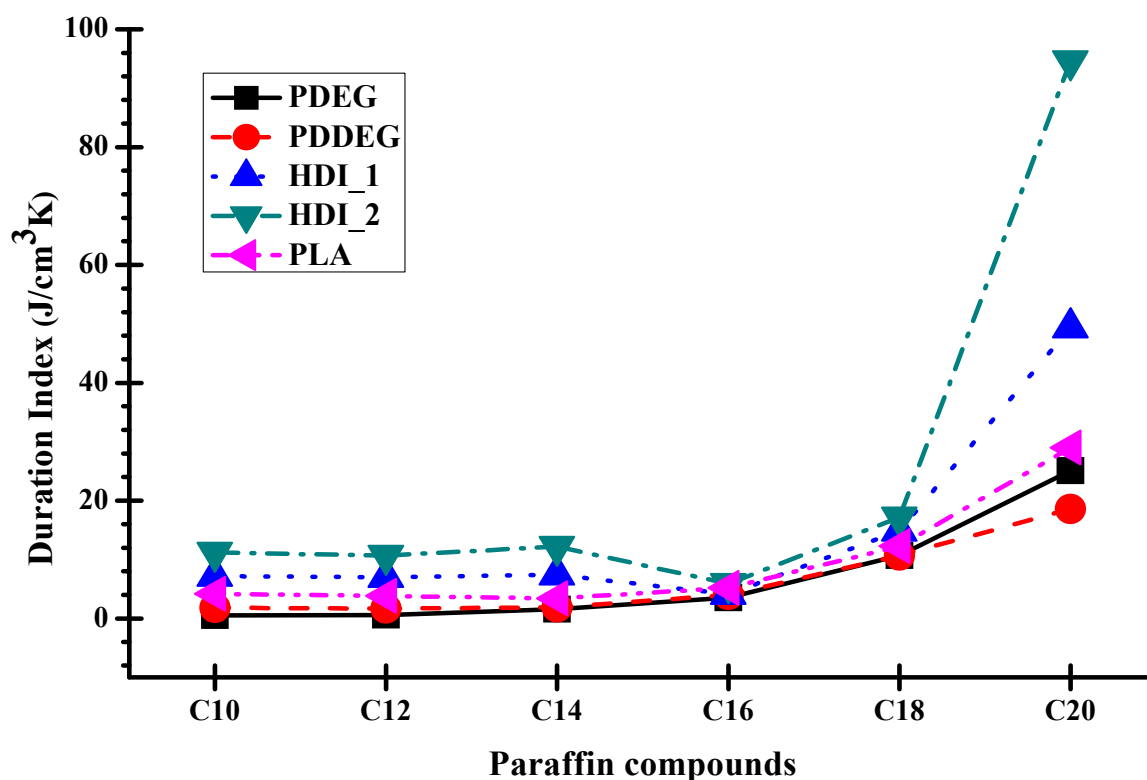


Figure 13: Duration index values for PCM compounds with different paraffin compounds

From all these studies, we conclude that, the optimum parameters for obtaining the PCM composite are to mix the polymer with paraffin in a 1:2 molar ratio, at 100°C for 14 h. Octadecane and HDI derivatives compounds show the best results of all studied paraffin-polymer compounds.

Table 7: Effect of different paraffin type on enthalpy, onset, peak temperature and duration index of second heating for PCM polymer composites

Polymer Compounds	Paraffin Type (No. of Carbon)*	2 nd Heating			DI** (J/cm ³ K)
		T _o (°C)	T _p (°C)	ΔH (J/g)	
PDEG	C ₁₀	23.4	25.2	8.50	0.5
	C ₁₂	22.8	24.5	10.20	0.6
	C ₁₄	21.7	23.3	31.10	1.6
	C ₁₆	17.7	19.0	85.30	3.5
	C ₁₈	25.1	27.0	159.10	10.7
	C ₂₀	32.5	35.0	140.20	25.1
PDDEG	C ₁₀	28.9	32.0	18.10	1.8
	C ₁₂	27.1	30.0	20.80	1.7
	C ₁₄	26.2	29.0	26.10	1.9
	C ₁₆	19.0	21.0	90.70	4.0
	C ₁₈	25.3	28.0	156.20	10.7
	C ₂₀	30.7	34.0	145.70	18.6
HDI_1	C ₁₀	33.2	38.0	34.45	7.2
	C ₁₂	33.0	37.8	34.92	7.0
	C ₁₄	33.2	38.0	35.57	7.4
	C ₁₆	17.5	20.1	100.10	4.1
	C ₁₈	27.5	31.5	189.30	14.9
	C ₂₀	34.5	39.5	155.40	49.4
HDI_2	C ₁₀	34.1	38.4	41.22	11.2
	C ₁₂	33.9	38.2	41.63	10.7
	C ₁₄	34.1	38.5	43.64	12.2
	C ₁₆	20.6	23.2	121.34	5.9
	C ₁₈	28.2	31.8	188.81	17.2
	C ₂₀	35.6	40.1	170.32	94.6
PLA Polylauryl acrylate [C ₁₅ H ₂₈ O ₂] _n	C ₁₀	31.5	39.0	29.10	4.2
	C ₁₂	30.7	38.0	29.80	3.8
	C ₁₄	29.9	37.0	30.00	3.4
	C ₁₆	20.2	25.0	110.20	5.2
	C ₁₈	26.5	32.8	160.90	12.3
	C ₂₀	32.7	40.5	155.00	29.0

* C₁₀: *n*-decane, C₁₂: *n*-dodecane, C₁₄: *n*-tetradecane, C₁₆: *n*-hexadecane, C₁₈: *n*-octadecane, C₂₀: *n*-eicosane

**DI Duration Index: based on ΔT from melt point to body temperature (37°C) and average density of 0.8 g/cm³

Reaction Condition: Molar Ratio: 1:2; Temperature: 100°C; Time 14h

T_o: Onset Temperature,

T_p: Peak Temperature,

ΔH: Enthalpy

2.3.2. Textile Application

The textiles (clothing, interior textiles, and technical textiles) are used as thermal insulators and adding PCM to such textile is expected to improve the insulating performance for suppressing temperature variations ⁽¹¹²⁾. The phase change materials play the role of a buffer in the insulator by storing and releasing heat under the change of environmental temperature ⁽¹¹²⁾. This effect has to be quantified for evaluating the efficiency of a PCM material.

The DSC results of coated cotton and wool fabrics with PCM polymer composites (HDI_1 and HDI_2) are illustrated in **Figure 14** and **Table 8**. It can be concluded that wool and cotton fabric can be coated with PCM polymer composite and the coated wool shows better results than coated cotton fabrics. The measured total resistance to dry heat transfer for treated cotton and wool fabric ranges from 0.11 – 0.13 clo (1 clo = 0.155 m²·°C/W).

Table 8: DSC and DI results of coated fabric with PCM polymer composites

Polymer	Fabric Type	1 st Heating			1 st Cooling			2 nd Heating			DI * (J/cm ³ K)
		T _o (°C)	T _p (°C)	ΔH (J/g)	T _o (°C)	T _p (°C)	ΔH (J/g)	T _o (°C)	T _p (°C)	ΔH (J/g)	
HDI_1	Cotton	24.2	29.5	189.2	17.8	21.3	175.3	24.5	29.5	194.8	12.4
	Wool	27.4	31.8	192.6	19.1	20.7	190.9	27.4	31.9	198.6	16.5
HDI_2	Cotton	25.2	30.4	190.5	18.5	22.7	179.1	25.4	31.1	215.3	14.8
	Wool	28.1	33.2	195.3	20.3	22.1	193.1	28.2	33.3	212.1	19.3

*DI Duration Index: based on ΔT from melt point to body temperature (37°C) and average density of 0.8 g/cm³

Reaction Condition: Time: 14h; Temperature: 100°C; M.R: Polymer: Octadecane (1:2)

T_o: Onset Temperature,

T_p: Peak Temperature,

ΔH: Enthalpy

For checking the stability of the composite, the treated fabric was heated from room temperature till 45°C, a temperature that is higher than the complete melting temperature of the PCM capsules. Then the fabric is put on a filter paper and kept at 45°C in the oven for 15 min. After 24 hours no oil drops are noticeable, which shows that although melting, the PCM material is still held up well by the polymer matrix. We consider that this is due to capillary forces existing between the polymer and the melted paraffin. ⁽¹¹³⁾

Figure 15 and **Figure 16** show the scanning electron microscope images of treated cotton and wool respectively before and after heating. It is clear that the PCM composites are held up well after heating.

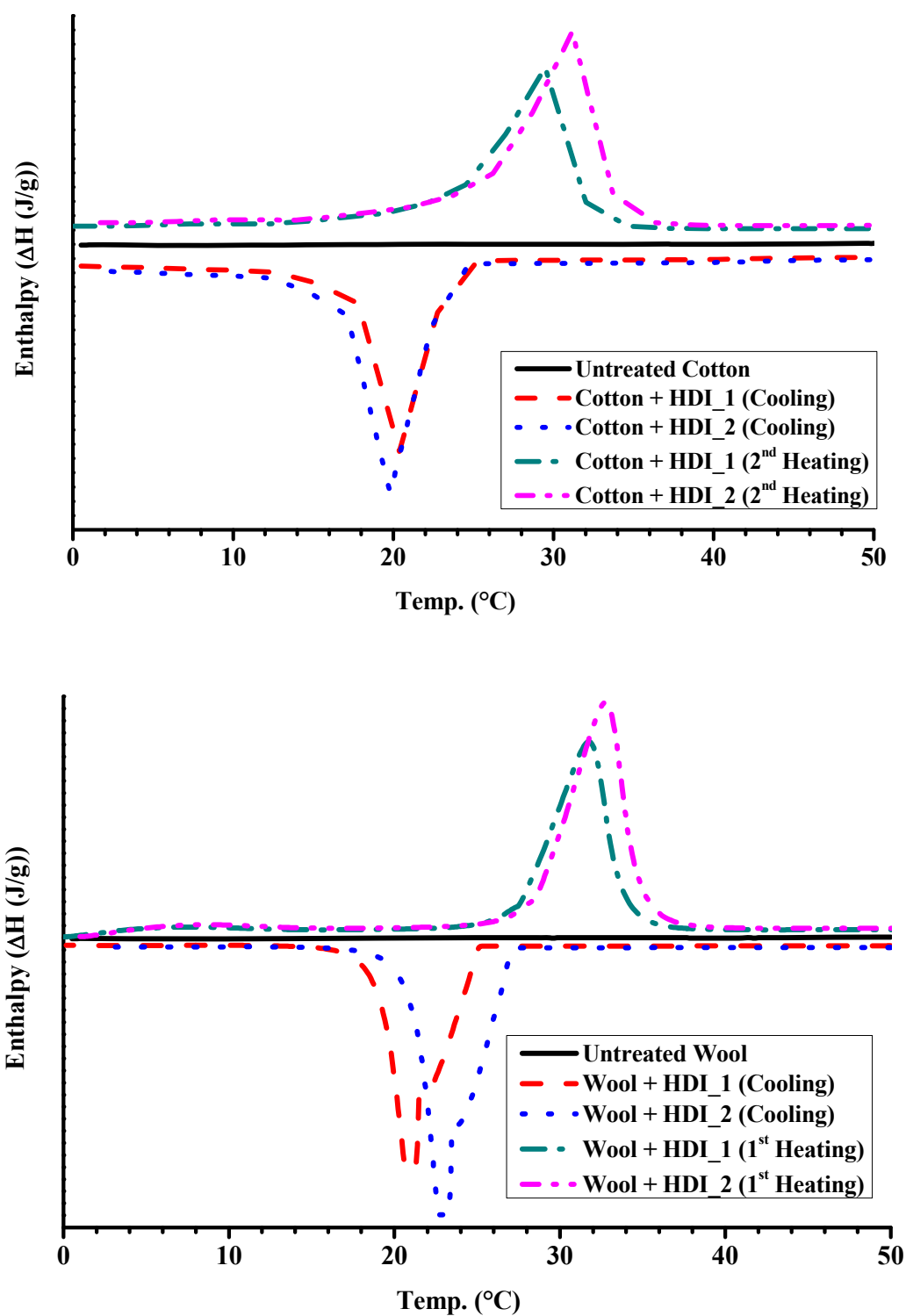


Figure 14: DSC curves of coated cotton and wool fabrics with HDI derivatives (cooling and 2nd heating)

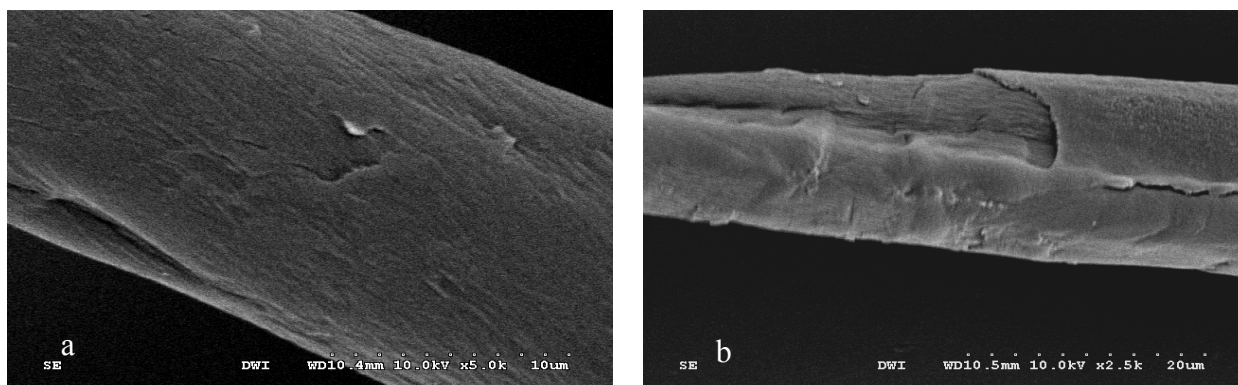


Figure 15: Scanning electron micrograph for coated cotton with HDI_2 derivative

a) after treatment b) after heating at 50°C for 15 min

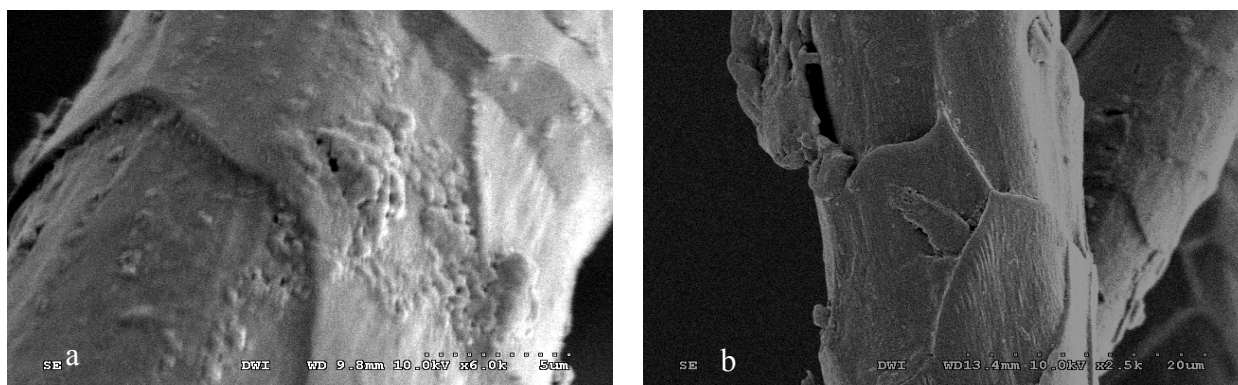


Figure 16: Scanning electron micrograph for coated wool with HDI_2 derivative

a) after treatment b) after heating at 50°C for 15 min

2.4. Conclusions

The preparation method of the PCM materials used in this study allowed us obtaining composites of polymer-PCM paraffin with good heat storage capacity and control of the temperature around the body temperature. The achieved enthalpies of PCM materials were found proportional to those of hydrocarbons in temperature intervals corresponding to the phase transitions of PCMs.

HDI derivatives synthesised during this work can host PCM-paraffin materials better than other polymers. Scanning electron microscope of treated cotton and wool before and after heating provide that, the PCM composites is still held up well by the polymer matrix after heating. We consider that, this is due to capillary forces existing between the polymer and the melted paraffin.

By applying the composites onto textile materials (wool and cotton fabrics), one achieves fabrics coated with PCM-polymer composites exhibiting good temperature control properties. Overall the coated wool fabric has better results than coated cotton fabrics.

3. Organic PCM/Polybehenyl Acrylate Composites for Textile Usage

3.1. Introduction

Poly(behenyl acrylate) is a polymer with long side chains (C_{22}), that we investigated for its ability to host phase change materials in the matrix. The polymerization of behenyl acrylate in bulk or in solution shows gel effect even though the polymerization is carried out above the glass transition temperatures (T_g). Due to the gel effect, considerable deviations from the normal kinetic parameters are observed in high-conversion polymerization. Onset of the gel effect is reported to occur between 20 and 40% conversion, depending on the temperature and the amount of initiator used.^(114, 115) During the radical polymerization, the conversion first increases according to first-order kinetics and then accelerates because of the gel effect, which is characterized by an increase of viscosity resulting from higher conversion and increase in chain length.^(114, 116)

During this part phase change materials (PCM) were developed from PCM/polymer composites and in textile composite systems to so-called "PCM-nonwovens" integrated. These fabrics are combining with textile insulation layers to effective thermal shielding; the optimum structure for both layer sequences and thicknesses may be optimized by calculation.

3.2. Experimental

3.2.1. Materials

1-Dodecanol ($CH_3(CH_2)_{11}OH$, 98.5%, Fluka), 1-hexadecanol ($CH_3(CH_2)_{15}OH$, 95%, Sigma Aldrich), 1-octadecanol ($CH_3(CH_2)_{17}OH$, 96 %, Merk), 1-docosanol ($CH_3(CH_2)_{21}OH$, 97 %, Merk), methyl dodecanoate ($CH_3(CH_2)_{10}COOCH_3$, 98 %, SAFK), methyl hexadecanoate ($CH_3(CH_2)_{14}COOCH_3$, 97%, Aldrich), methyl octadecanoate ($CH_3(CH_2)_{16}COOCH_3$, 96%, Aldrich).

Behenyl acrylate (BA, NK Ester AB-H), 2-hydroxyethyl acrylate (HEA, Aldrich), anisole (Aldrich), alkoxyamine initiator *N-tert*-butyl-*N*-(1'-diethylphosphono-2,2'-dimethylpropyl)-*O*-(2-carboxyl-prop-2-yl) (Blocbuilder[®] initiator, registered trademark of Arkema), free nitroxide *N-tert*-butyl-*N*-(1'-diethylphosphono-2,2'-dimethylpropyl)-nitroxide (SG-1, Arkema), ethanol, chloroform and diethyl ether (Aldrich).

Benzoyl peroxide (BPO, $(C_6H_5C=O)_2O_2$, 75%, Sigma-Aldrich), 1,1'-Azobis(cyclohexanecarbonitrile) (AICN, 98%, Aldrich), 2,2'- Azobis(2-methylpropionitrile) (AIPN, $\geq 98\%$, Fluka)

3.2.2. *Methods*

3.2.2.1. **Preparation of PCM/Polymer Composite based on Poly Behenyl Acrylate**

Poly(behenyl acrylate) is a polymer with long side chain (C_{22}) that we investigated for its ability to host phase change materials in the matrix. As PCMs we tested several alcohols and methyl esters, namely: 1-dodecanol ($CH_3(CH_2)_{11}OH$), 1-hexadecanol ($CH_3(CH_2)_{15}OH$), 1-octadecanol ($CH_3(CH_2)_{17}OH$) and 1-docosanol ($CH_3(CH_2)_{21}OH$), methyl dodecanoate ($CH_3(CH_2)_{10}COOCH_3$), methyl hexadecanoate ($CH_3(CH_2)_{14}COOCH_3$) and methyl octadecanoate ($CH_3(CH_2)_{16}COOCH_3$).

Two different methods are used to prepare the PCM/polymer composites, namely i) solid solvent polymerization of behenyl acrylate followed by mixing with paraffin alcohol or ester compound, ii) in-situ solid–solid polymerization of behenyl acrylate in presence of PCM.

3.2.2.1.1. *Solid – solvent polymerization*

a) Homo-polymerizations of behenyl acrylate

Behenyl acrylate (2 g, 5.2×10^{-3} mol) was weighed in a schlenk flask and dissolved in anisole (2 ml). Blocbuilder[®] initiator (20 mg, 5.2×10^{-5} mol) and SG-1 (1.5 mg, 5.2×10^{-6}) were added to the mixture and was bubbled with nitrogen for at least 30 minutes to deoxygenate the solution. The polymerization mixture was immersed in an oil bath at 110°C. Samples were withdrawn at time 0 and after 24 hours and analysed by 1H NMR spectroscopy. After 24 hours polymerization time, the reaction mixture was precipitated in ethanol (600 ml) without cooling followed by filtration over a porosity 3 filter. A second precipitation was required to remove all residual monomers. Therefore, the polymers were re-dissolved in chloroform (5–10 ml) and precipitated in ethanol (600 ml) followed by filtration and drying over night at vacuum (10^{-2} mbar) yielding the homopolymer BA in 27% ($X_p = 35\%$, $M_{n,th} = 13600$ g/mol, $M_{n,NMR} = 20000$ g/mol) (**PBA_I**). All homopolymerized compounds were performed following the same procedure and are listed in **Table 9**.

Table 9: Homopolymerization of BA: starting materials and results.¹⁾

No	BA g (mmol)	PBA (g)	X _p ²⁾ (%)	M _{n,th} ³⁾ (g/mol)	M _{n,NMR} ⁴⁾ (g/mol)
PBA_I	2 (5.2)	1.25	35	13600	20000
PBA_II	2 (5.2)	1.6	n.d.	n.d.	28400
PBA_III	5 (13.1)	3	69	26700	29700

¹⁾ Nitroxide mediated polymerization was performed in Anisole (50wt%), with SG-1 0.1 mol% in respect with the monomer and a monomer-to-initiator ratio of 100 : 1 mol.

²⁾ Monomer conversion determined by ¹H NMR spectroscopy.

³⁾ Theoretical number average molecular weight (M_{n,th}) calculated from the monomer conversion.

⁴⁾ Number average molecular weight determined by ¹H NMR spectroscopy.

b) Co-polymerizations of behenyl acrylate with 2-hydroxyethyl acrylate

Behenyl acrylate (5 g, 13.1×10^{-3} mol) was weighed in a schlenk flask and dissolved in anisole (5.5 ml). 2-hydroxyethyl acrylate (HEA, 0.5 g, 4.4×10^{-3} mol), Blocbuilder[®] initiator (BB, 20 mg, 5.2×10^{-5} mol) and SG-1 (1.5 mg, 5.2×10^{-6}) were added to the mixture and was bubbled with nitrogen for at least 30 minutes to deoxygenate the solution. The polymerization mixture was immersed in an oil bath at 110°C. Samples were withdrawn at time 0 and after 24 hours and analysed by ¹H NMR spectroscopy. After 24 hours polymerization time, the reaction mixture was precipitated in ethanol/diethyl ether (3/1 v/v) without cooling followed by filtration over a porosity 3 filter. A second precipitation was required to remove all residual monomers. Therefore, the polymers were re-dissolved in chloroform (5 – 10 ml) and precipitated in ethanol/diethyl ether (3/1 v/v) followed by filtration and drying over night at vacuum (10^{-2} mbar) yielding the copolymer P(BA₇₇-co-HEA₂₃) in 42% (X_{p,BA} = 49%, X_{p,HEA} = 68%, M_{n,th} = 26900 g/mol, M_{n,NMR} = 23000 g/mol, M_{n,SEC} = 16100 g/mol, PDI = 1.13) (PBA/HEA_I). All copolymerized compounds were performed following the same procedure and are listed in **Table 10**.

Table 10: Copolymerization of BA with HEA: starting materials and results.¹⁾

No	BA g (mmol)	HEA g (mmol)	P(BH) g	X _{p,BA} ²⁾ (%)	X _{p,HEA} ²⁾ (%)	M _{n,th} ³⁾ (g/mol)	M _{n,SEC} ⁴⁾ (g/mol)	PDI, SEC ⁴⁾
PBA/HEA_I	5 (13.1)	0.50 (4.4)	2.31	49	68	26900	16100	1.13
PBA/HEA_II	5 (13.1)	1.52 (13.1)	3.17	38	73	23300	24000	1.25
PBA/HEA_III	5 (13.1)	4.57 (39.4)	4.58	53	95	31600	17600	1.34

¹⁾ Nitroxide mediated polymerization was performed in Anisole (50wt%), with SG-1 0.1 mol% in respect with the monomer and a monomer-to-initiator ratio of 100 : 1 mol.

²⁾ Monomer conversion determined by ¹H NMR spectroscopy.

³⁾ Theoretical number average molecular weight (M_{n,th}) calculated from the monomer conversion.

⁴⁾ Number average molecular weight and polydispersity index determined by SEC-THF chromatography.

3.2.2.1.2. *In-situ Solid–Solid polymerization of behenyl acrylate in presence of PCM compounds*

Behenyl acrylate was mixed with different PCM compounds with different ratio 2:1 1:1, 1:2 and 1:4 molar fractions; BA: PCM respectively, at 100°C during 14 h. In addition, the effect of different initiator on preparation of PCM/polymer composites was studied by reaction between behenyl acrylate and the paraffin alcohol or ester compounds in presence of AICN or AIPN or BPO as initiator, (1.25 % of the total weight) at 100°C for 14 h and hold at 60°C for 6h.

3.2.3. *Measurements*

3.2.3.1. Differential Scanning Calorimetry (DSC)

Differential scanning calorimetry was carried out in a Perkin Elmer DSC differential scanning calorimeter under nitrogen flow (20 mLmin⁻¹). Samples (5–15 mg weighed to 1 mg precision) was heated from 0 to 70°C at a heating rate of 10°C min⁻¹ and kept at high temperature for 2 minutes to erase any thermal history. Subsequently, they are cooled with 10°C min⁻¹ until 0°C. After 2 minutes at the low temperature, a second heating run with the same heating rate of 10°C min⁻¹ performed. Melting temperature and enthalpy were evaluated from the fusion peaks.

3.2.3.2. NMR Measurements

¹H liquid NMR spectra were recorded on a Bruker DPX-400 FT-NMR spectrometer at 400 MHz, using CDCl₃ as solvent.

3.2.3.3. Size Exclusion Chromatography Analysis (SEC)

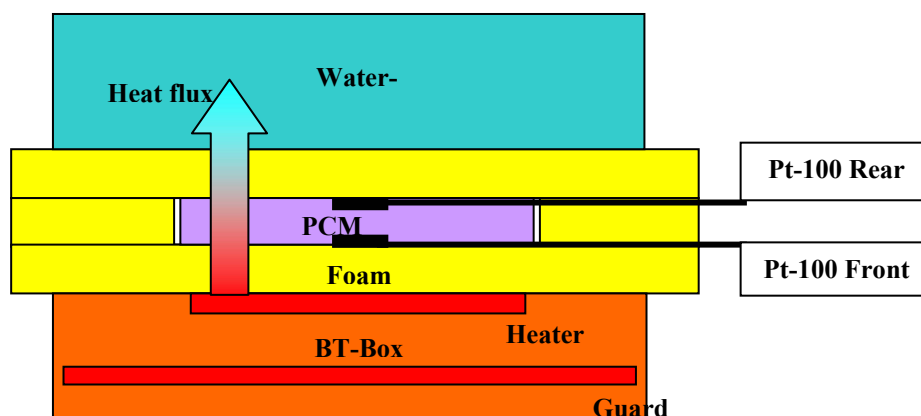
Size exclusion chromatography analyses (SEC) were carried out using THF (with addition of 250 mg/L 2,6-di-tert-butyl-4-methylphenol) as eluting solvent. A high pressure liquid chromatography pump (ERC HPLC-Pumpe Model 6420) and a refractive index detector (WGE Dr. Bures, Model ETA 2020) with a flow rate of 1.0 mL/min were used. A pre-column with the length of 50 mm, the diameter 8 mm and the nominal pore widths of 50 Å and four columns with MZ SD plus gel were applied. The length of each column was 300 mm, the diameter 8 mm and the nominal pore widths were of 50, 10², 10³ and 10⁴ Å. Calibration was achieved using poly(methyl methacrylate) (PMMA) standards.

3.2.3.4. Scanning Electron Microscope (SEM)

Scanning Electron Microscopy HITASHI S-3000 microscope S, at 15-kV acceleration voltage, after gold coating was use to study the surface morphology and the cross section of the composite films.

3.2.3.5. PCM Heat Transfer Measure

The device for measuring the heat transfer through the phase change material while heating has been home done. It uses two Pt-100 resistive thermometers for measuring the temperatures on the two faces (front and rear) of the PCM layer while applying a constant heat gradient from the heat box (front) towards water box (rear). The layer of PCM has 5 mm thickness, and the assembly is insulated with styropor foam. Schematically sketch of the device is shown in **Scheme 5**, and the device is illustrated in **Figure 17**.



Scheme 5: General scheme of the heat transfer measurement of a PCM

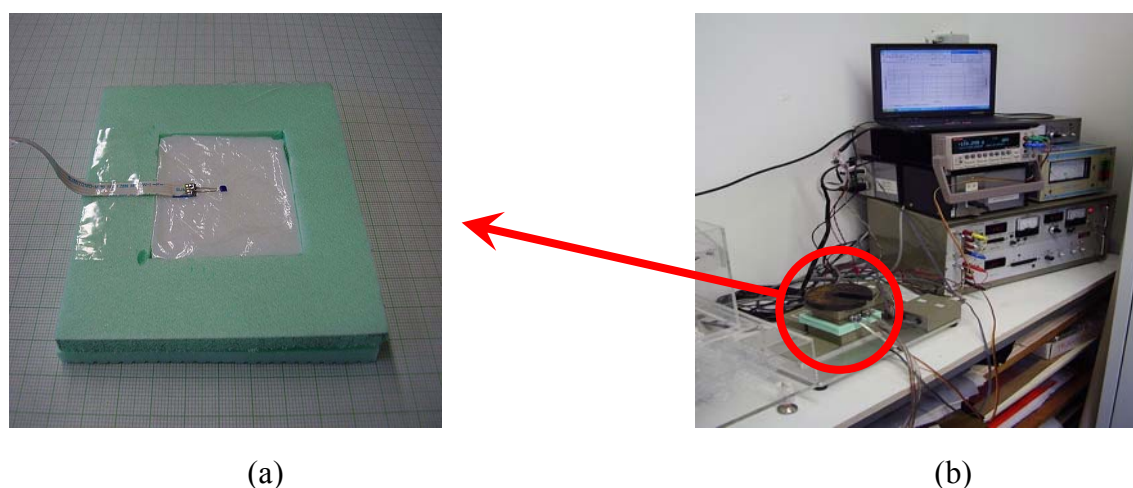


Figure 17: The experimental setup: a) thermometer applied on the face of the phase change material and b) the device with the side instruments for control of heat flow and recording temperature

3.3. Result and Discussion

3.3.1. Characterization of the Poly(behenyl acrylate)

By comparing the ^1H NMR spectra for behenyl acrylate with its polymer as illustrated in **Figure 18**, we found that, the integration peaks of H from double bond (6.05, 5.59 and 6.27) decrease after polymerization. Comparing the ^{13}C NMR spectra for behenyl acrylate and its polymer in **Figure 19**, one observe that the peaks of C from double bond (128.2 and 131.3) disappeared after polymerization. These data are compatible with IR data.

IR spectra for poly(behenyl acrylate) in **Figure 20** show that the intensity of C=C at (1635) is much lower than in behenyl acrylate.

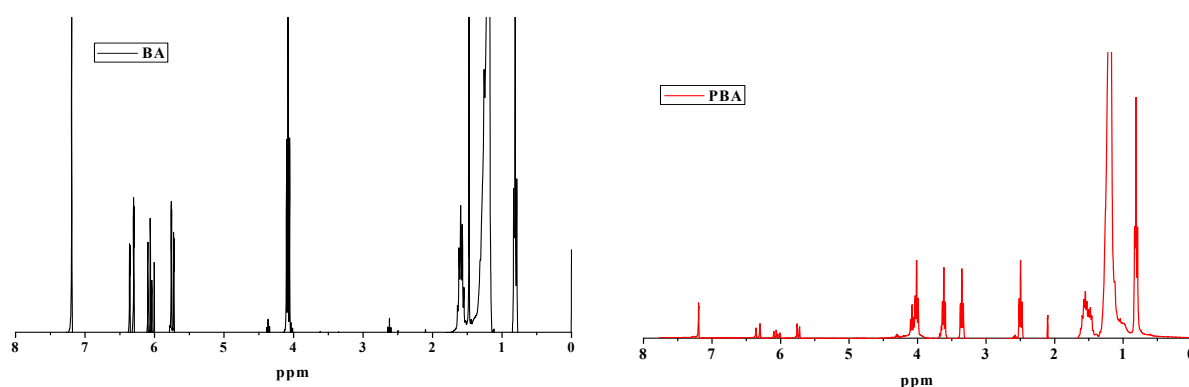


Figure 18: ^1H NMR spectra of behenyl acrylate and its polymer

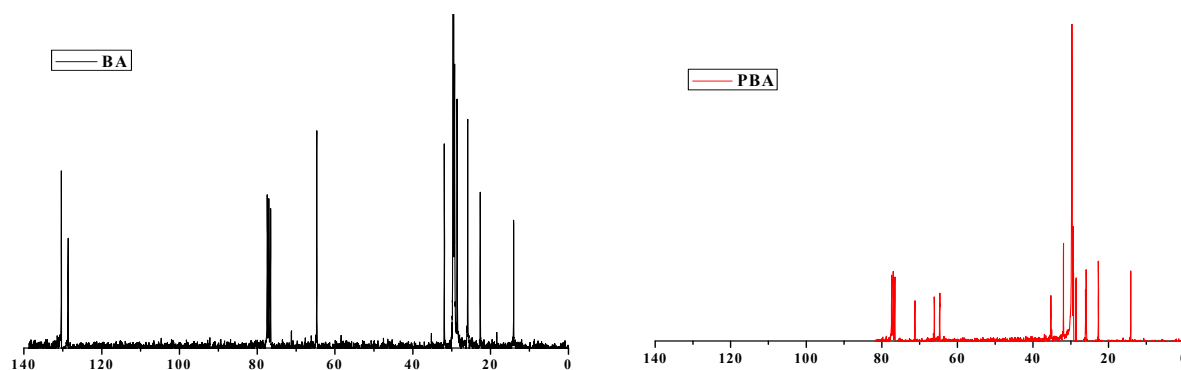


Figure 19: ^{13}C NMR spectra of behenyl acrylate and its polymer

3.3.2. Characterization of the PCM/polymer composite

The composites were measured on DSC, with a temperature programme of $10^\circ\text{C}/\text{min}$. We used a cycle of heat-cool-heat between 0°C and 80°C and measured the temperature (onset temperature) and heat of the phase transition from the second heating curve.

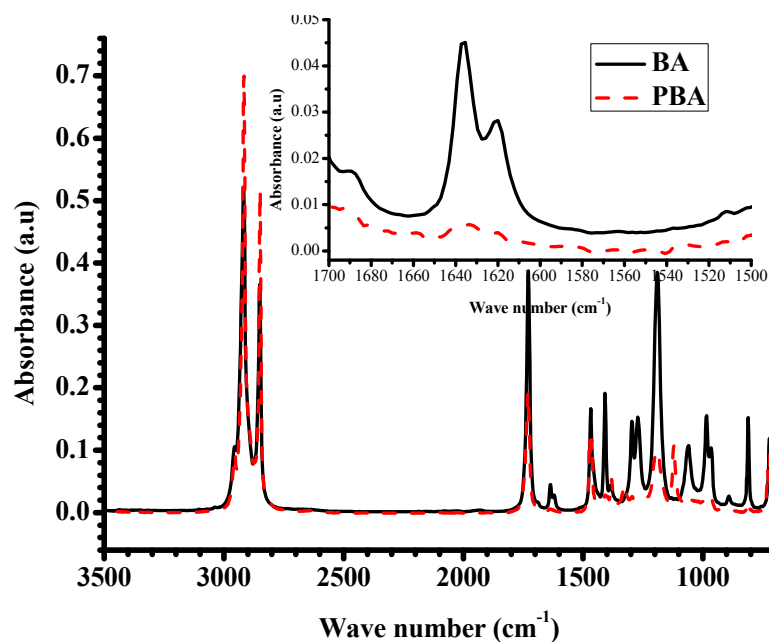


Figure 20: IR spectra of behenyl acrylate and its polymer

IR, Raman and NMR analysis were used to provide the absence of double bond in the acrylate monomer, DSC analysis was used to determine the melting point and enthalpy, heat flow was measured.

IR and Raman spectra for PBA/C₁₈H₃₇OH and PBA/C₁₇H₃₅COOCH₃ are illustrated in **Figure 21** and **Figure 22** respectively, and show that the intensity of C=C peak for behenyl acrylate (1630 – 1640; IR and 1603; Raman) for PBA/C₁₇H₃₅COOCH₃ is lower than PBA/C₁₈H₃₇OH and both of them are much lower than behenyl acrylate itself.

¹H and ¹³C NMR theoretical and experimental spectra were presented in **Figure 23** – **Figure 26**. One can observe that, in ¹H NMR spectra, the bands for the hydrogen of the double bond of behenyl acrylate at 6.05, 6.27 and 5.59 ppm are disappeared in both PCM/polymer composites which indicates the opening of the double bond during the polymerization process of behenyl acrylate. In addition, ¹³C NMR analysis provides similar result like ¹H NMR.

DSC spectra of PBA/C₁₇H₃₅COOCH₃ and PBA/C₁₈H₃₇OH given in **Figure 27** show the behaviour of these composites during second heating. It shows that, PBA/C₁₈H₃₇OH has only one peak at 51.7°C which is near to the peak of PBA itself, and PBA/C₁₇H₃₅COOCH₃ has two peaks at 33.7 and 55.3°C which are assigned to the encapsulated PCM material and PBA itself respectively. The enthalpy of the PBA/ C₁₈H₃₇OH composite is higher than PBA/C₁₇H₃₅COOCH₃ composite. All the melting point and enthalpies data for heating – cooling – heating system are listed in **Table 11**.

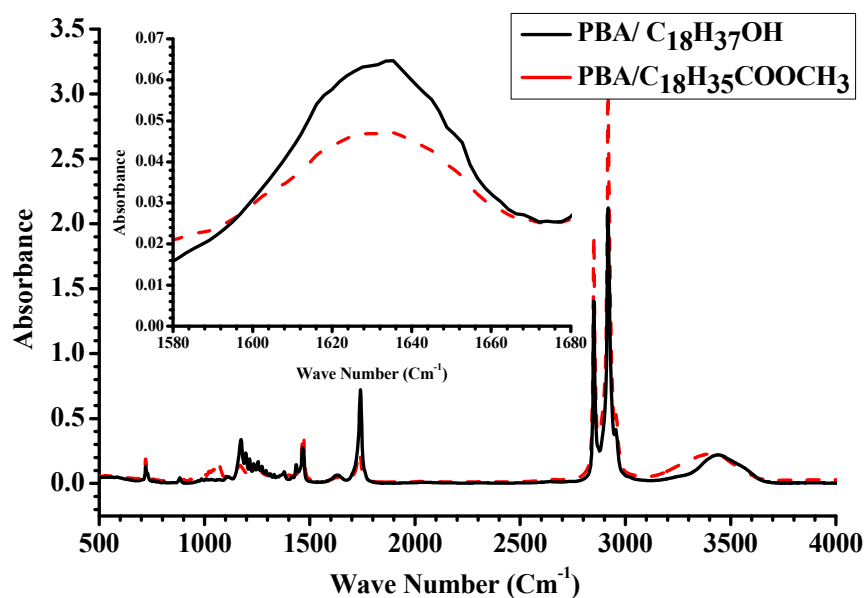


Figure 21: IR spectra of PBA/C₁₇H₃₅COOCH₃ and PBA/C₁₈H₃₇OH composites

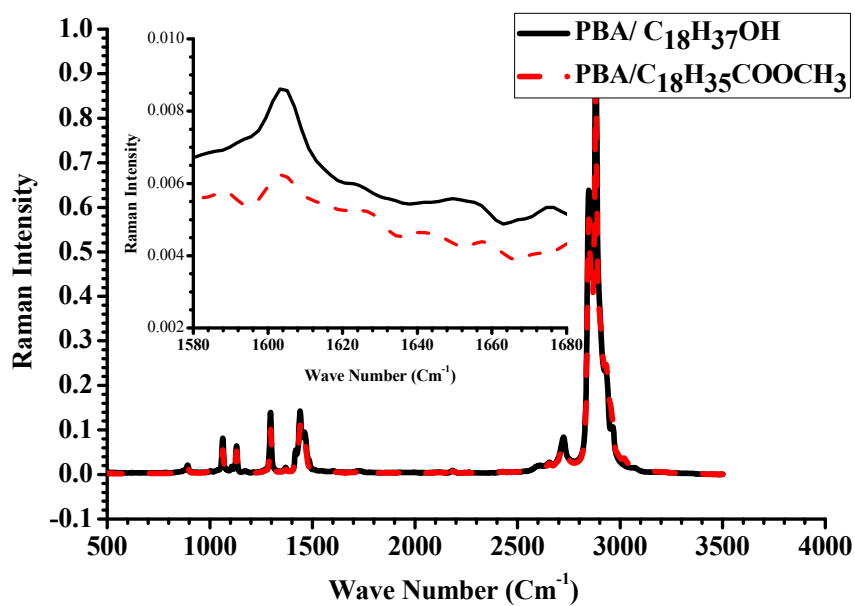
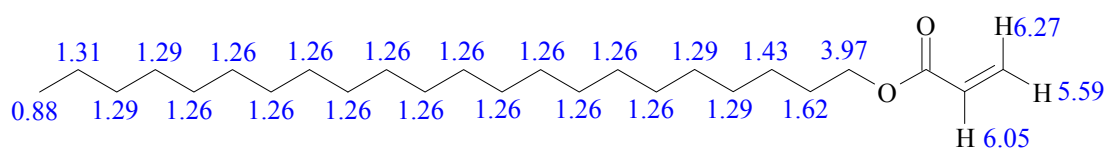
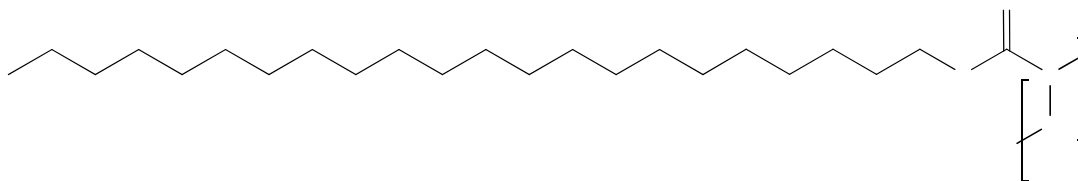


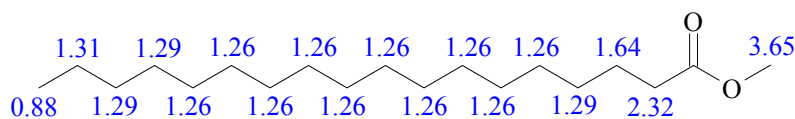
Figure 22: Raman spectra of PBA/C₁₇H₃₅COOCH₃ and PBA/C₁₈H₃₇OH composites



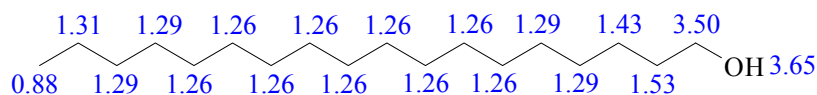
Behenyl acrylate



Poly(behenyl acrylate)



Methyl octadecanoate



n-Octadecanol

Figure 23: ^1H NMR theoretical shifts for behenyl acrylate, poly(behenyl acrylate), methyl octadecanoate and n-Octadecanol

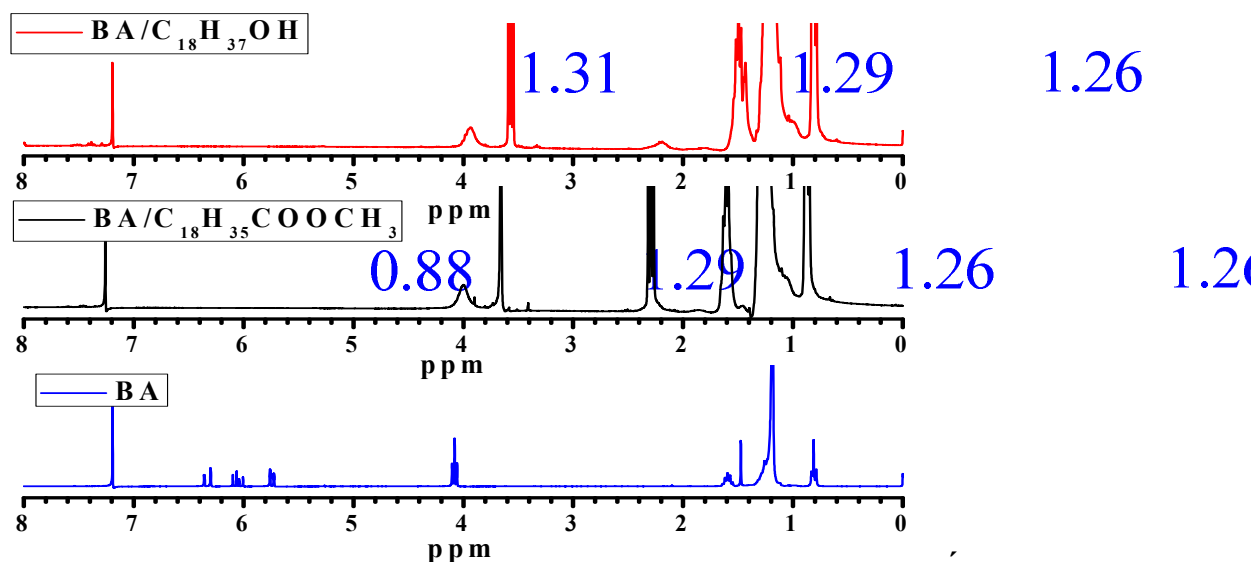
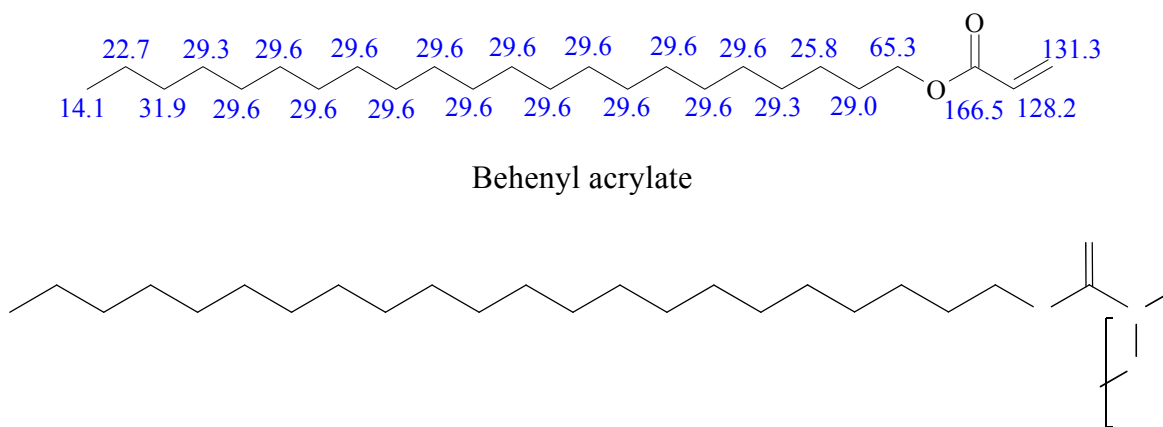
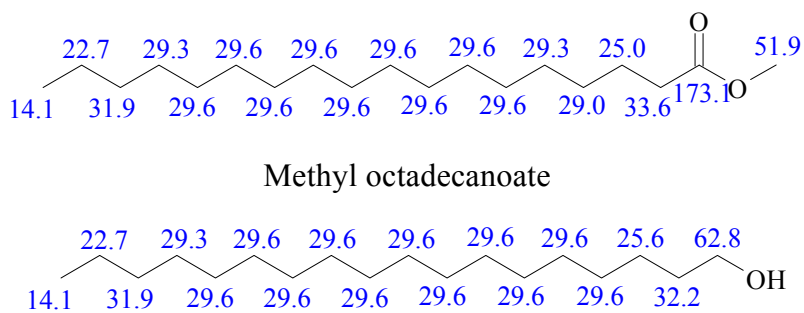


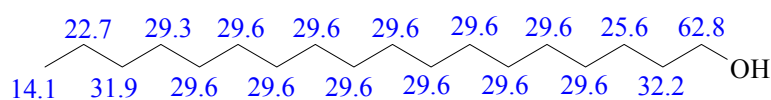
Figure 24: ^1H NMR experimental shifts for PBA/ $\text{C}_{17}\text{H}_{35}\text{COOCH}_3$ and PBA/ $\text{C}_{18}\text{H}_{37}\text{OH}$ composites



Poly(behenyl acrylate)



Methyl octadecanoate



n-Octadecanol

Figure 25: ^{13}C NMR theoretical shifts for behenyl acrylate, poly(behenyl acrylate), methyl octadecanoate and n-Octadecanol

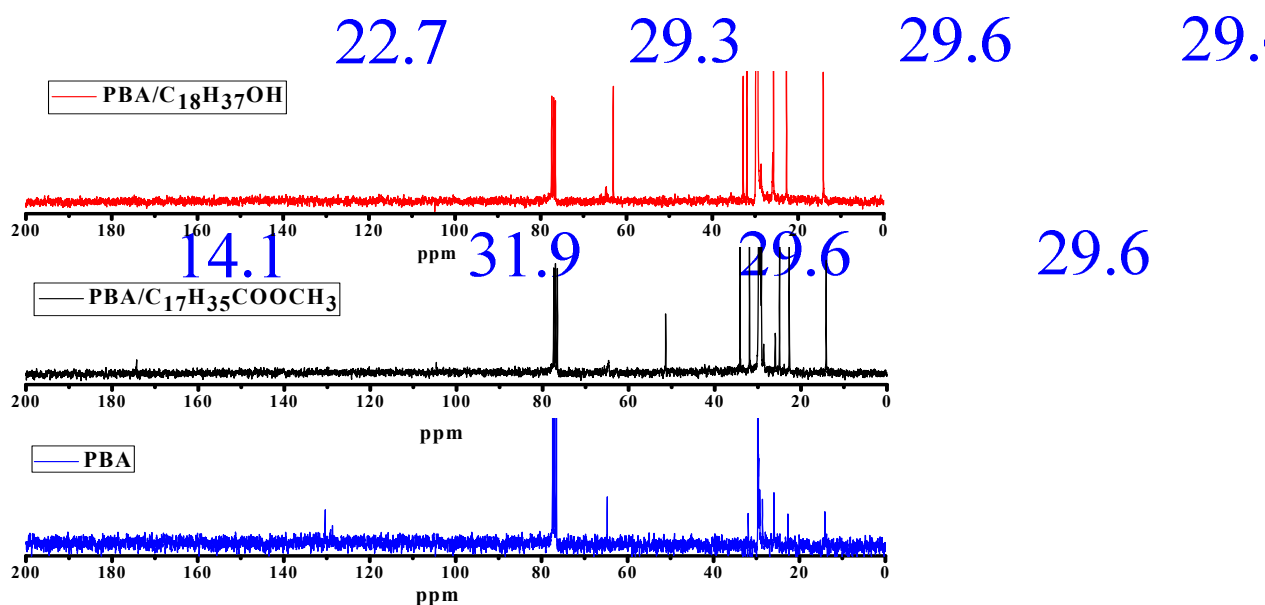


Figure 26: ^{13}C NMR experimental shifts for PBA/ $\text{C}_{17}\text{H}_{35}\text{COOCH}_3$ and PBA/ $\text{C}_{18}\text{H}_{37}\text{OH}$ composites

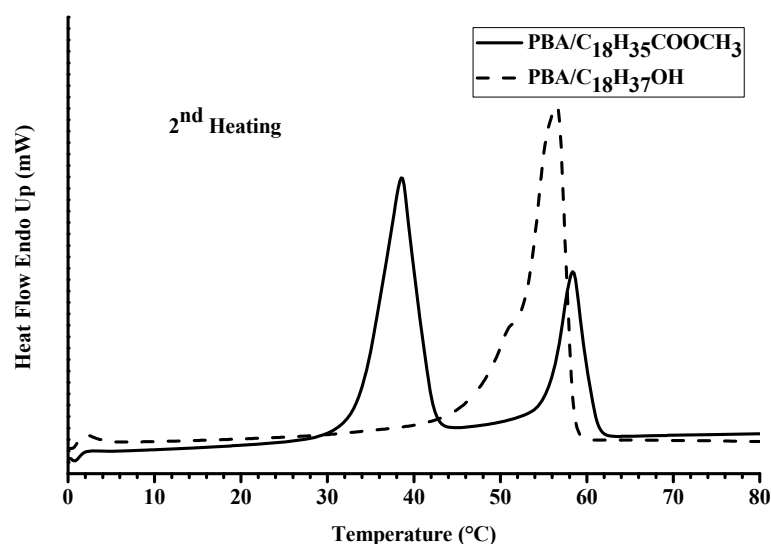


Figure 27: DSC spectra for PBA/C₁₇H₃₅COOCH₃ and PBA/C₁₈H₃₇OH composites

Table 11: DSC data for PBA/C₁₇H₃₅COOCH₃ and PBA/C₁₈H₃₇OH composites

PCM/Polymer Composite	1 st Heating		1 st Cooling		2 nd Heating	
	T _p (°C)	ΔH (J/g)	T _p (°C)	ΔH (J/g)	T _p (°C)	ΔH (J/g)
PBA/C ₁₇ H ₃₅ COOCH ₃	35.2	102.0	30.8	-84.7	33.7	94.3
	60.3	48.5	50.0	-45.7	55.3	44.0
PBA/C ₁₈ H ₃₇ OH	53.4	178.0	47.0	-145.8	51.7	150.8

T_p: peak temperature

ΔH: enthalpy

As shown in **Figure 28** the PCM material is retained inside the PBA polymer matrix, which meaning that the PBA can be used as a PCM carrier to keep the PCM material well through the polymer matrix disregarding the PCM melting. That is because the melting point of the PBA is higher than the melting point of the PCM material itself. Therefore, one can say the PCM material is retained inside the PBA matrix between the branched alkyl chains (behenyl) which help the PCM material to hold well without any leaking.

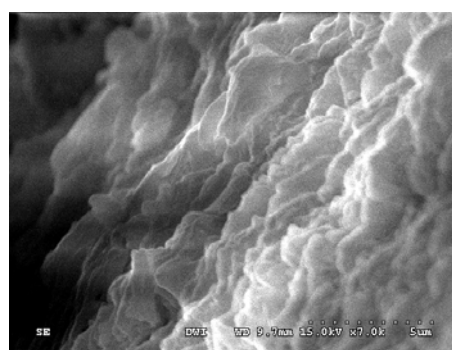
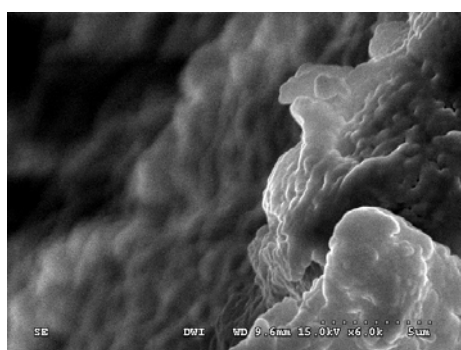


Figure 28: SEM micrograph for organic PCM material retained in PBA matrix

3.3.2.1. Comparison between PCM/polymer composites based on homo-polymer and co-polymer of BA

Poly(behenyl acrylate) homo-polymer (PBA_I) and co polymer with 2-hydroxyethyl acrylate (PBA/HEA_I) were mixed with methyl octadecanoate $C_{17}H_{35}COOCH_3$ in order to infiltrate it between the branched chain of the polymer matrix. The mixing of these compounds occurred at 100°C for 24 h. The melting temperature and enthalpies of resulted composites were measured using DSC and the data for onset temperature, peak temperature and enthalpies for the polymers and their composites as well as the duration index (DI) are given in **Table 12**. The specific heat values (C_p) of these polymers and its composites are illustrated in **Figure 29**.

Table 12: DSC data for PBA_I and PBA/HEA_I and their composites with $C_{17}H_{35}COOCH_3$

Materials	1 st Heating			Cooling			2 nd Heating			Duration index J/(cm ³ K)
	T _o (°C)	T _p (°C)	ΔH (J/g)	T _o (°C)	T _p (°C)	ΔH (J/g)	T _o (°C)	T _p (°C)	ΔH (J/g)	
PBA_I	67.4	72	108.1	63.3	61.3	-96.4	67.1	71.8	58.2	----
PBA_I + $C_{17}H_{35}COOCH_3$	34.9	40.2	64.3	53.3	51.3	-68.4	34.3	38.5	56.1	29.92
PBA/HEA_I	71.1	75.3	82.2	64.8	61	-93.6	70.4	75.3	74.2	----
PBA/HEA_I + $C_{17}H_{35}COOCH_3$	34.9	42.2	99.8	52.6	49	-114.6	35.5	39.9	78.8	21.74

Duration index DI, based on ΔT from melt point to body temperature (37°C) and average density of 0.8 g/cm^3

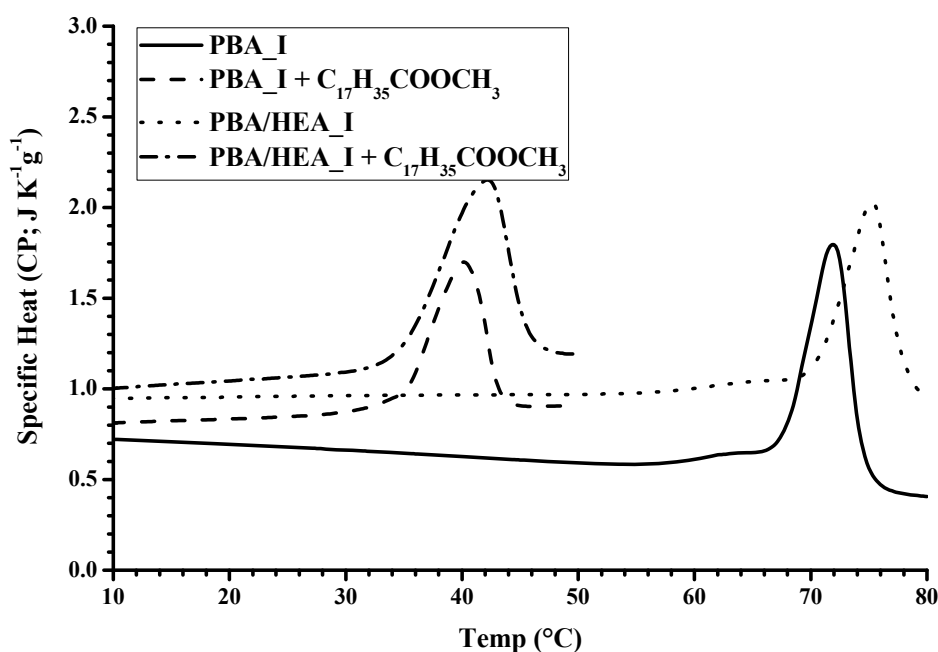


Figure 29: Specific heat for PBA_I and PBA/HEA_I and their composites with $C_{17}H_{35}COOCH_3$

3.3.2.2. Study the effect of the poly(behenyl acrylate) concentration on different PCM/polymer composites

Figure 30 shows the enthalpy measured for the various PCM/polymer composites. They also show that the formation of the PCM/polymer composite does not modify the phase transition process of the PCM, indicating that poly(behenyl acrylate) plays the role of a hosting matrix. As it appears from **Figure 31**, the temperature values of phase change process are not significantly affected by the formation of the polymer composite.

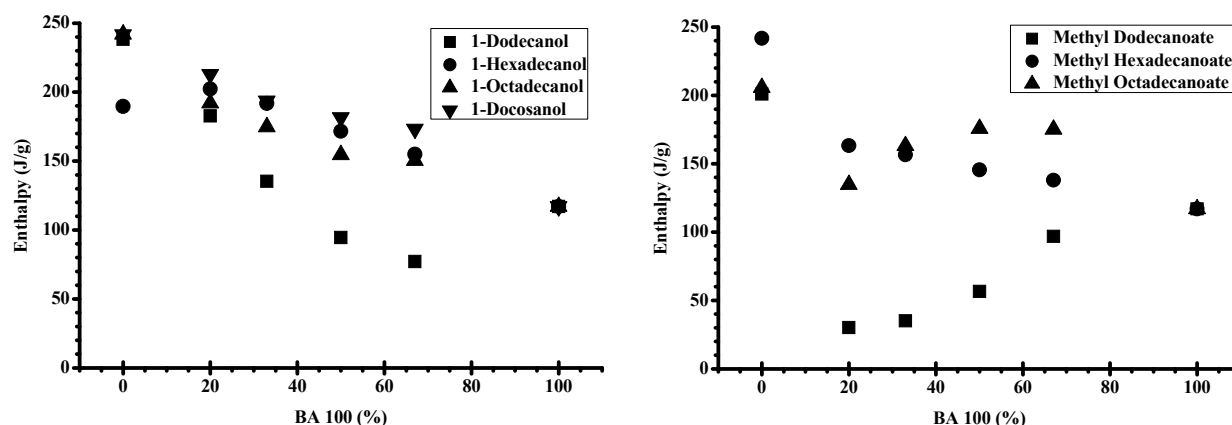


Figure 30: Enthalpy values of phase change process for the PCM/polymer composites

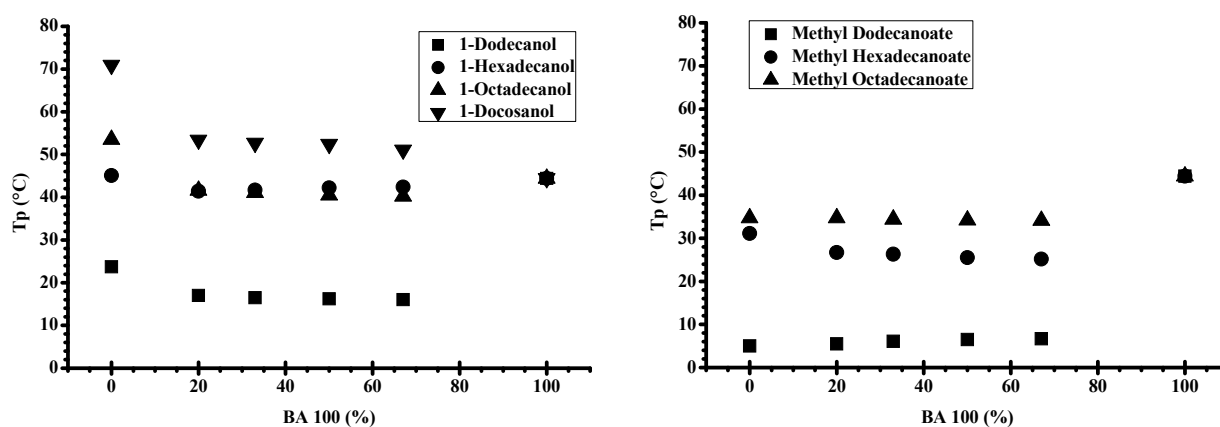


Figure 31: Temperature values of phase change process for the PCM/polymer composites

3.3.2.3. Effect of heat on the behaviour of PCM/polymer composite

At heating and cooling the PCM changes its phase from solid to liquid and back. When PCM becomes liquid the polymer is expected to be kept in the matrix by capillary forces. **Figure 32** gives three snapshots from an investigation on a heating stage of the composite of methyl octadecanoate/poly(behenyl acrylate). The three temperatures are before, during and after the phase transition of methyl octadecanoate. The snapshots are similar at heating and at cooling, showing the reversibility of the phenomenon.

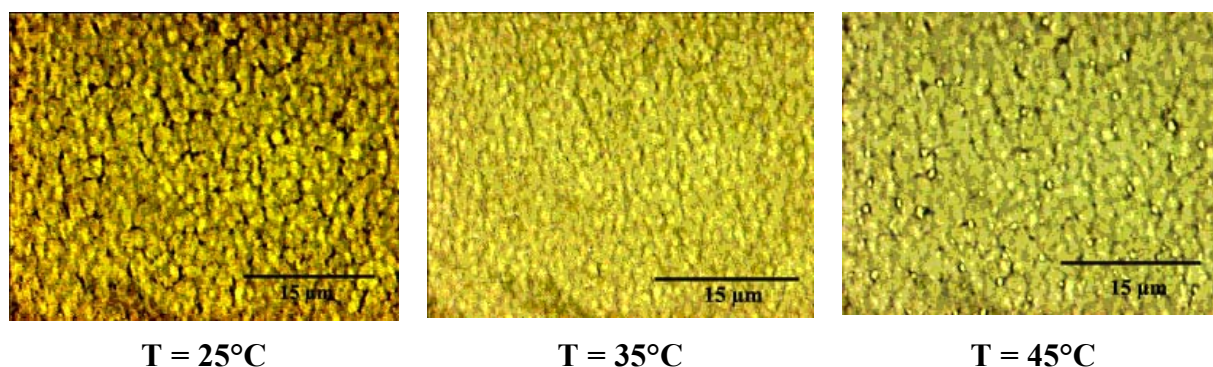


Figure 32: Behaviour of PBA/C₁₇H₃₅COOCH₃ composite during heating with 10°C/min

3.3.2.4. Stability of PCM-polymer composite at storing

The PCM – polymer composites were investigated for their stability at storing by evaluating if one observes physical separation of mixtures in molar ratio 1:2 of monomer to PCM stored at room temperature up to 30 days. Visual inspection (**Figure 32**) and DSC investigations of the temperature and enthalpy of melting after various storing intervals (see **Figure 33** and **Figure 34**) showed that poly(behenyl acrylate) forms homogeneous and stable mixtures with both n-octadecanol and with methyl octadecanoate.

For checking the stability of the composite, we have put a couple of milligrams on a filter paper and kept at 45°C in the oven. After 24 hours no oil drops were observed which shows that although melting, the PCM material is still held up well by the polymer matrix.

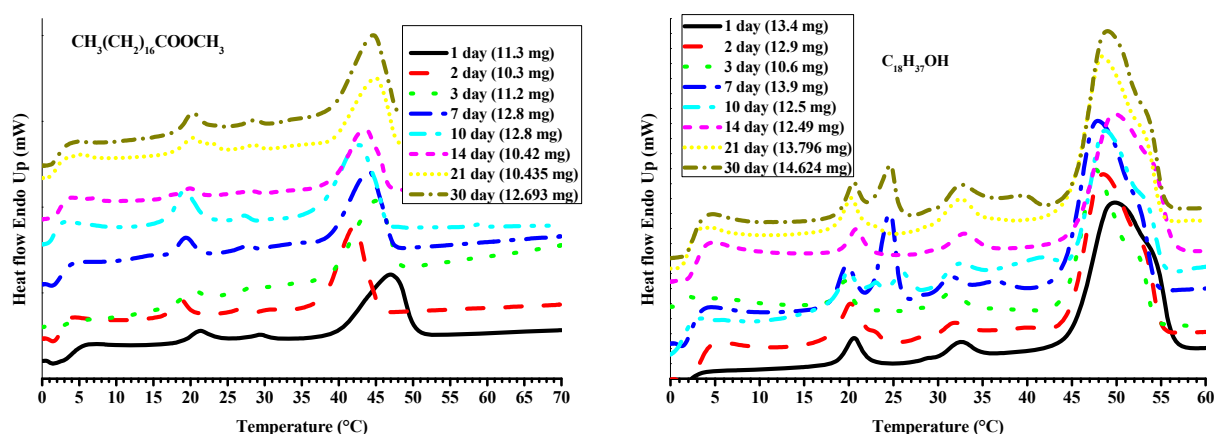


Figure 33: DSC graphs of PCM/polymer composites stored at room temperature for PBA/C₁₇H₃₅COOCH₃ and PBA/C₁₈H₃₇OH composites

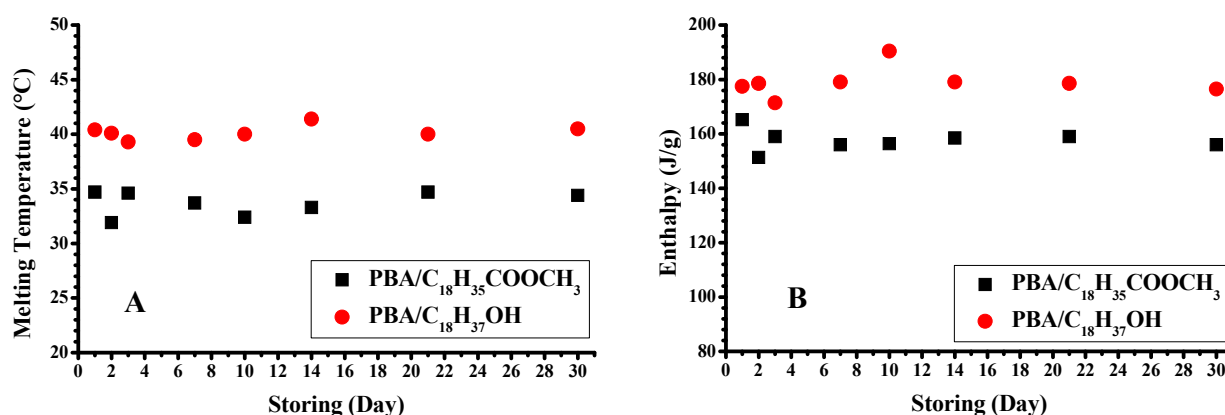


Figure 34: Storing stability at room temperature of PBA/C₁₇H₃₅COOCH₃ and PBA/C₁₈H₃₇OH composites in terms of temperature and enthalpy of melting

3.3.3. Applying the PCM/polymer composite on clothing insulation materials

The textiles (clothing, interior textiles, and technical textiles) are used as thermal insulators and adding PCM to such textile is considered to improve the insulating performance for suppressing temperature variations. The phase change materials play the role of a buffer in the insulator by storing and releasing heat under the change of environmental temperature. This effect has to be quantified for evaluating the efficiency of a PCM material.

The literature mention the computerized thermal manikin used to simulate the heat loss from a human being to a cooler environment and to measure the insulation value of the clothing systems ^(46, 47).

The manikin provides the total resistance to dry heat transfer, measure the insulation value of the clothing systems and is defined by ($R = \frac{\Delta T \times A}{H}$, **Equation 8**), provided by a material of area (A), having the temperature difference of the two sides of the material, $\Delta T = T_F - T_R$ (F , face, and R , rear, of the material) and through which passes a known heat flow, (H). The value for textiles is given in “clo” ($\text{m}^2 \cdot ^\circ\text{C}/\text{W}$), $1 \text{ clo} = 0.155 \text{ m}^2 \cdot ^\circ\text{C}/\text{W}$, which is the unit for clothing insulation adopted from studies of hygienic comfort ^(46, 47).

The design of insulation materials containing PCM makes use of a 3-layer sandwich model composed of (hot side) – insulator – PCM – insulator – (cold side), as schematically shown in **Figure 35**.

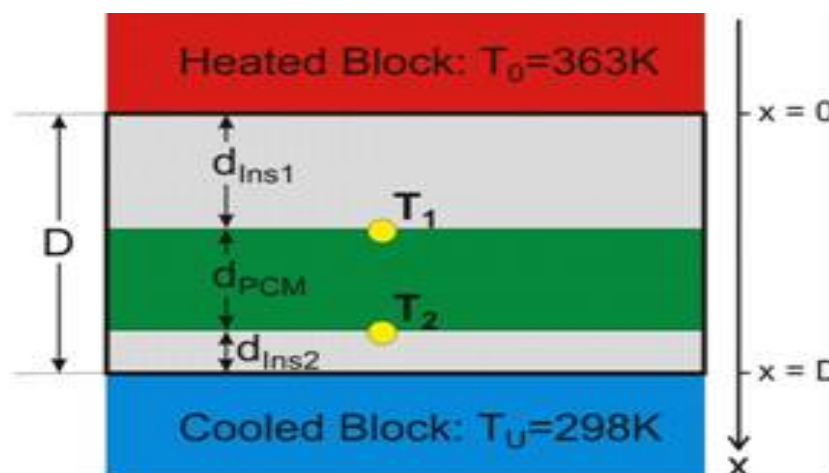


Figure 35: Three-layer sandwich model of an insulator with PCM

To design the insulation one needs to choose proper type of PCM (melting/freezing temperature, latent heat) and to optimize the thicknesses of insulator sides (d_{Ins1} and d_{Ins2} , respectively) and of the PCM material (d_{PCM}) for protecting against a given heat flux during so-called "active protection" time, which is the time of complete melting of PCM at given temperatures of hot and cold sides of the material (T_0 and T_u respectively).

For measuring directly the active protection time we developed a device schematically shown in **Scheme 5** which provides controlled temperatures on the hot and cold sides of a sandwich of insulator-PCM-insulator; while the heat flow passes, the temperatures of front and rear sides (in respect to the heater) of PCM layer are measured. The thickness of the composite layer was of 5 mm, the heat flow of 280 W/m^2 and the area of the material of 25 cm^2 .

For a model system, the insulator foam is styropor, each layer of 5 mm thickness. The hot side is kept at 80°C by an electric heater and the cold side is kept at 22°C by a water tank. The temperatures on the two sides of the PCM material are measured by two Pt-100 thermosensors.

As it appears, the measuring of the difference of temperature between the two sides of a material characterizes the insulation efficiency. We measured one of the prepared PCM/polymer composites ($\text{PBA/C}_{17}\text{H}_{35}\text{COOCH}_3$) using the heating programme shown in **Figure 36**.

The measurement gives the temperature of the two sides of the material, as in **Figure 37**, from which one obtains the temperature difference (**Figure 37**). The temperature difference, recorded versus time while passing a constant heat flow from Face to Rear side of the material, as plotted in **Figure 38**, allows finding the time during which the PCM buffers the heat flow (the time during which the material changes from solid to liquid).

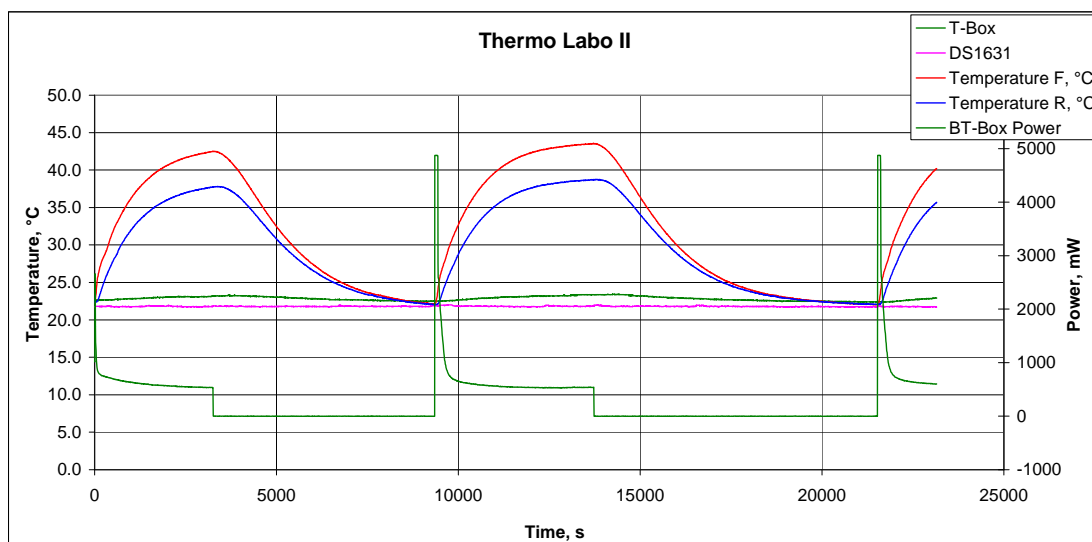


Figure 36: The temperature programme used for measuring the insulator property of a PCM/polymer composite

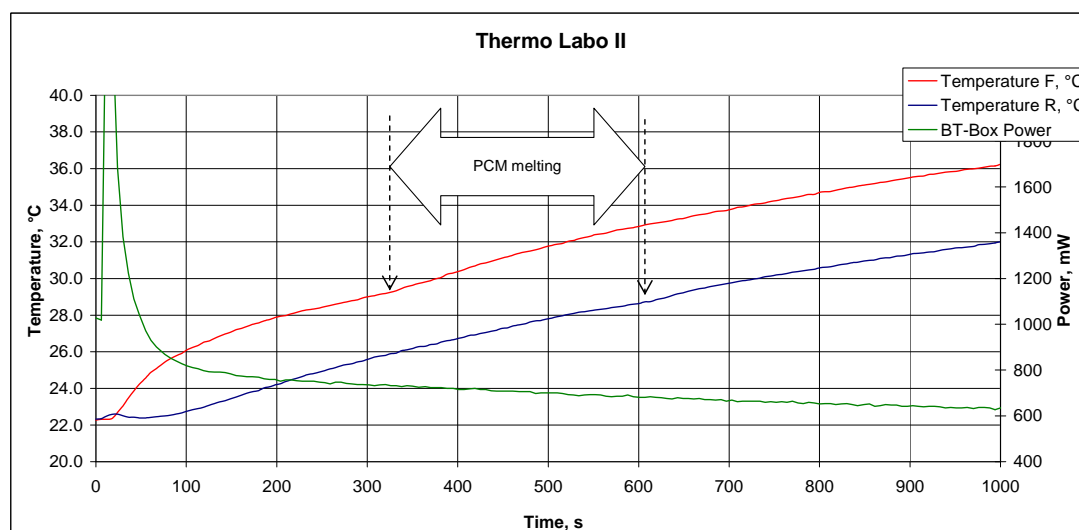


Figure 37: The temperature recorded on the two sides of the PCM/polymer composite

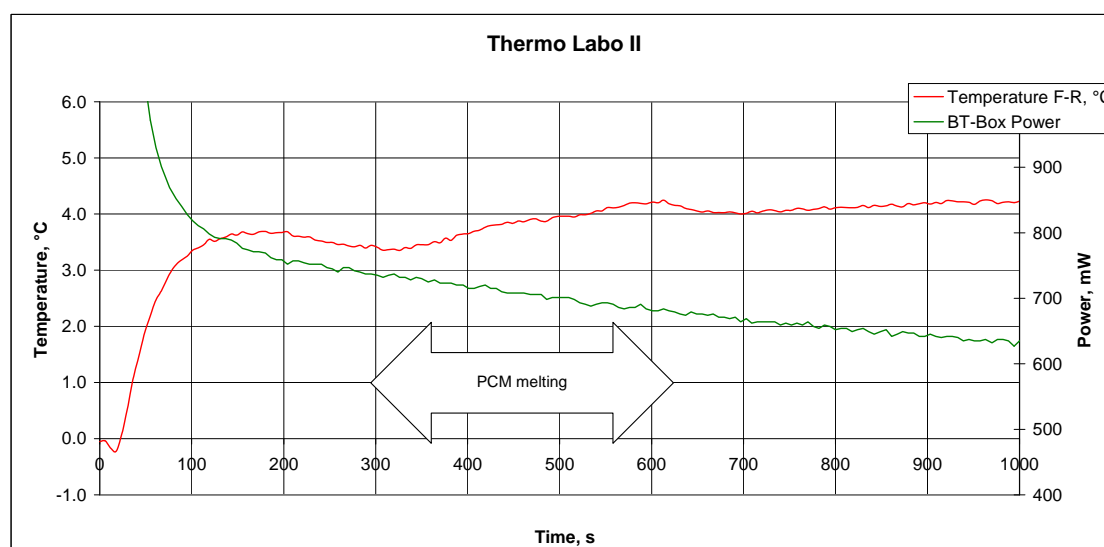


Figure 38: The difference temperature for a constant heat flow

As the measurements indicate, for the flow of 280 W/m^2 the phase change material secures 300 seconds of buffering, which is the time for the whole material to melt under the given conditions.

For the temperature difference during the melting process of 5 degrees between front and rear surface of the material which was measured, and for a constant heat flow of about 700 mW through the surface of 25 cm^2 (the flow of 280 W/m^2) the total resistance to dry heat transfer is calculated at 0.11 clo (or $0.018 \text{ m}^2 \cdot ^\circ\text{C/W}$).

3.4. Conclusions

The data from IR, Raman spectroscopy and NMR analysis show that, the polymerization process of behenyl acrylate ended under the experimental conditions, and all the peaks assigned to double bonds are not presence any more in the polymer mixtures. The DSC data show that the melting point of polybehenyl acrylate is around 65°C .

Although we did not notice significant differences in terms of temperature and heat values of phase transition process, we appreciate that the method of homo polymerizing of the behenyl acrylate, which then mixes with PCM allows controlling better the product properties, than if the co-polymerisation method.

As it results, both the n-octadecanol/poly(behenyl acrylate) composite, and the methyl octadecanoate/poly(behenyl acrylate) composite can be used for storing heat. The PCM crystals are accommodated by the polymer matrix and above the melting transition of the PCM compound the capillary forces prevent the liquid wax from free flow.

The results show the feasibility of this approach. After changing from solid to liquid phase, the capillary forces of PBA network keep PCMs flow in the polymer network. The system does not separate by storing and exhibits consistent results.

Heating and cooling under microscope a composite of poly(behenyl acrylate) and methyl-octadecanoate allowed watching the melting and crystallization of the PCM hosted in the loops of the polymeric network.

For measuring the effect of heat insulation on the treated textile materials, we have developed a device, which can provide the size and duration of the effect on a textile. The measurements carried out on one of the PCM/polymer composite (poly(behenyl acrylate) with methyl octadecanoate) showed the thermal insulation effect of the material.

4. Inorganic Encapsulation of Inorganic PCM for Textile Usage

4.1. Introduction

The inorganic phase change materials are largely used for energy storage in various applications including building insulation. They have the important advantage of having high storage density (high enthalpy change at phase transition). On the other side they have the disadvantages of overcooling and corrosion, which impede on their use.

During the present work we evaluated six different hydrated inorganic salts for using as inorganic phase change materials, namely: calcium nitrate tetrahydrate ($\text{Ca}(\text{NO}_3)_2 \cdot 4\text{H}_2\text{O}$), calcium chloride hexahydrate ($\text{CaCl}_2 \cdot 6\text{H}_2\text{O}$), sodium sulphate decahydrate ($\text{Na}_2\text{SO}_4 \cdot 10\text{H}_2\text{O}$), disodium hydrogen phosphate dodecahydrate ($\text{Na}_2\text{HPO}_4 \cdot 12\text{H}_2\text{O}$), ferric nitrate nonahydrate ($\text{Fe}(\text{NO}_3)_3 \cdot 9\text{H}_2\text{O}$), and manganese (II) nitrate hexahydrate ($\text{Mn}(\text{NO}_3)_2 \cdot 6\text{H}_2\text{O}$). **Table 13** lists the melting point and enthalpy of fusion for the salts as measured from DSC experiments.

The temperature and heat of fusion given in **Table 13** indicate that sodium sulphate decahydrate and disodium hydrogen phosphate dodecahydrate are the most appropriate salts for textile PCM application.

Table 13: The melting temperature and the heat of phase transition for several inorganic salt hydrates

Salt	Formula	Melting temp.(°C)	Enthalpy of fusion (kJ/mole)
Calcium nitrate tetrahydrate	$\text{Ca}(\text{NO}_3)_2 \cdot 4 \text{H}_2\text{O}$	42	31.05/132 J/g ⁽¹¹⁷⁾
Calcium chloride hexahydrate	$\text{CaCl}_2 \cdot 6\text{H}_2\text{O}$	29.5	43.40/200 ⁽¹¹⁷⁾
Sodium sulphate decahydrate	$\text{Na}_2\text{SO}_4 \cdot 10\text{H}_2\text{O}$	32	78.20/240-245 ⁽¹¹⁸⁾
Disodium hydrogen phosphate dodecahydrate	$\text{Na}_2\text{HPO}_4 \cdot 12\text{H}_2\text{O}$	34.5	94.9/265 ⁽¹¹⁸⁾
Ferric nitrate nonahydrate	$\text{Fe}(\text{NO}_3)_3 \cdot 9\text{H}_2\text{O}$	48.5	77.0/190 ⁽¹¹⁹⁾
Manganese (II) nitrate hexahydrate	$\text{Mn}(\text{NO}_3)_2 \cdot 6\text{H}_2\text{O}$	24.8	40.26/140 ⁽¹²⁰⁾

There are various methods for encapsulating the inorganic phase change materials⁽⁴⁸⁾ but the microencapsulation is still a challenge, because of the corrosivity of inorganic salts^(34, 35). For overcoming this we considered the encapsulation in silica based capsules by using poly(ethoxysiloxane) (PAOS, which was synthesized by the polycondensation of tetraethoxysilane as described elsewhere^(49, 50), see structure in **Figure 39**) to produce capsules with the core made of hydrated salt.

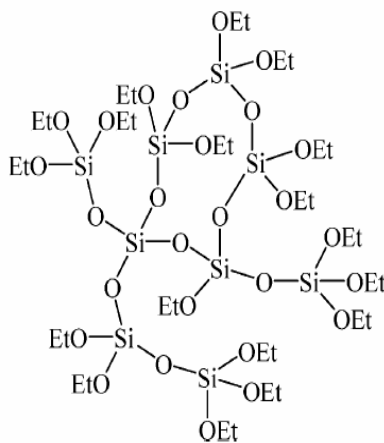
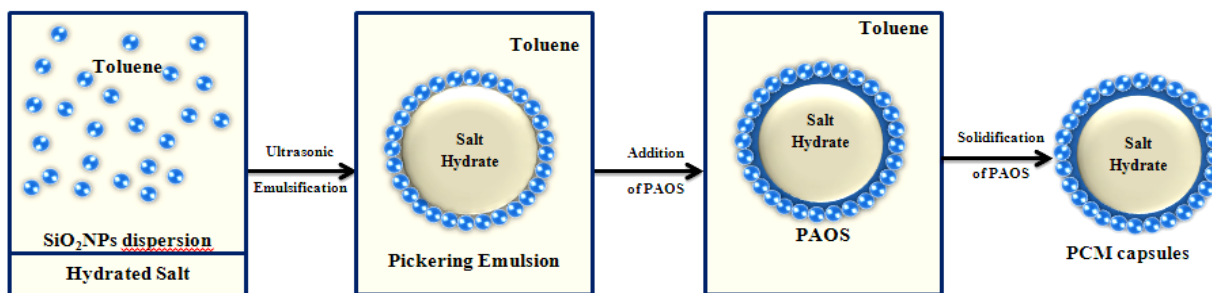


Figure 39: Molecular structure of poly(ethoxysiloxane) (PAOS)

Silica has several advantages over traditional organic materials. It is an inert, transparent, stable, biocompatible and non-toxic material which makes it the ideal solid matrix for addition of other functionalities.

Though many techniques have been developed for the preparation of capsules with different compositions and structures, the synthesis of inorganic capsules in a controllable manner is still a challenge. We developed a versatile strategy based on Pickering emulsion ^(121, 122) to synthesize pure silica nanoparticles with designed structure and properties.

The method for preparation of the silica nanoparticles is outlined in **Scheme 6**. Water-in-oil emulsion (w/o) was used as a soft template for the synthesis of PCM capsules.



Scheme 6: Schematic illustration of the preparation of the inorganic PCM capsules based on silica nanoparticles ⁽¹²³⁾

4.2. Experimental

4.2.1. Materials

Tetraethyl orthosilicate (TEOS), trimethoxy (octadecyl)silane (MODS), poly(ethoxysiloxane) (PAOS), sodium sulphate decahydrate $\text{Na}_2\text{SO}_4 \cdot 10\text{H}_2\text{O}$ disodium hydrogen phosphate dodecahydrate $\text{Na}_2\text{HPO}_4 \cdot 12\text{H}_2\text{O}$, ethanol, toluene, hydrochloric acid and ammonia, all of reagent purity, were acquired from Aldrich Sigma. Polypropylene (PP) grains were received from Sabic.

4.2.2. Methods

4.2.2.1. Preparation of PCM-Silica Capsules

4.2.2.1.1. Preparation of hydrophobic silica particles

Tetraethyl orthosilicate (TEOS) (208.33 g/mole, 1.67 ml; 7.5×10^{-3} mole) was mixed with 2.5 ml ammonia 25%, dissolved in 50 ml ethanol in closed round flask (100 ml) and stirred at 200 rpm for three day at room temperature. The trimethoxy (octadecyl)silane (MODS) (374.67 g/mole 200 μl ; 4.713×10^{-4} mole) was added drop by drop while stirring at 200 rpm, and the mixture was kept under stirring for another three days at the same speed of 200 rpm. The precipitated particles were separated by removing the solvent with centrifuge at 11000 rpm for 10 – 20 min. The precipitated particles were washed several times with toluene until the ethanol was completely removed. Finally, the particles were re-dispersed in 30 ml toluene to form homogenous dispersion.

4.2.2.1.2. Preparation of inorganic PCM capsules

1 mL silica dispersion was dissolved in 8.5 mL toluene in a dry round flask, and mixed with inorganic salts in various ratio of silica to inorganic salt, namely: 5:95, 10:90, 15:85, 20:80 and 25:75 (wt/wt) respectively, and the pH was adjusted at pH = 1 by using 1 mL HCl. The mixture was then emulsified by ultrasonic action for 30 min, after which 0.6 mL from 20% PAOS in toluene was added to the emulsion drop by drop. The emulsion was further kept under gentle stirring at melting temperature of the inorganic salt for at least three days for allowing PAOS to solidify in order to form the capsules. The precipitate was washed with a mixture of ethanol and toluene two - three times, followed by once with hexane and twice with toluene, then dried and used for the further analysis.

4.2.2.2. Preparation Film from PCM-Silica Capsules and Polypropylene

The laboratory extruder from DSM Research BV X-Plore was used (see **Figure 40**) for manufacturing the films of polypropylene and PCM capsule mixture by extrusion under a flow of nitrogen. The films were preferred over the fibres, because in case of fibres the change in capsule size could block the nozzles of the spinneret. The capsules were added up to 5% (weight) of the PP grains and the mixture was melted in a twin screw extruder, the temperature being kept at 200°C from top to bottom. The mixing speed was 100 rpm and the screw speed was 35 U/min, the drawing speed at 850 mm/min and the torque was 30 rpm. The extruded film was 90 – 100 µm thick.



Figure 40: X-plore extruder for the production of polymer films

4.2.2.3. Coating of Wool and Cotton Fibres/Fabrics with PCM Compound

A coating method was applied to prepared PCM materials with 100% cotton and wool fibres. Coating material is a water soluble synthetic dispersion, commercially available for fabrics, that was polyurethane based, anionic, with 45–48% active content. Fixing agent comprising melamine resins with low formaldehyde content, which was miscible in water, nonionic and of 8–9 pH value was used for cross linking.

Recipes were prepared for 1:1 and 1:1.5 mixtures of the coating material and the PCM materials. Ten units coating material were stirred at 600 rpm for 5 min and then 10 or 15 units PCM material were mixed while increasing the stirring rate up to 1000 rpm for the next 15 min. 1.5% fixing agent was blended and stirring rate was halved for the last 2–3 min.

The fabrics were immersed into the coating dispersion solution at 40–50°C, coated fabric samples were fixed in a drying oven for 15 min and the temperature increased gradually from 60 to 80°C and then conditioned for the subsequent 24 h.

To determine the actual incorporation percentages of the PCM materials transferred to the sample, which depends also on the coating thickness, we weighed the coated and uncoated pieces of fabric.

4.2.3. Measurements

4.2.3.1. Differential Scanning Calorimetry (DSC)

DSC measurements for measuring the melting and the crystallization behaviour of the substances were carried out on Perkin Elmer DSC and on Netzsch DSC 204. The measurements were run using nitrogen flow at 20 mL/min as purge gas. The weighted samples, each of approximately 7 mg, were closed in aluminium pans, which were perforated prior to be placed in DSC device. An empty aluminium pan was used as reference. The temperature programme consisted of heating, cooling and heating steps. Temperature ranged from 0°C to 70°C, with 10 K·min⁻¹. The melting temperature and enthalpy ΔH were evaluated from the onset and area, respectively, of the peaks recorded during the second heating. DSC temperature and heat flow was calibrated with indium.

4.2.3.2. Scanning Electron Microscopy (SEM)

Scanning electron microscope (SEM) measurement of the PCM capsules was carried out on Hitachi 5-4800 FESEM (Field-Emission SEM). The electron beam accelerating voltage was set at 120 kV. The capsules were dispersed in toluene, and one drop of the dispersion was trickled on a piece of form var-carbon coated copper grid. Before placed into the SEM, the copper grid was dried in air under ambient conditions.

Surface morphology and the cross section of the composite films were studied using scanning electron microscope HITACHI S-3000 microscope S, at 15 kV acceleration voltage, after gold coating.

4.2.3.3. Mechanical Properties

The film of PP/PCM was measured for mechanical properties on a Miniature Materials Tester (MiniMat2000 by Rheometric Scientific). Prior to measurement the sample was kept for 24 hours at 22°C and relative humidity of 65%. After mounting the sample in the tester it is stretched with a constant rate of 0.1 mm/min under a load of 20 N until the break.

4.3. Result and Discussion

4.3.1. Encapsulation into Silica Particles

The weight ratio of hydrophobic silica particles to PCM salt ranged from 5:95 to 10:90, for preserving as much as possible of heat storage ability. The ratio is further decreased in the final product because the amount of PAOS which forms the shell is not well controllable. The obtained capsules properties are illustrated in **Table 14** and the capsules were measured on DSC (see **Figure 41**). The values obtained from the DSC measurements are listed in **Table 15**. Scanning electron microscope micrograph show that the particle size is within the micrometer range (2-3 μ can be detected) (see **Figure 42**). Results in **Table 15** indicate that the encapsulation preserves the effect of PCM, but the size of the effect is reduced according to the overall percentage of salt to silica capsule. It appears also that the heat transmission coefficient of the silica shell shifts the phase transition peak to higher value, and also rounds the endothermic peak shape.

Table 14: Properties of PCM capsules from hydrated inorganic salts with silica particles

PCM capsules	capsules radius (nm)	Wall Thickness (nm)
$\text{Na}_2\text{SO}_4 \cdot 10\text{H}_2\text{O}$ + Silica	60 – 125	10 – 30
$\text{HNa}_2\text{PO}_4 \cdot 12\text{H}_2\text{O}$ + Silica	45 - 80	10 - 20

Table 15: DSC data for PCM materials from hydrated inorganic salts with silica particles

Material	1 st Heating		2 nd Heating	
	T_o (°C)	ΔH (J/g)	T_o (°C)	ΔH (J/g)
$\text{Na}_2\text{SO}_4 \cdot 10\text{H}_2\text{O}$	27.9	234.6	27.2	230.2
$\text{Na}_2\text{SO}_4 \cdot 10\text{H}_2\text{O}$ + Silica	27.3	38.6	29.0	35.4
$\text{HNa}_2\text{PO}_4 \cdot 12\text{H}_2\text{O}$	37.4	266.7	37.4	250.0
$\text{HNa}_2\text{PO}_4 \cdot 12\text{H}_2\text{O}$ + Silica	36.6	69.3	36.3	70.1

T_o : Onset Temp (°C)

ΔH : Enthalpy, (J/g)

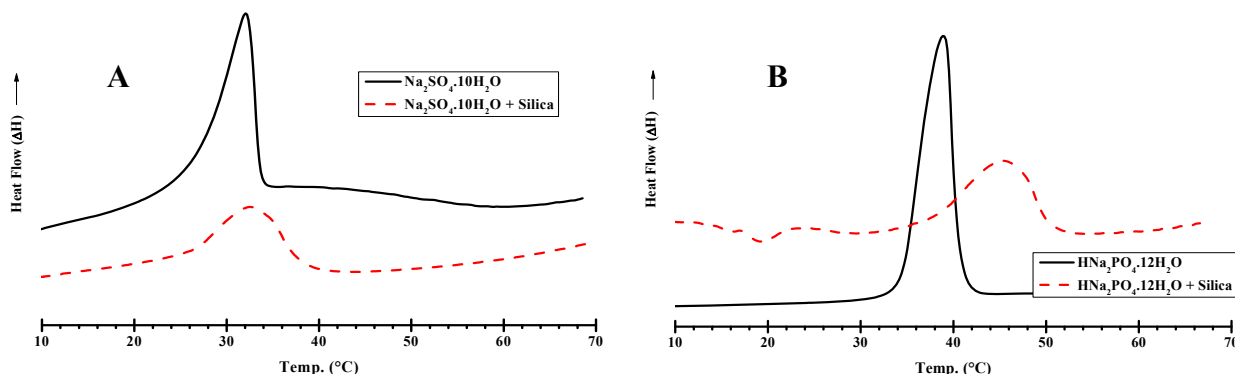


Figure 41: The DSC plots of silica capsules containing $\text{Na}_2\text{SO}_4 \cdot 10\text{H}_2\text{O}$ (A) and $\text{HNa}_2\text{PO}_4 \cdot 12\text{H}_2\text{O}$ (B)

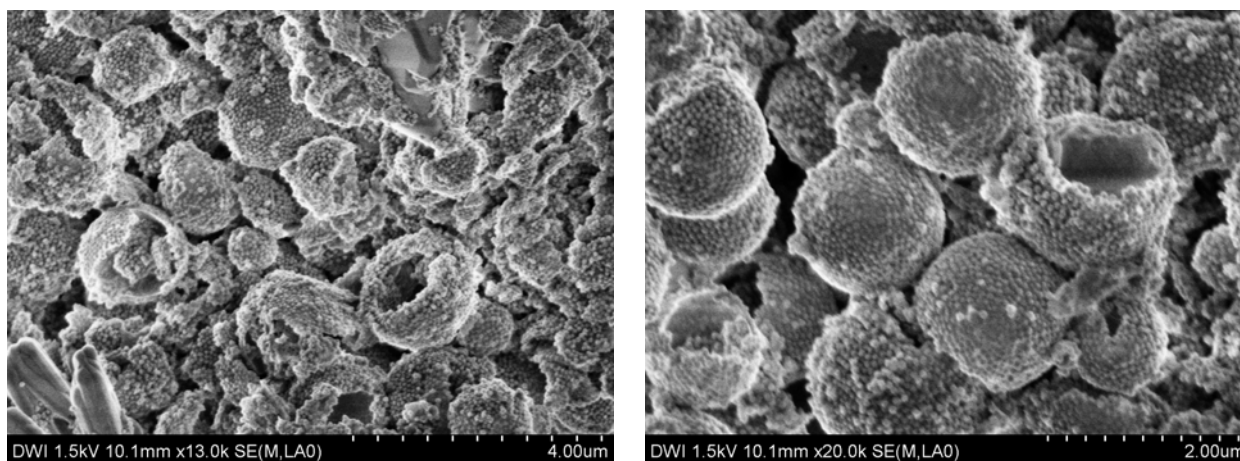


Figure 42: Inorganic PCM ($\text{Na}_2\text{HPO}_4 \cdot 12\text{H}_2\text{O}$) encapsulated in silica particles

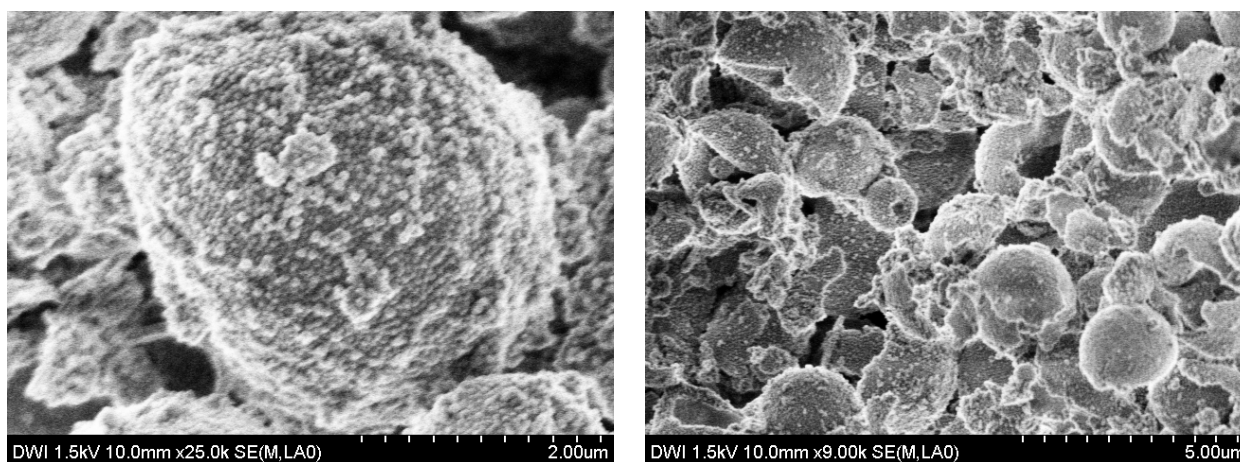


Figure 43: Inorganic PCM ($\text{Na}_2\text{SO}_4 \cdot 10\text{H}_2\text{O}$) encapsulated in silica particles

4.3.2. Textile Application

The DSC results of coated cotton and wool fabrics with inorganic PCM polymer composites ($\text{Na}_2\text{SO}_4 \cdot 10\text{H}_2\text{O}$ + Silica and $\text{HNa}_2\text{PO}_4 \cdot 12\text{H}_2\text{O}$ + Silica) are listed in **Table 16**. One may conclude that wool and cotton fabrics can be coated with inorganic PCM polymer composite. The abrasion/washing tests indicate a fairly good stability of the thermal buffer effect imparted by coating.

Table 16: DSC and DI results of coated fabric with inorganic PCM polymer composites

Polymer	Fabric Type	2 nd Heating			
		After treatment		After washing	
		T _o (°C)	ΔH (J/g)	T _o (°C)	ΔH (J/g)
$\text{Na}_2\text{SO}_4 \cdot 10\text{H}_2\text{O}$ + Silica	Cotton	28.8	34.1	29.2	32.2
	Wool	28.9	36.8	28.8	35.8
$\text{HNa}_2\text{PO}_4 \cdot 12\text{H}_2\text{O}$ + Silica	Cotton	36.5	68.2	36.9	67.4
	Wool	36.7	72.5	37.2	71.3

T_o: Onset Temperature °C,

ΔH: Enthalpy J/g

4.3.3. Polypropylene Film with PCM-Silica Capsules

Polypropylene (PP) is a highly versatile polymer used mainly for interior textiles. We chose this material to embed PCM silica capsules, for increasing its heat storing capacity. The PP grains were mixed with 5% PCM-silica capsules and the film was extruded at 200°C as described previously.

The elongation at break of 6% was recorded for films with 5% PCM capsules. This is within the range recorded for pure PP film (5 – 6%), indicating that the capsules do not affect the mechanic properties of the polypropylene film.

The DSC plots of the PP film embedding 5% PCM capsules with sodium sulphate decahydrate, or disodium hydrogen phosphate dodecahydrate, respectively, are shown in **Figure 44**, along with the plot of a PP film, for temperature ranging from room temperature to 80°C with 10°C/min.

One observes the endothermic peak of PCM capsules with sodium sulphate decahydrate around 53°C due to the phase transition (melting) of sodium sulphate decahydrate. The size of the effect is very small, at about 2 J/g materials, and can be increased by increasing the amount of PCM capsules added to PP film.

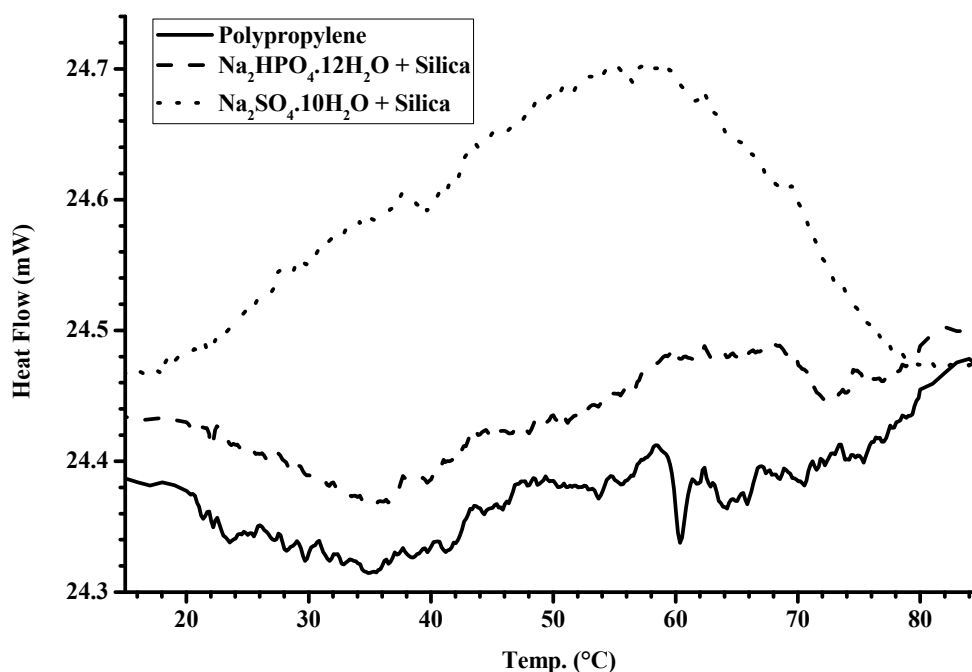


Figure 44: DSC plots of films of PP and PP with PCM capsules from Na₂SO₄·10H₂O, HNa₂PO₄·12H₂O

Figure 45 shows the SEM micrographs of the PCM-silica capsules distributed in the cross-section of a polypropylene film extruded from polypropylene melt with 5% added capsules. The micrographs indicate a homogeneous distribution of the capsules in the PP film, showing a good compatibility of the additive and polymer matrix.

For the textile use the methodology set up for films can be transferred for fibres. The fibres with encapsulated PCM materials are the most advantageous technique to merge the expected enriched heat performance with the other textile properties on the same product. Also it is a good way to avoid the interaction of the PCM materials with the skin. The incorporation of PCM capsules into textiles in the form of a core-shell matrix brings many opportunities such as less evaporation and minimum interaction with the environment, increased heat transfer area and long shelf-life of the garment.

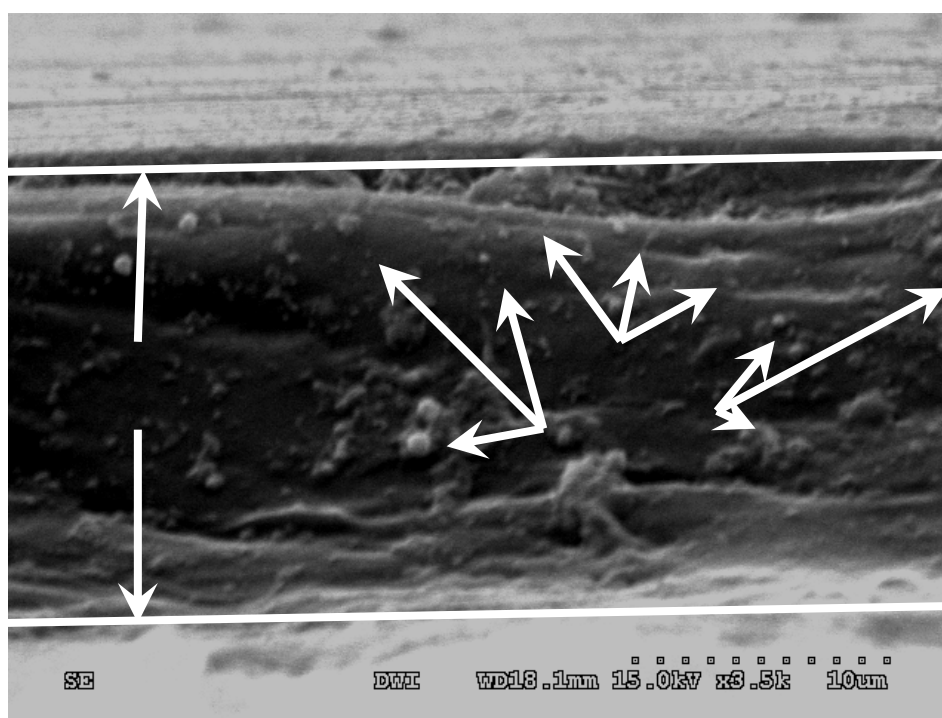


Figure 45: Cross-section of poly propylene film with 5% PCM capsules

4.4. Conclusions

We have investigated the possibility to encapsulate inorganic PCM in an inorganic, silica-based capsule, and used the capsules for coating or infiltrating them on/into films/fibre.

Pure inorganic silica capsules were prepared using PAOS. The capsules contain inorganic hydrated salt inside. We successfully produced silica-based microcapsules with sodium sulphate decahydrate, and disodiumhydrogen phosphate dodecahydrate respectively. The

microcapsules, which show retaining good phase change property, were embedded in a film of the polypropylene at the extruding stage. The basic mechanical properties of the new material do not differ from those of the pure polypropylene. The DSC data indicate that the effect of the phase change material (melting of the salt), is measurable also in the film. the capsules were also used for coating textiles of wool, or cotton. The DSC data indicates that the effect is preserved after washing of the textile.

Summing up, we have produced polymer-inorganic PCM materials which show potential for being used in textile industry for interior textile composition.

5. Polyvinylcaprolactam-Co-Polymer Microgels to Handle Gloss Properties of Natural Fibres

5.1. Introduction

Microgels play an important role in living systems and are of broad interest for a large variety of industrial products (e.g. as storage and separation media) ⁽¹²⁴⁾. In recent years, especially thermo-sensitive systems like poly(*N*-isopropylacrylamide) (PNIPAM), microgels have attracted much attention ^(68, 125, 126), because the viscoelastic characteristics can be easily controlled by changing the temperature. Moreover, the bio-adhesive properties of these materials point to possible applications as drug delivery systems ⁽¹²⁴⁾.

Lustre is one of the factors in the selling of fabrics which can be influenced by fabric design ⁽¹²⁷⁻¹³⁷⁾. There are signs of a style trend or fashion interest in “white on white” in men’s shirting. ⁽¹³²⁾ ASTM ^(62, 63) defines luster or contrast gloss as: “The appearance characteristics of a surface that reflects more in some directions than it does in other directions, but not of such gloss as to form clear mirror images.” To be more specific to textiles, the Textile Institute defined luster ^(64, 65) as “The display of different intensities of light, reflected both specularly and diffusely from different parts of a surface exposed to the same incident light.”

In this study we used three different types of microgels (based on poly(*N*-vinylcaprolactam); PVCL) for coating the surface of hair, cotton and wool fibres, respectively, and investigated the way the coating affects the lustre.

5.2. Experimental

5.2.1. Materials

Untreated cotton and wool fibres, *N*-vinylcaprolactam (VCL, C₈H₁₃NO, M.wt.: 139.19 g/mol, Aldrich) and purified by distillation, vinylimidazole (VIm, C₅H₆N₂, M.wt.: 94.12 g/mol, Aldrich), acetoacetoxyethyl methacrylate (AAEM, C₁₀H₁₄O₅, M.wt.: 214.21, Aldrich) and purified by conventional methods and then vacuum distilled under nitrogen, and itaconic acid dimethyl ester (IADME, C₇H₁₀O₄, M.wt.: 158.154, Fluka) were purified by distillation under vacuum. Initiator 2,2’-azobis(2-methylpropionamidine) dihydrochloride (AMPA, M.wt.: 271.19, Aldrich) and used as received, cross-linker *N,N*’-methylene bis(acrylamide) (BIS, M.wt.: 154.17, Aldrich) was used without further purification and Deionized water D₂O

(99.9%, KMF GmbH, Germany) was employed as polymerization medium, were used as received, the chemical structure of used ingredients is shown in **Figure 46**.

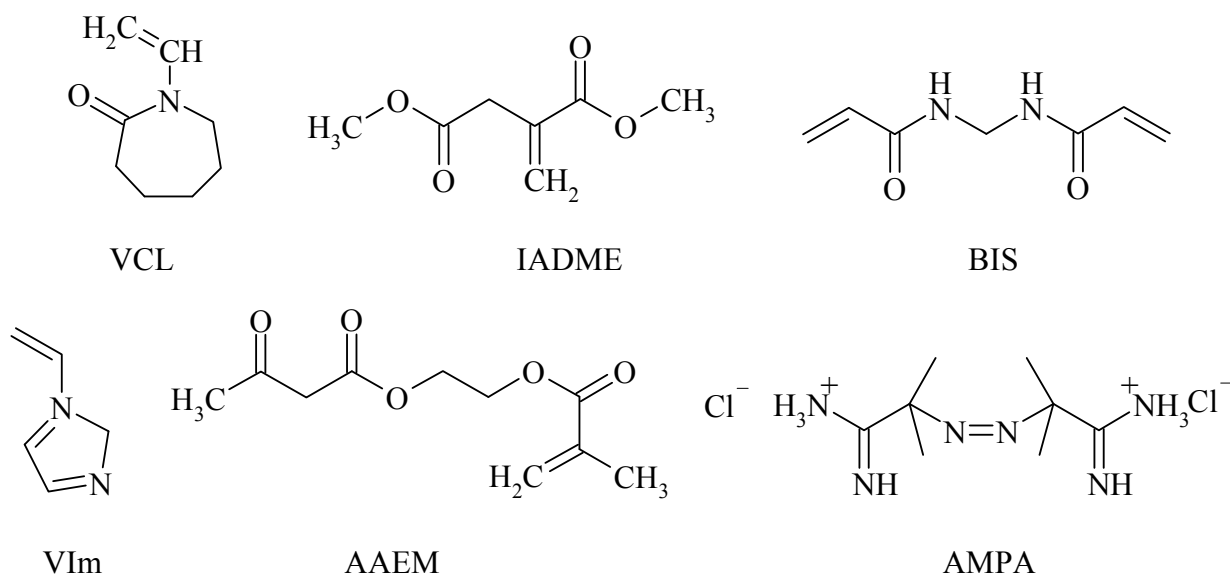


Figure 46: Different material structures used in preparation of microgel compounds

5.2.2. Methods

5.2.2.1. Synthesis of Amphoteric, Anionic and Neutral Microgels

The synthesis of VCL/AAEM and VCL/IADME and VCL/IADME/VIm microgels has been reported elsewhere.⁽¹³⁸⁻¹⁴⁰⁾ The polymerization procedure can be described as follows. Appropriate amounts of monomer(s) and cross linker (the amounts of ingredients used for polymerization process as well as some important microgel characteristics are shown in **Table 17**) were dissolved in deionizer water. Double wall glass reactor 250 mL equipped with stirrer and reflux condenser was purged with nitrogen. Solution of the monomers was placed into reactor and stirred for 1 h at 70°C under continuous purging with nitrogen. After that, the 5 ml aqueous solution of initiator was added under continuous stirring. Reaction was carried out for 8 h at the same temperature. Synthesized VCL/IADME and VCL/IADME/VIm microgels were treated with NaOH to hydrolyse ester bonds in IADME and obtain itaconic acid (IA) having two carboxylic groups.

Microgels were purified by dialysis with Millipore Dialysis System (cellulose membrane, MWCO 100 000) for **MG_3** (pH = 6) and (VIVA-Flow50, 50000 MWCO, poly(ether sulfone)) for both **MG_2** (pH = 8) and **MG_1** (pH = 4 and 8). The microgel was redispersed in deionised water (D₂O) and the particle concentration was adjusted to 2 wt%.

Table 17: Ingredients used for the synthesis of different microgels

Microgel	VCL		IADME		AAEM		VIm		BIS	AMPA	H ₂ O	Solid content (%)	pH
	(g)	mol %	(g)	mol %	(g)	mol %	(g)	mol %					
MG_1	1.76	85	0.35	15	–	–	0.014	1	0.06	0.05	150	0.5	amphoteric pH
MG_2	1.77	85	0.35	15	–	–	–	–	0.06	0.05	150	0.41	Negative pH 8
MG_3	1.88	85	–	–	0.34	15	–	–	0.06	0.05	150	1.04	Positive pH 4

5.2.2.2. Fibre Treatment

Cotton and wool fibres are treated with three types of microgels at different pH (4 and 8, respectively) for 20 min at room temperature, and at 50°C. The treated fibres were dried at room temperature overnight and used for further investigation. **Table 18** shows the treatment parameters for each experiment.

Table 18: The conditions for fibre treatment with different microgels

Fibre type	Microgel compound	pH = 4		pH = 8	
		Room Temp.	50°C	Room Temp.	50°C
Cotton	MG_1	√	√	√	√
	MG_2	–	–	√	√
Wool	MG_1	√	√	√	√
	MG_3	√	√	–	–

5.2.3. Measurements

5.2.3.1. Liquid state NMR Measurements

Proton NMR spectra of the VCL, AAEM, VIm and IADME monomers as well as of the microgel were measured on liquid state Bruker NMR spectrometer operating at 600 MHz. For these measurements 2wt% of the amphoteric microgel dissolved in D₂O was used.

5.2.3.2. Scanning Electron Microscope (SEM)

SEM images of the microgel colloids were taken with Gemini microscope (Zeiss, Germany). Microgel dispersions were diluted with deionized water, dropped onto cleaned glass support

and dried at room temperature. Samples were coated with thin Au/Pd layer for increasing the contrast and quality of the images. Pictures were taken at a voltage of 4 kV.

Fibre snippets were coated with thin Au/Pd layer to increase the contrast and quality of the image. The surface morphology of the fibres was studied using scanning electron microscope HITASHI S-3000 microscope S, at 15-kV acceleration voltage.

5.2.3.3. Gloss measurement

A gloss measuring device produced by OMT-Germany was used to measure the reflected and dispersed light at wavelength ranging from 380 to 900 nm and angle ranging from 15 to 75°, for an incident white light (D65) at 45°. The reflected light measured under an angle ranging from 35 to 55° was taken as specular light. The wavelength considered for calculations ranged from 400 to 650 nm.

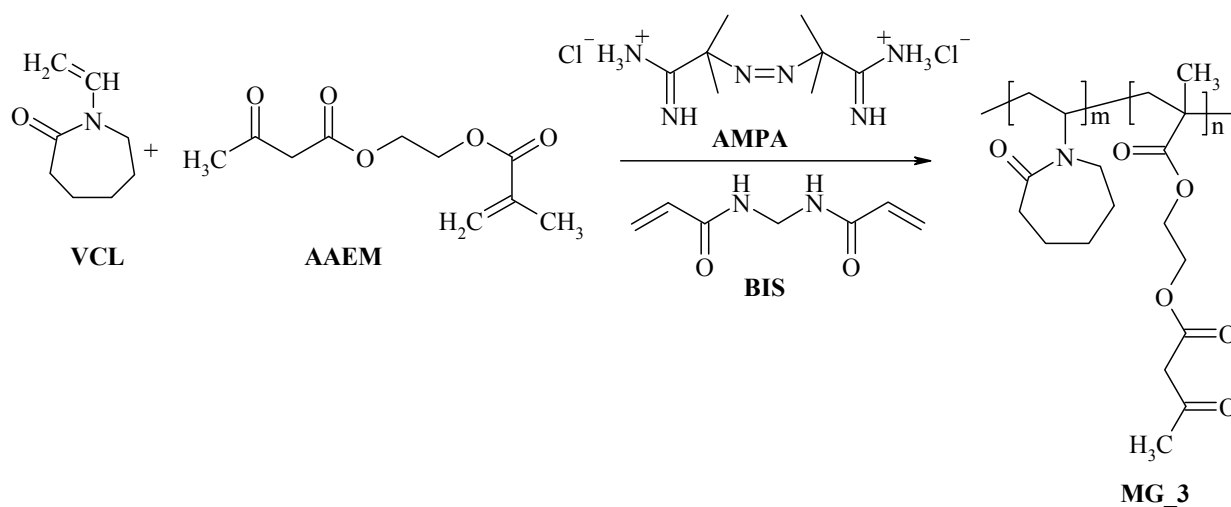
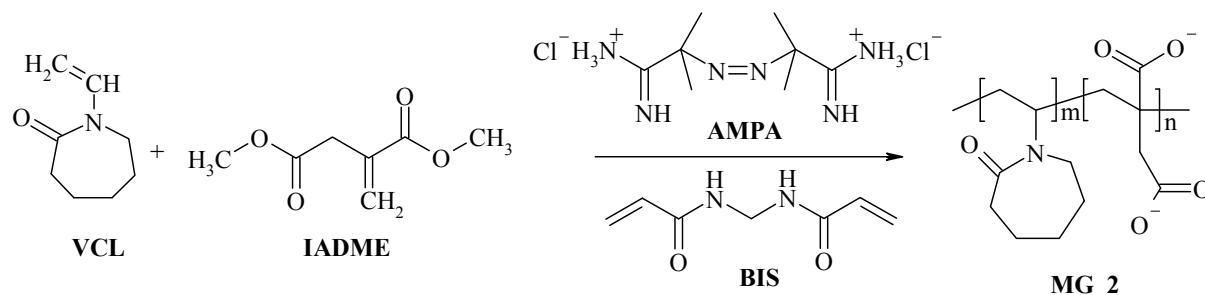
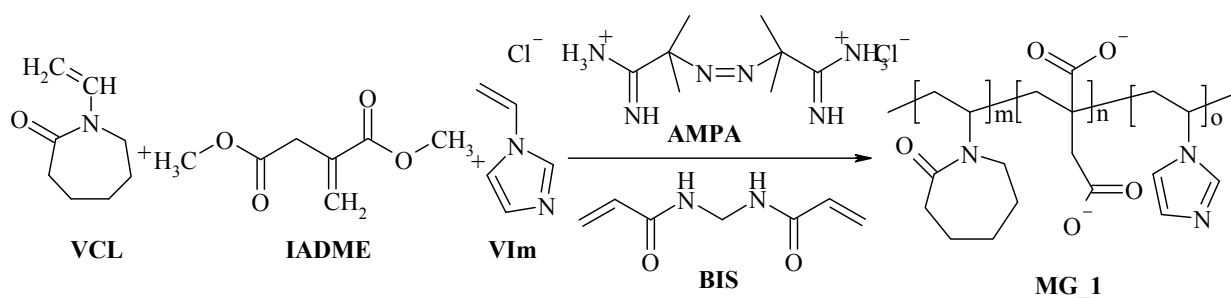
5.3. Result and Discussion

Thermo-sensitive microgels based on VCL have been prepared in surfactant-free conditions. Incorporation of hydrophilic co-monomers (VIm or IADME) improves colloidal stability of obtained particles. In previous studies we found that the microgels have core-shell structure due to fast consumption of more reactive acrylic monomers ⁽¹³⁸⁾.

5.3.1. Microgel Synthesis

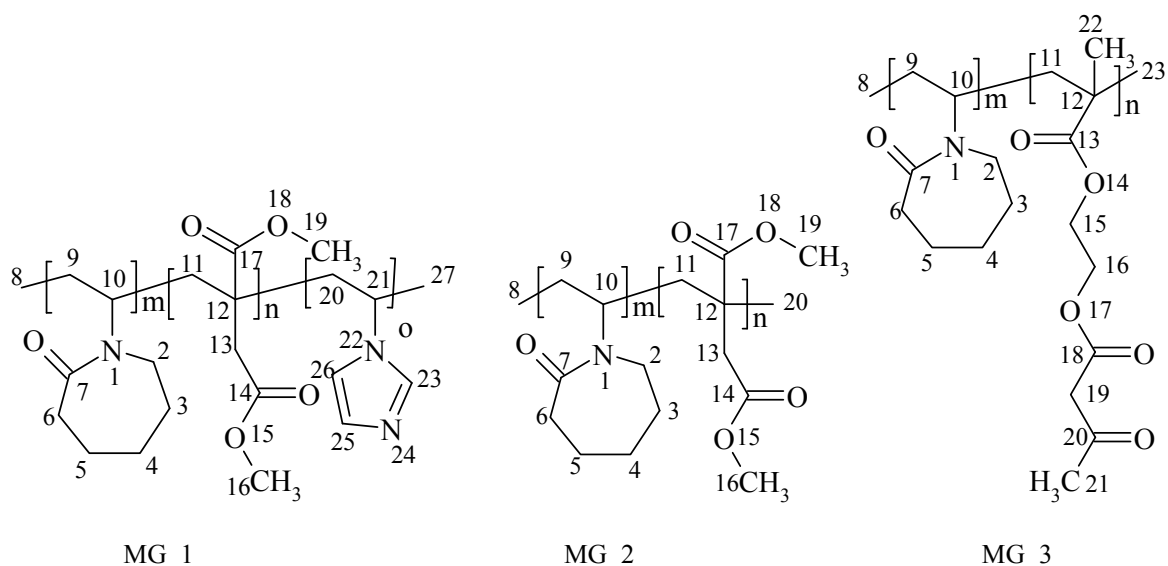
The preparation of thermo-sensitive microgels by copolymerization of VCL, IADME and AAEM has been introduced first in earlier publication ⁽¹³⁸⁻¹⁴⁰⁾ and the use of VCL/AAEM microgels as carrier for polypyrrole, ^(141, 142) magnetite, ⁽¹⁴³⁾ ZnS, ⁽¹⁴⁴⁾ and Ag ⁽¹⁴⁵⁾ nanoparticles has been reported recently. In this study, these microgels will be used to coat the wool and cotton fibres in order to change the gloss properties of these fibres.

The different schemes for preparation of the different microgel which are used in this article are shown in **Scheme 7**, **Scheme 8** and **Scheme 9**.



5.3.1.1. Chemical Composition of Microgels

^1H -NMR and ^{13}C -NMR spectra of the VCL and IADME monomers as well as of the different microgels were measured. In the resulting NMR spectra, all the prepared microgels compounds are identified, and the entire expected signals exists. The chemical shifts of ^1H -NMR and ^{13}C -NMR for these microgels are listed below:



MG_1: ^1H NMR: $\delta = 1.28 - 1.38$ (d, 4H, H^8 , H^9); $1.49 - 1.60$ (m, 2H, H^3); $1.72 - 1.79$ (m, 2H, H^4); $1.75 - 1.89$ (t, 2H, H^{11}); $1.98 - 2.00$ (m, 2H, H^5); $2.02 - 2.07$ (t, 2H, H^{20}); $2.10 - 2.20$ (t, 2H, H^6); $2.66 - 2.72$ (m, 1H, H^{13b}); $2.40 - 2.72$ (m, 2H, H^{13b}); $3.36 - 3.48$ (t, 2H, H^2); $3.62 - 3.71$ (d, 2H, H^{16} , H^{19}); $3.73 - 3.79$ (m, 1H, H^{10}); $3.85 - 3.95$ (t, 2H, H^{21} , H^{27}); $6.62 - 6.68$ (m, 1H, H^{25}); $7.12 - 7.25$ (m, 1H, H^{26}) and $7.82 - 7.88$ (d, 1H, H^{23}).

^{13}C NMR: $\delta = 20.4(\text{C}^9)$; $26.9(\text{C}^4, \text{C}^5)$; $30.8(\text{C}^{12})$; $31.8(\text{C}^3)$; $33.3(\text{C}^{20})$; $38.1(\text{C}^6)$; $38.9(\text{C}^{11})$; $41.9(\text{C}^{13})$; $43.1(\text{C}^2)$; $45.0(\text{C}^{21})$; $55.3(\text{C}^{10})$; $50.8(\text{C}^{16})$; $53.9(\text{C}^{19})$; $121.2(\text{C}^{26})$; $130.2(\text{C}^{25})$; $139.6(\text{C}^{23})$; $172.3(\text{C}^{14})$; $174.8(\text{C}^7)$ and $175.9(\text{C}^{17})$.

MG_2: ^1H NMR: $\delta = 1.28 - 1.38$ (d, 4H, H^8 , H^9); $1.49 - 1.60$ (m, 2H, H^3); $1.72 - 1.79$ (m, 2H, H^4); $1.75 - 1.89$ (t, 2H, H^{11}); $1.98 - 2.00$ (m, 2H, H^5); $2.08 - 2.20$ (t, 2H, H^6); $2.66 - 2.72$ (m, 1H, H^{13a}); $2.86 - 2.98$ (m, 2H, H^{13b} , H^{20}); $3.36 - 3.48$ (t, 2H, H^2); $3.62 - 3.71$ (d, 2H, H^{16} , H^{19}) and $3.73 - 3.79$ (m, 1H, H^{10}).

^{13}C NMR: $\delta = 19.4(\text{C}^9)$; $26.9(\text{C}^4, \text{C}^5)$; $31.8(\text{C}^3)$; $33.6(\text{C}^{13})$; $36.0(\text{C}^{11})$; $38.1(\text{C}^6)$; $38.6(\text{C}^{12})$; $43.1(\text{C}^2)$; $50.8(\text{C}^{16})$; $53.9(\text{C}^{19})$; $172.3(\text{C}^{14})$; $174.8(\text{C}^7)$ and $175.9(\text{C}^{17})$.

MG_3: ^1H NMR: $\delta = 1.16 - 1.22$ (m, 3H, H^{22}); $1.28 - 1.38$ (d, 4H, H^8 , H^9); $1.49 - 1.70$ (m, 2H, H^3); $1.72 - 1.85$ (m, 4H, H^4 , H^{11}); $1.98 - 2.00$ (m, 2H, H^5); $2.08 - 2.20$ (t, 2H, H^6); $2.22 - 2.31$ (d, 3H, H^{21}); $2.42 - 2.51$ (d, 1H, H^{23}); $3.36 - 3.48$ (t, 4H, H^2 , H^{19}); $3.72 - 3.78$ (m, 1H, H^{10}) and $4.28 - 4.42$ (m, 4H, H^{15} , H^{16}).

^{13}C NMR: $\delta = 17.2(\text{C}^{22})$; $19.4(\text{C}^9)$; $26.9(\text{C}^4, \text{C}^5)$; $31.0(\text{C}^{21})$; $31.8(\text{C}^3)$; $33.6(\text{C}^{12})$; $38.1(\text{C}^6)$; $38.6(\text{C}^{11})$; $43.1(\text{C}^2)$; $50.3(\text{C}^{19})$; $58.9(\text{C}^{10})$; $62.3(\text{C}^{16})$; $62.9(\text{C}^{15})$; $167.1(\text{C}^{18})$; $174.8(\text{C}^7)$; $175.9(\text{C}^{13})$ and $202.7(\text{C}^{20})$.

5.3.1.2. Microgel Morphology

The SEM images of the various microgels in **Figure 47**, **Figure 48** and **Figure 49** indicate that independently of their chemical composition they have a narrow particle size distribution. The diameter of the particles in all microgels ranges from 200 to 300 nm.

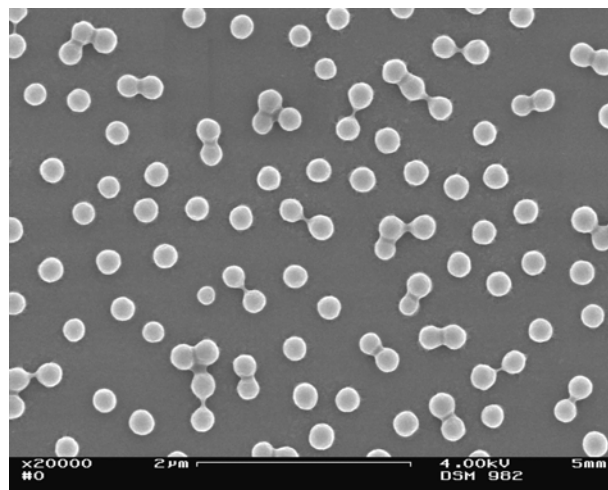


Figure 47: SEM image of VCL/IADME/VIm (MG_1) microgel

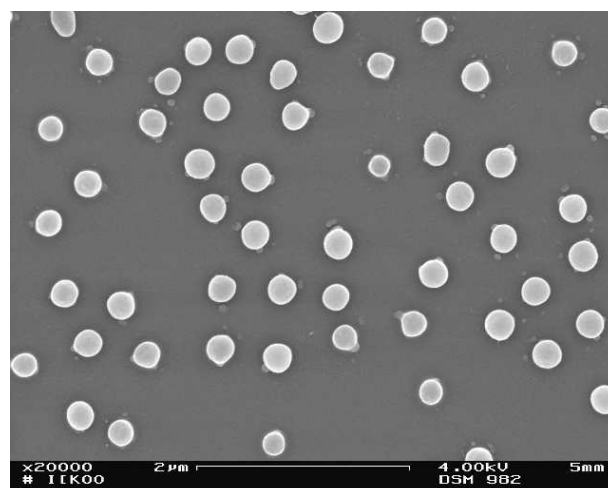


Figure 48: SEM image of VCL/IADME (MG_2) microgels

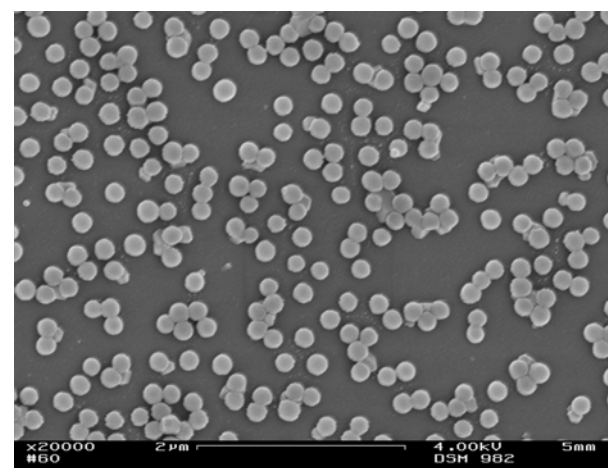
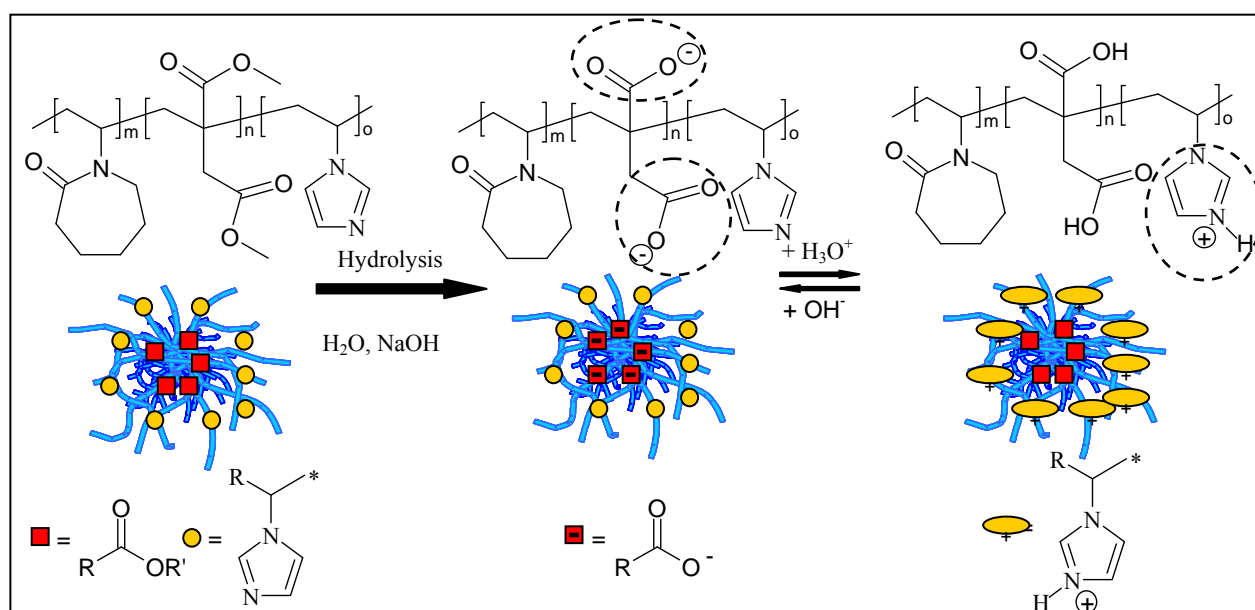


Figure 49: SEM image of VCL/AAEM (MG_3) microgels

5.3.2. Microgel Deposition of Fibres

As it was shown in the previous works,^(138, 141, 142) the microgel MG_1 is a pH sensitive microgel. The microgel has negative charge in alkaline medium (pH around 8), and positive charge in acidic medium (pH around 4). The hydrolysis of this microgel occurs according to **Scheme 10**. It is clear that, in acidic medium the shell of the microgel has positive charge and the ability to interact with negatively charged surfaces is very high, and the reverse is true in alkaline medium. Consequently, this microgel deposits well onto both fibres (cotton and wool). The microgel MG_2 has negative charge at pH 8 and may be used to deposit onto cotton fibre. The microgel MG_3 is almost neutral and has a weak positive charge at pH 4 and deposits onto wool fibre.



Scheme 10: Hydrolysis effect of MG_1 microgel in different pH medium

The microgel MG_1 has amphoteric properties (have positive or negative charge depending on the pH treatment medium) and it was applied onto cotton, wool fibres at pH 4 and 8, in two different temperatures (25 and 50°C). It is clear that, for cotton fibres the amount of deposited microgel onto the surface increases by increasing the temperature in both pHs medium. Also, the nanoparticles deposit onto the surface at pH 8 more than at pH 4 (**Figure 50**). Furthermore, wool fibre at pH 4 has more deposited nanoparticles than at pH 8 even by increasing the temperature. One can observe that, most particles are deposited on the scales of wool at room temperature. The deposition of the particles covers the whole surface by increasing the temperature. At pH 8 the particles has good distribution onto whole wool fibres surface but do not cover it completely.

Second microgel MG_2 has negative charge and it was applied onto cotton fibre only at pH 8, at two different temperatures 25 and 50°C respectively. One can see that, the microgel has the affinity to deposit onto the cotton surface at room temperature (**Figure 51**). The microgel particles appear as spherical objects on fibre. Increasing the temperature till 50°C causes increasing of the deposition of the microgel onto the surfaces. The images show the formation of a coating film onto cotton surface.

Third microgel MG_3 has neutral charge (slightly positive charge resulted during presence of cationic initiator in the preparation method), and it was applied onto wool fibre only at pH 4, at two different temperatures 25 and 50°C respectively. Generally the ability of the microgel to deposit onto wool surface fibre is high (**Figure 51**).

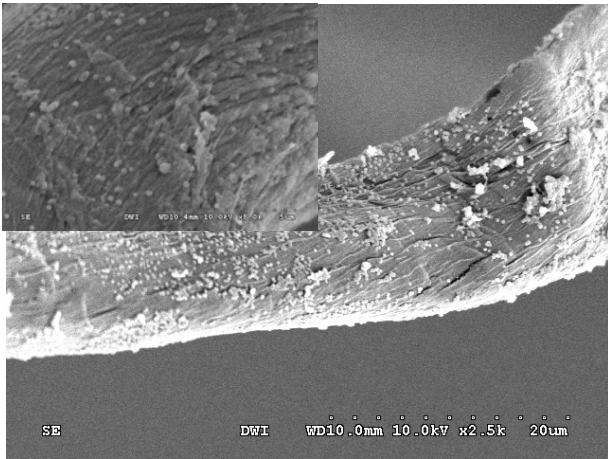
5.3.3. Gloss Measurement

We define the DWI Gloss Index by considering that the specular reflected light surface is the light reflected under an angle which ranges from 35° to 55°. The volume of specular reflected light to the total volume of reflected light is taken as a measure of DWI Gloss Index:

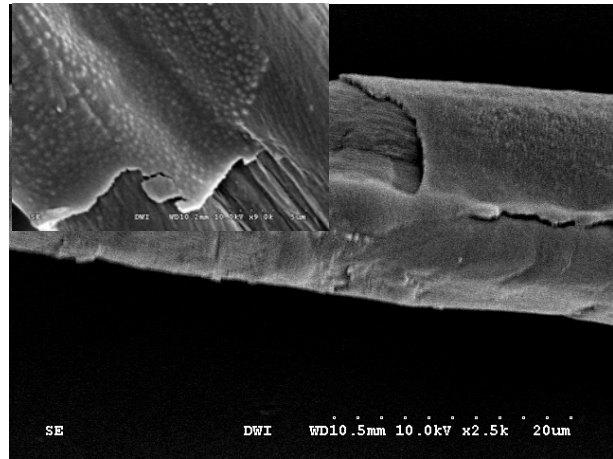
$$DWI\ GlossIndex = \frac{\int_{35^{\circ}}^{55} (LightSurface) dAngle}{\int_{15}^{75} (LightSurface) dAngle}$$

This definition is the extrapolation of the gloss index defined for measurements under a single wavelength ⁽¹⁴⁶⁾ and the wavelength from 400 – 650 nm (visible wavelength).

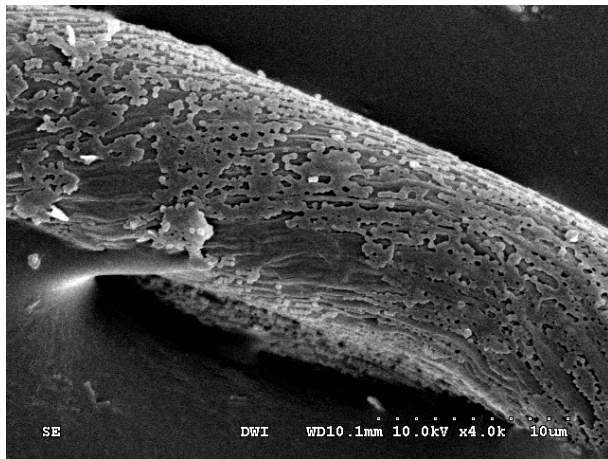
All the results measured and calculated as described above are shown in **Figure 53** and **Figure 54** for cotton and wool fibres respectively. These figures show the relative change of cotton and wool gloss, namely the ratio of DWI Gloss Index versus those of the white reference.



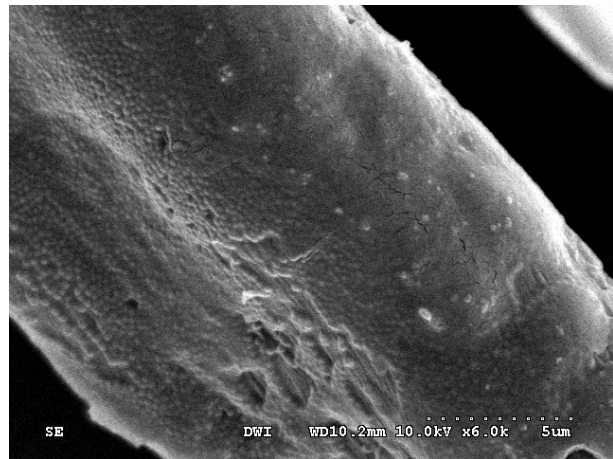
Cotton (25°C) – (MG_1) – pH = 4



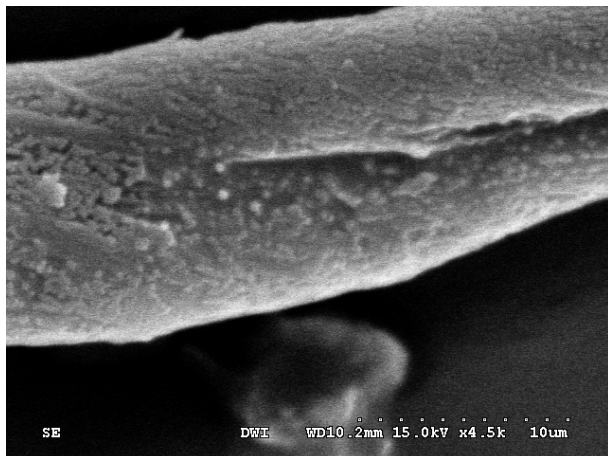
Cotton (50°C) – (MG_1) – pH = 4



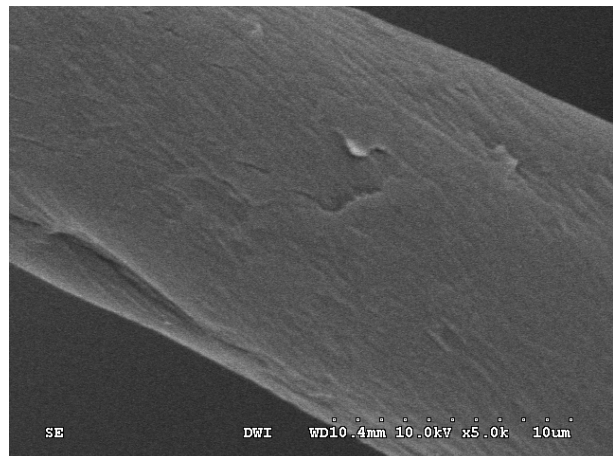
Cotton (25°C) – (MG_1) – pH = 8



Cotton (50°C) – (MG_1) – pH = 8

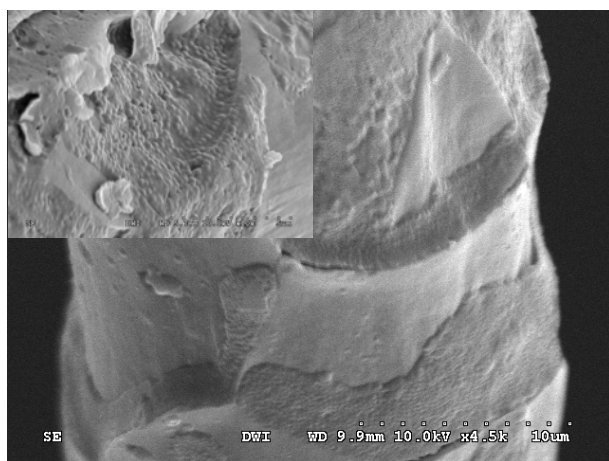


Cotton (25°C) – (MG_2) – pH = 8

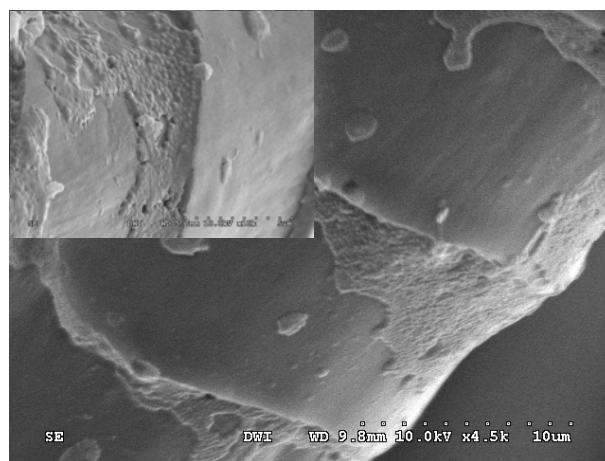


Cotton (50°C) – (MG_2) – pH = 8

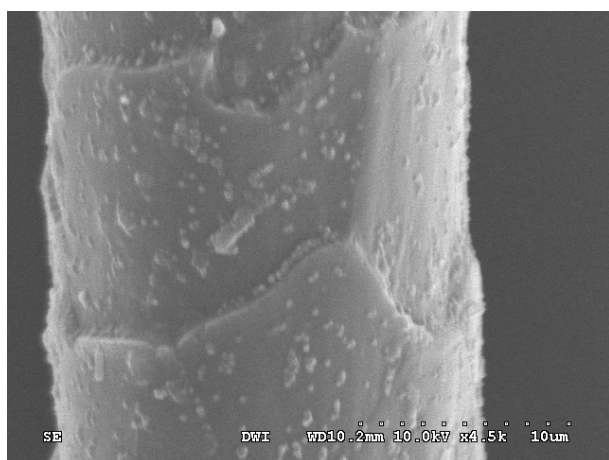
Figure 50: SEM image of treated cotton fibres using microgels MG1 and MG2.



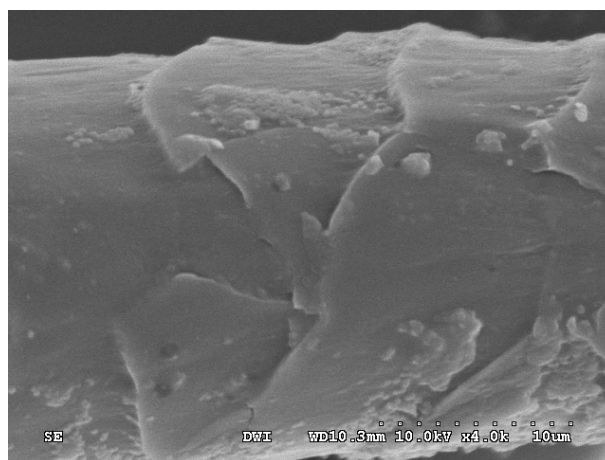
Wool (25°C) – (MG_1) – pH = 4



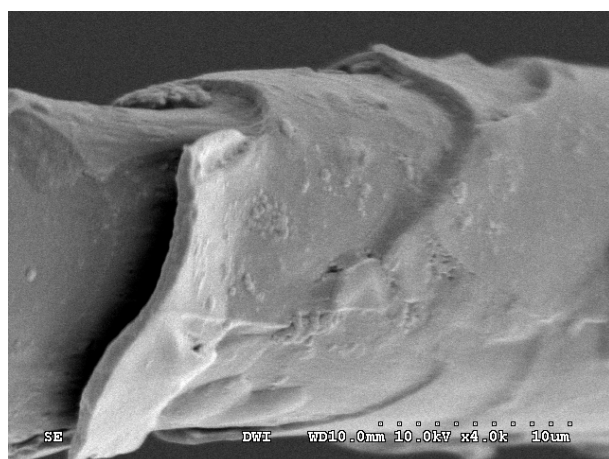
Wool (50°C) – (MG_1) – pH = 4



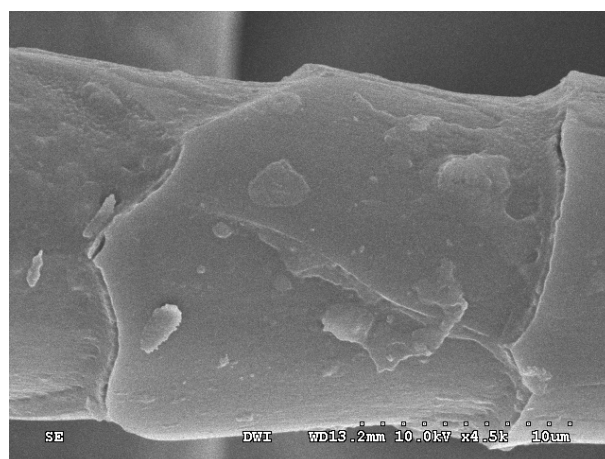
Wool (25°C) – (MG_1) – pH = 8



Wool (50°C) – (MG_1) – pH = 8



Wool (25°C) – (MG_3) – pH = 4



Wool (50°C) – (MG_3) – pH = 4

Figure 51: SEM image of treated wool fibres using microgels MG1 and MG3.

A measurement for untreated cotton and wool fibres against standard white colour are shown in **Figure 52**. The intensity of the reflected light measured at all wavelengths and angles gives the surface plotted below.

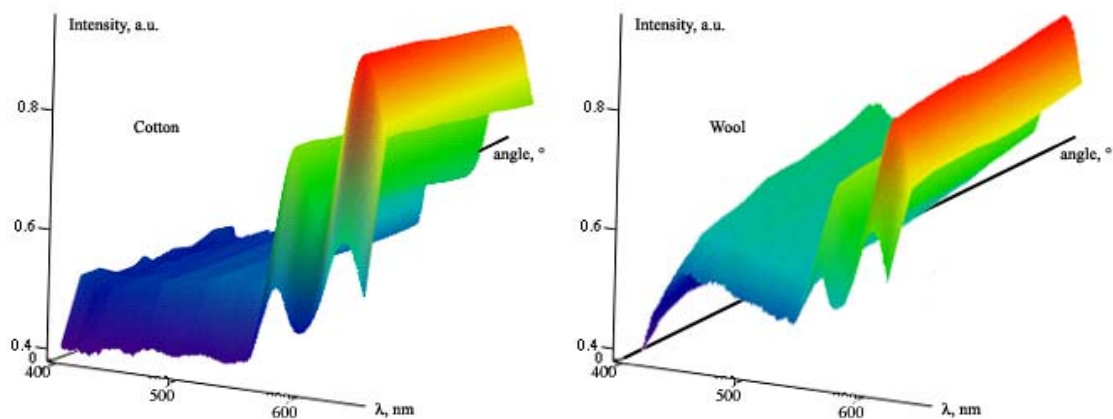


Figure 52: The light surface for cotton and wool fibres

For cotton fibres, **Figure 53** shows that the coating with any of microgels decreases the lustre of treated cotton fibre (expressed as DWI gloss index) under all treatment conditions. In addition, the gloss index of the cotton fibres treated with MG_2 at pH 8, room temperature, has a lower gloss index than all the other samples. It is clear that the treatment with MG_2 at pH 8 and 25°C (room temperature) reduces the gloss more than the other treatment conditions. The washing process of the treated fibre does not affect the gloss index property, meaning that the microgel is still on the fibre surface.

By comparing the data of gloss index, and SEM photo of treated cotton fibres, we found that cotton fibres coated with a monolayer of microgel particles have less lustre than untreated cotton. This may be attributed to the size of the microgel particles making the coating film, which have the ability to absorb the light more than the cotton surface itself.

Figure 54 shows the gloss index of wool fibres treated with MG_1 and MG_2. It shows that the lustre of treated wool fibre (expressed as DWI gloss index) increases after any treatment. The gloss index of the wool fibres treated with MG_1 at pH 8, 25°C (room temperature) has the highest gloss index of wool fibres. The washing of the treated fibres decreases the gloss index which comes close to those of the untreated fibres. This indicates that the treatments are temporary for wool fibres and can be easily removed by washing.

The gloss index data and the SEM images suggest that the wool fibres having the particles arranged as dots on the surface have also a high lustre. This may be attributed to the small and spherical size of the microgel particles which deposit onto the surface as random islands and which may therefore increase the gloss index compared to the untreated fibres. These values decrease after washing, which indicates that the treatment is temporary.

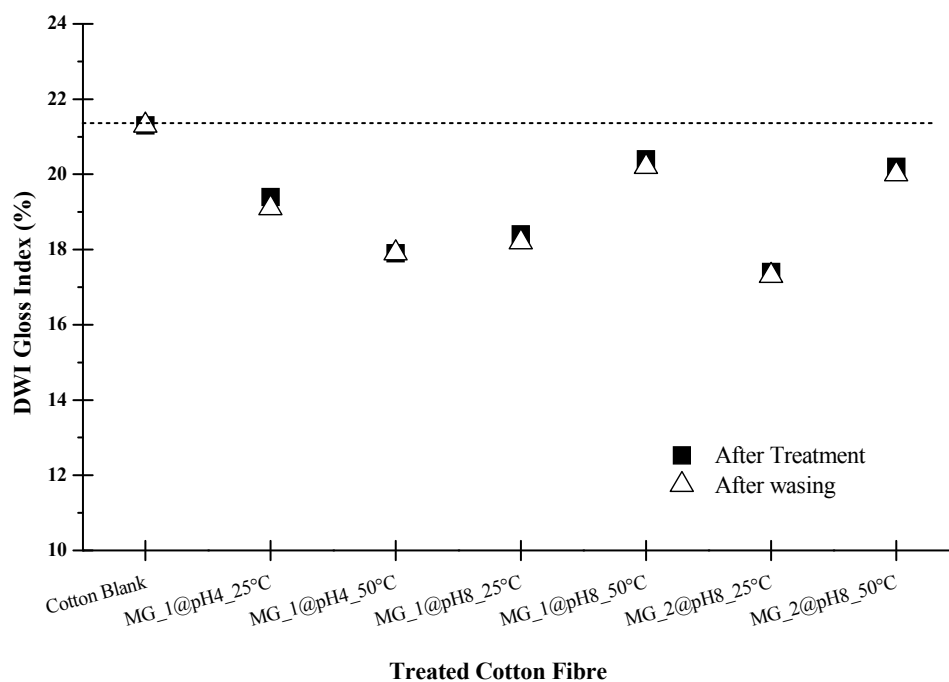


Figure 53: Gloss index values of treated cotton fibre with various microgels
Visible wavelength (400 – 650 nm) and selected angle 35 – 55°

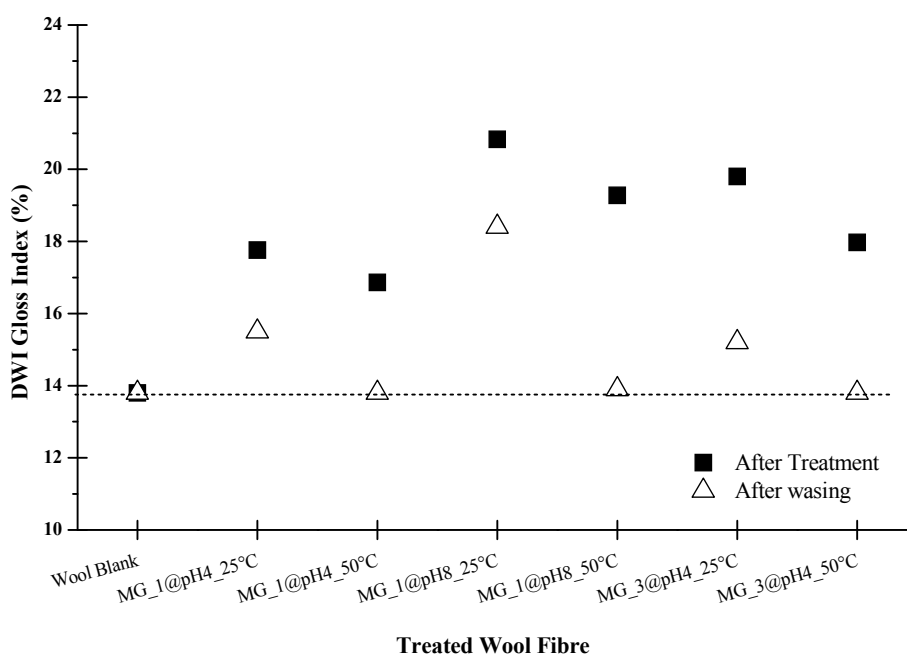


Figure 54: Gloss index values of treated wool fibre with various microgels
Visible wavelength (400 – 650 nm) and selected angle 35 – 55°

5.4. Conclusions

Three different microgels based on poly(N-vinylcaprolactam) (PVCL) and vinylimidazole (VIm), acetoacetoxyethyl methacrylate (AAEM) and itaconic acid dimethyl ester (IADME) were prepared and used to coat different fibre surfaces. The structures of the prepared microgel were confirmed with ^1H -NMR and ^{13}C -NMR. Scanning electron microscopy indicates that the diameter of the particles ranges from 200 to 300 nm for all microgels. The fibres were treated for 30 min at room temperature or 50°C, respectively, and at pH of 4, or 8, respectively. The fibres were examined by scanning electron microscopy and measured for gloss.

Scanning electron microscope images prove that the microgels behave differently depending on the surface of the fibre, chemistry of the microgel and parameters of the treatment (pH and temperature). The gloss measurement of the fibres confirms the results from scanning electron microscopy. As it appears, if the microgel coat the fibre surface with a thin layer film the gloss index decreases; if the coating forms small islands, (the microgels are held together and make randomised islands), the gloss index increases. One may understand from this that the increasing of the gloss index is given by a special distribution of the microgel particles on the investigated surface. The arrangement of particles in dots randomized the reflected light which helps increasing the gloss index.

The chemistry of the microgel affects the deposition of the particles on the fibre surface, the microgel behaving differently at the same pH on different fibres. The use of VIm monomer into microgel structure allows controlling the gloss index by handling the pH and the temperature of the treatment.

Summing up it appears that, by controlling the structure of the microgel layer by adjusting the pH and temperature of the coating process, one may control the resulted gloss index of any fibre.

6. Deposition of Functionalized Polyethylenimine-Dye onto Cotton and Wool Fibres

6.1. Introduction

The use of the PEI in the fibre pre-treatment favours to a great extent the adsorption of a reactive dye onto fibres, and could be very interesting for textile industry because it produces a strong increase of antimicrobial activity ⁽⁵⁴⁾.

Since PEI has three types of amine group (primary, secondary and tertiary), the high density of primary, secondary and tertiary amino groups exhibiting protonation only on every 3rd or 4th nitrogen at pH 7 confers significant buffering capacity to the polymers over a wide pH range. This property, known as 'proton sponge property' ⁽¹⁴⁷⁾ is likely one of the crucial factors for the high transfection efficiencies obtained with these polymers.

The adsorption behaviour can most probably be ascribed to pure electro-sorption behaviour where the initial increase is linked to a coiling of the polyelectrolyte with increasing salt concentration. Since the fibres are highly porous, this will allow the polymer to enter some of the large pores of the fibre wall. This will in turn lead to a higher polyelectrolyte adsorption⁽⁵⁹⁾.

Pille *et al* ⁽⁸⁶⁾ reported that, the bound lipid layer onto the surface of wool causes the colloids to be not adsorbed onto untreated fibre. After removing the lipid layer, there is a monolayer adsorbed onto the surface by treatment with much diluted solution. This indicates that the lipid layer represents a major adsorption barrier for the cationic polymer particles. As pointed out by Van De Ven ⁽¹⁴⁸⁾ and by Lindström ⁽⁸⁸⁾ during the adsorption the following processes occur:

- Transport of the polyelectrolytes from the solution to the fibre surface (the definition of the available fibre surface is dependant on the molecular mass of the polyelectrolyte)
- Attachment of the polyelectrolyte on the fibre surface
- Detachment of the polyelectrolyte from the fibre surface

In this study we use new agents for carrying colour to wool and cotton fibres based on polyethyleneimine modified with quaternary ammonium group and reactive dye molecules. The used polymers have cationic charges required for a good adsorption to the fibre since they interact with the fibre surface which carries negative charges. ⁽⁶⁰⁾ The paper presents the system and some results of the isotherm and kinetic studies on its sorption by wool and cotton fibres.

6.2. Experimental

6.2.1. Materials

Glycerol ($C_3H_8O_3$, Acros), dimethyl carbonate ($C_3H_6O_3$, Acros), 1,4-diazaobicyclo[2.2.2]octane (DABCO, $C_6H_{12}N_2$, Aldrich), pyridine (C_5H_5N , Aldrich), phenyl chloroformate ($C_7H_5ClO_2$, Acros), 3-dimethylamino-1-propylamine ($C_5H_{14}N_2$, Aldrich), 2-chloro-4-nitrobenzenediazonium chloride ($C_6H_3N_3O_2Cl$, Fluka), aminopropylmethyl aniline ($C_{10}H_{16}N_2$, Aldrich), methyl iodide (CH_3I , Acros), acetic acid (CH_3COOH , Aldrich), ammonia (NH_4OH , Aldrich) and sodium carbonate ($NaCO_3$, Aldrich), sodium sulphate (Na_2SO_4 , Acros), poly(ethylene imine) (PEI, water free $M_w=25000$ g/mol, Aldrich, **Figure 55**), dichloromethane (CH_2Cl_2 , Acros), toluene (Acros) and *N,N*-dimethylformamid (DMF, Acros) dimethylsulfoxide (DMSO, Acros), were used as received. Tetrahydrofuran (THF, Fluka) was dried over sodium and distilled before use. Bleached cotton and wool fibres used for application.

Basic Red 51 **Figure 55**, *Chemical name*: 2-[[[(4-Dimethylamino)phenyl]azo]-1,3-dimethyl-1H-imidazolium chloride, *Trade name*: Vibracolor Ruby Rot; MIP 2985, Emp. Formula: $C_{13}H_{18}ClN_5$, M_w : 279.6 g/mol

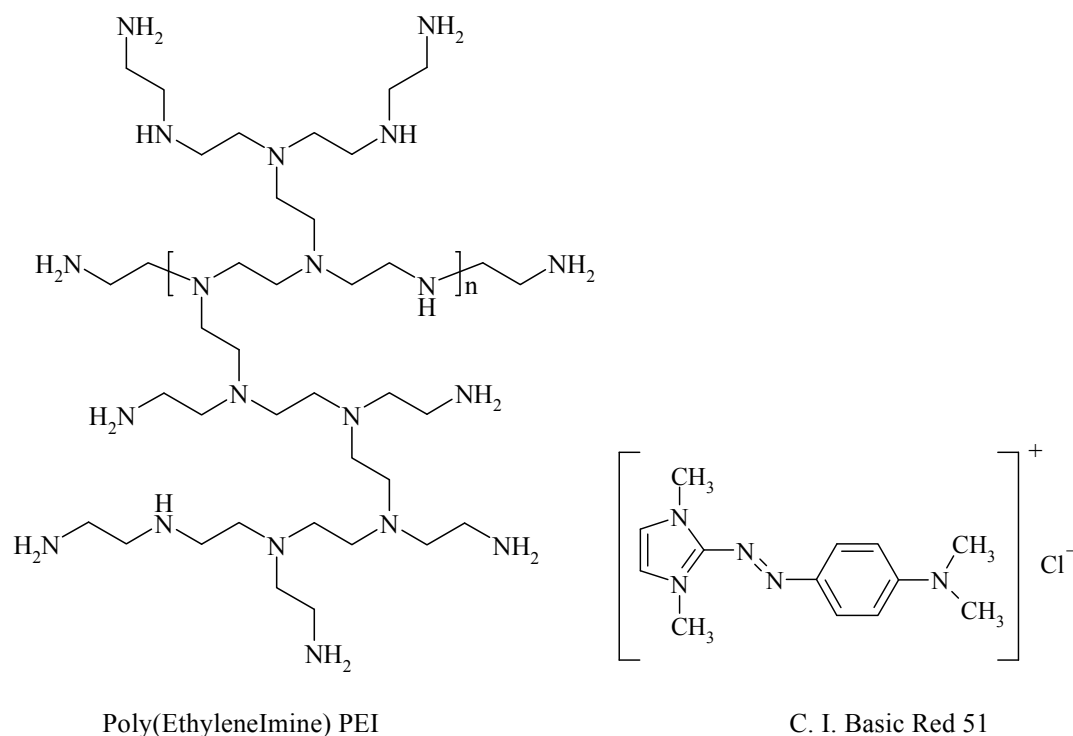
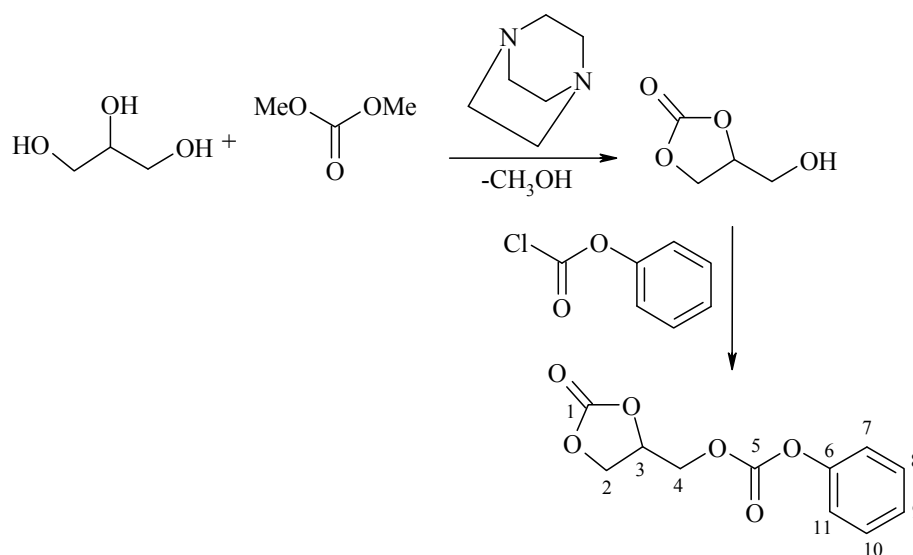


Figure 55: Chemical structure of PEI and C. I. Basic Red 51

6.2.2. Methods

6.2.2.1. Synthesis of Quaternary Ammonium Salt (QI)

Preparation of quaternary ammonium salt (QI) occurred in two steps, the first step is to prepare (2-oxo-1,3-dioxolan-4-yl)methyl phenyl carbonate according **Scheme 11**: Glycerol (10 g, 109 mmol), dimethyl carbonate (29.2 g, 326 mmol) and DABCO (121 mg, 1.08 mmol) were mixed and heated at 75°C for 10 h. After distillation of formed methanol and excess of dimethyl carbonate obtained glyceryl carbonate. The glyceryl carbonate (30 g, 254 mmol) and Pyridine (22 g, 278.13 mmol) were dissolved in THF (310 mL). The solution was cooled to 0°C, and a solution of phenyl chloroformate (43.7 g, 279.2 mmol) was added drop-wise to keep the temperature below 5°C. The reaction was stirred overnight at room temperature. The formed pyridine hydrochloride was removed by filtration and the solution was washed three times with water and brine. The organic phase was dried over Na₂SO₄ and the filtrate was diluted with 200 mL diethylether and was washed with equal volume (300 mL each) of water, 0.1% hydrochloric acid, 0.1% sodium hydroxide and 5% brine solution. in rotary vacuum (20 mbar, 40°C). The crude product formed was recrystallized from 350 mL chloroform at 40°C and a fine colourless powder of (2-oxo-1,3-dioxolan-4-yl)methyl phenyl carbonate was obtained. ¹H NMR and ¹³C NMR corresponded to the data reported in the literature ⁽¹⁴⁹⁾.



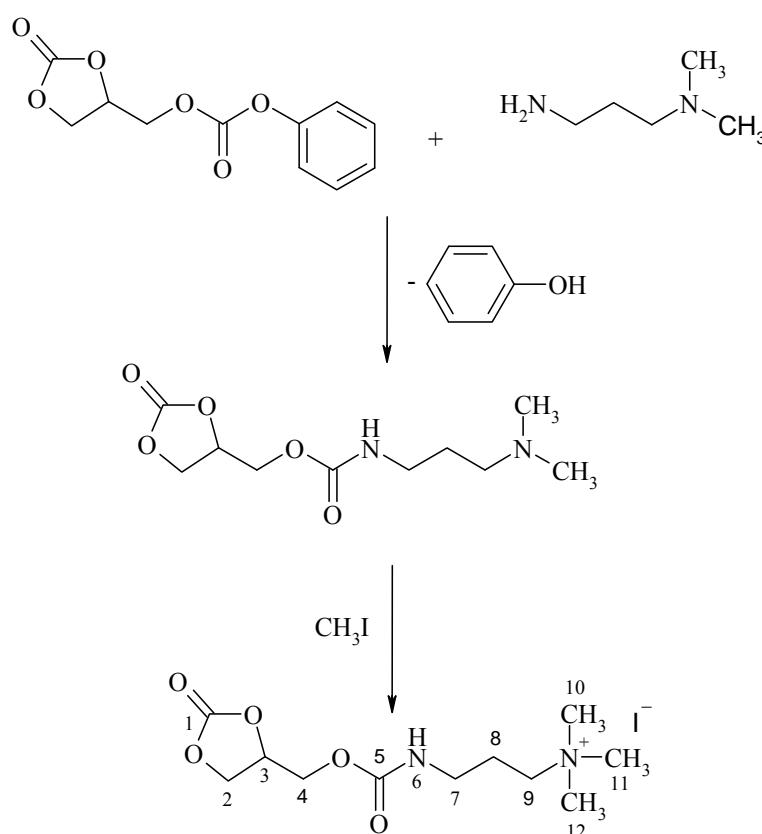
2-oxo-1,3-dioxolan-4-yl)methyl phenyl carbonate

Scheme 11: Scheme to preparation of 2-oxo-1,3-dioxolan-4-yl)methyl phenyl carbonate

¹H NMR (DMSO-*d*₆): δ= 4.39 (m, 1H, H²); 4.46 (m, 1H, H⁴); 4.53 (m, 1H, H⁴); 4.62 (m, 1H, H²); 5.11 – 5.18 (m, 1H, H³); 7.25 – 7.45 (m, 5H, phenyl) ppm

¹³C NMR (DMSO-*d*₆): δ= 65.7 (C²); 67.5 (C⁴); 74.0 (C³); 121.2 (2C, C⁷, C¹¹); 126.3 (C⁹); 129.6 (2C, C⁸, C¹⁰); 150.6 (C⁶); 152.70 (C⁵); 154.60 (C¹) ppm.

The second step is to prepare the quaternary ammonium salt (*N,N,N*-trimethyl-3-(((2-oxo-1,3-dioxolan-4-yl)methoxy)carbonylamino)propan-1-ammonium iodide) (**QI**) according to **Scheme 12**. The dicarbonate (10 g, 42.01 mmol) obtained in the first step was dissolved in 100 mL dry THF and cooled to 0°C. Solution of 3-dimethylamino-1-propylamine (4.29 g, 42.01 mmol) in 21 mL dry THF was then added drop-wise and temperature was kept below 5°C. The reaction mixture was stirred at this temperature for two hour and then stirred at room temperature for 20 hours. A solution of methyl iodide (11.92 g, 84 mmol) in 60 mL dry THF was added drop-wise under intensive stirring within 3 h and the solution was stirred for additional 1 hour at 60°C. The formed white powder was filtered and washed with dry THF (10 mL × 3 times) dried in vacuum 10⁻² mbar to obtained light yellow solid. ¹H NMR and ¹³C NMR corresponded to the data reported in the literature ⁽¹⁴⁹⁾.



N,N,N-trimethyl-3-(((2-oxo-1,3-dioxolan-4-yl)methoxy)carbonylamino)propan-1-ammonium iodide

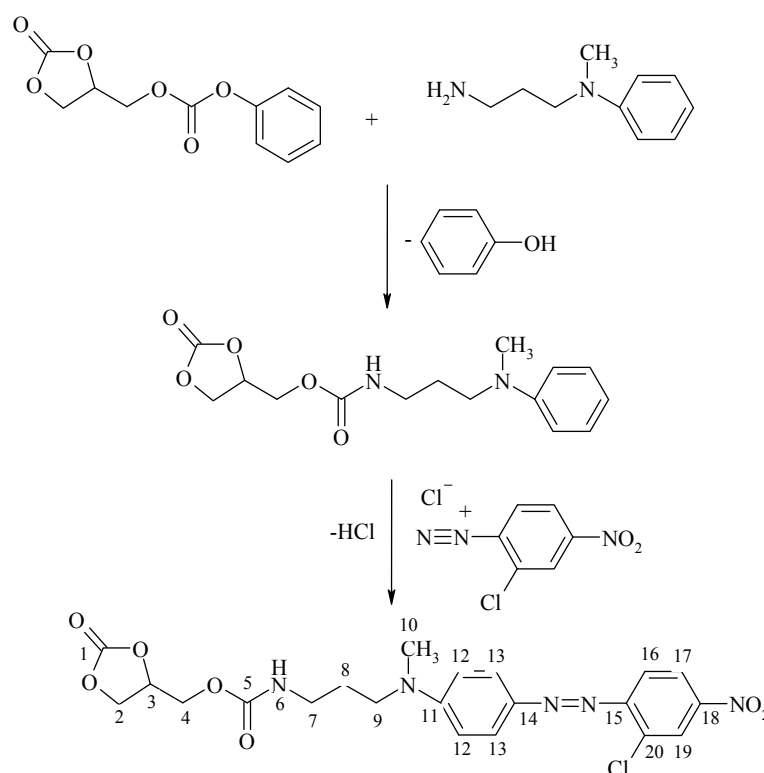
Scheme 12: Scheme of the second step to prepare the quaternary ammonium salt (**QI**)

¹H NMR (DMSO-*d*₆): δ= 1.74 – 1.95 (m, 1H, H⁸); 3.00 – 3.20 (m, 11H, H⁷, H¹⁰, H¹¹, H¹²); 3.25 – 3.45 (t, 2H, H⁹); 4.10 – 4.34 (m, 3H, H², H⁴); 4.59 (t, 1H, H²); 4.96 – 5.14 (m, 1H, H³); 7.39 (t, 1H, H⁶) ppm

¹³C NMR (DMSO-*d*₆): δ= 22.9 (C⁸); 37.3 (C⁷); 52.3 (3C, C¹⁰, C¹¹, C¹²); 63.2 (C⁹); 66.9 (C⁴); 74.6 (C³); 154.6 (C⁵); 155.70 (C¹) ppm.

6.2.2.2. Synthesis of the Reactive Dyestuff (RD)

Preparation of the reactive dye (2-oxo-1,3-dioxolan-4-yl)methyl 3-((4-((2-chloro-4-nitrophenyl) diazenyl) phenyl) (methyl) amino) propylcarbamate (RD) is illustrated in **Scheme 13**: 2-oxo-1,3-dioxolan-4-yl)methyl phenyl carbonate (Dicarbonate) was dissolved in dry THF and the solution was cooled to 0°C. Next the solution of amine in dry THF was added dropwise so that the temperature does not overcome 5°C. The reaction mixture was stirred at RT for additional 20 h. The solvent was removed by distillation (40°C, 30 mbar). The raw product dissolved in CH₂Cl₂ was extracted with water, NaOH (5%), (HCl 5%) and brine to give (after evaporation of solvent) a yellow oil. This yellow oil was dissolved in CH₂Cl₂ and then 2-chloro-4-nitrobenzenediazonium chloride added dropwise during 2 hour, the mixture left for stirring for 20 h at 60°C, then the solvent was removed by extraction in water, NaOH 5%, HCl 5% to give finally (after evaporating the solvent) a dark red oily product, which was used without further purification.



(E)-(2-oxo-1,3-dioxolan-4-yl)methyl 3-((4-((2-chloro-4-nitrophenyl)diazenyl)phenyl)(methyl)amino)propylcarbamate

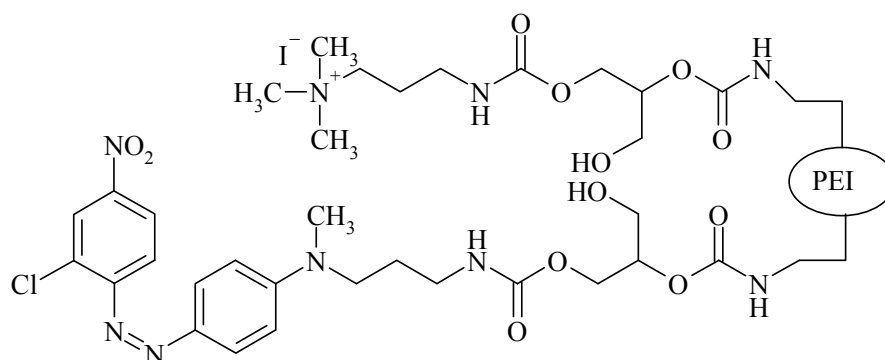
Scheme 13: Scheme to prepare the reactive dyestuff (RD)

¹H NMR (DMSO-*d*₆): δ = 1.68-1.82 (m, 2H, H⁸); 2.95-3.20 (m, 5H, H¹⁰, H⁷); 3.43-3.60 (t, 2H, H⁹); 4.15-4.40 (m, 3H, H^{4a}, H²); 4.50-4.65 (t, 1H, H^{4b}); 4.95-5.10 (m, 1H, H³); 6.80-6.95 (d, 2H, H¹²); 7.45-7.55 (m, 1H, H⁶); 7.70-7.80 (d, 1H, H¹⁶); 7.80-7.90 (d, 2H, H¹³); 8.15-8.25 (d, 1H, H¹⁷); 8.35-8.45 (d, 1H, H¹⁹).

^{13}C NMR ($\text{DMSO-}d_6$): $\delta = 26.7$ (C^8); 38.08 (C^{10}); 38.36 (C^7); 49.37 (C^9); 63.15 (C^2); 65.88 (C^4); 74.84 (C^3); 111.70 (C^{12}); 117.92 (C^{16}); 123.30 (C^{17}); 125.68 (C^{19}); 126.61 (C^{13}); 132.28 (C^{20}); 143.29 (C^{14}); 146.65 (C^{15}); 152.30 (C^{18}); 152.98 (C^{11}); 154.69 (C^1); 155.68 (C^5).

6.2.2.3. Synthesis of Functionalized Polyethylenimine-Dye

1 g of PEI was dissolved in 10 mL of DMF. The mixture of RD and QI with different ratio (see results in **Table 19**) was dissolved in 20 mL of DMF and added to the PEI solution. The reaction mixtures were immersed in the oil bath at 60°C . After 48h, DMF was removed by evaporation under reduced pressure to give an intensively red powder. The prepared functionalized polyethylenimine-dye (FPEI) was used without further purification for deposition onto fibres. The structure of functionalized polyethylenimine-dye (FPEI) is schematically presented in **Scheme 14**.



Scheme 14: Structure of functionalized polyethylenimine-dye (FPEI)

Table 19: Composition of modified poly(ethyleneimine)s (FPEI)

FPEI	RD functionalized dyestuff		QI cationic functionalized dyestuff	
	Weight (g)	Mol-%*	Weight (g)	Mol-%*
FPEI_1	1.15	100	-----	00
FPEI_2	0.92	80	0.16	20
FPEI_3	0.69	60	0.33	40
FPEI_4	0.46	40	0.51	60
FPEI_5	0.23	20	0.67	80

*refers to amount of primary amine in poly(ethyleneimine) structure.

6.2.2.4. The Pre-treatment of the Fibres

The cotton and wool fibres were washed before coating with the FPEI compounds. The treatment aimed to remove the waxy materials and impurities from the outer surface of the fibres. Cotton fibres were washed with Na_2CO_3 solution 2 g/L, and wool fibres were washed with CH_2Cl_2 for 15 min.

6.2.2.5. Deposition onto Cotton and Wool Surfaces

The deposition was performed from a solution of 0.2 g/L functionalized poly(ethyleneimine)s in water at 50 and 90°C for wool and cotton respectively; pH 5, 7 and 9 (pH was adjusted using acetic acid and sodium carbonate); and liquor ratio 1: 20 were used for the deposition. The tresses of fibres were immersed in polymer solution and left for 30 min, after which the fibres were taken out of the solution, washed with water for 15 min in presence of non-ionic detergent 2 g/L and sodium carbonate 0.2 g/L at 90 and 50°C for cotton and wool respectively, then dried at 100°C for 5 min.

6.2.3. Measurements

6.2.3.1. NMR Measurements

^1H NMR spectra were recorded on a Bruker DPX-400 FT-NMR spectrometer at 400 MHz, using DMSO as solvent.

6.2.3.2. Adsorption and Isothermal Studies

Five known concentrations for each FPEI compound were prepared and measured using a UV-visible spectrophotometer (model HP 8452 A Diode Array) at $\lambda_{\text{max}} = 498$ for making the calibration standard curve. This allows us converting the measured absorbance into concentration in order to monitoring the amount of FPEI adsorbed onto the fibres before and after washing.

For each experimental treatment run, 1g cotton or wool was placed into 250 mL flask containing FPEI solution at a liquor ratio 1:20. The FPEI solution is of 0.2 mg/mL, and pH of 7 and 9 for wool and cotton respectively; the pH of the solution was controlled by the addition of CH_3COOH or Na_2CO_3 solutions. The flask was agitated in a shaking water bath at a constant speed of 100 rpm for 30 min. For each washing run, the treated cotton or wool fibre was placed into 250 mL flask containing detergent 2 g/L during 20 min at 50 and 90°C for

wool and cotton respectively in a Liquor Ratio of 1:20. The fibres were then rinsed with cold water for 90 sec.

All the rinsed fibres were measured for colour strength with a Data colour device (model 3890, Marl Co, Germany). The residual solutions were also analysed for the residual FPEI concentration by measuring absorbance at $\lambda_{\text{max}}=498$ using UV-vis spectrophotometer (model HP 8452 A Diode Array).

For kinetic studies, after the treatment or washing, sampling was done at 0, 30, 60, 90,...1800 seconds. 1 mL of the sampled aqueous phase was measured for the residual concentration of FPEI using a UV-vis spectrophotometer, and then put back into the treatment or washing solution for keeping the concentration constant.

For isotherm studies, solutions of various FPEI concentrations ranging from 0.05 to 6 mg/mL were prepared in separate 100 mL conical flasks. 1g of fibres was transferred into each of the conical flasks. After 30 min, the fibres were rinsed with hot water for 90 sec and dried. The washing experiment was carried out for each treated fibre separately suitable condition as written before, and then the fibres were analysed with Data colour.

The absorbance measured was then converted to concentration. Duplicate experiments were performed in parallel to check the results.

6.2.3.3. Colour Measurements

The extent of coloration and the spectral reflectance values of the treated dyed fibre samples were measured at the wavelength of maximum absorbance using a computerized automatic filter spectrophotometer (Data colour device model 3890, Marl Co., Germany). The colour intensity (ΔE) and the relative colour strength (K/S) of the untreated and treated cotton fibres was measured.

The relative colour strength (expressed as (K/S) values) was assessed by applying the Kubelka–Munk equation as follow: ⁽¹⁵⁰⁾

$$K/S = \frac{(1-R)^2}{2R} - \frac{(1-R_o)^2}{2R_o} \quad \text{Equation 9}$$

where: K: is the absorption coefficient, S: is the scattering coefficient, R_o : is the reflectance of uncoloured (white) sample and R: is the reflectance of coloured sample

6.3. Results and Discussion

6.3.1. Synthesis of Reactive Dyestuff (RD)

Reactive dyestuff was obtained in two-steps, the first step is by reaction (2-oxo-1,3-dioxolan-4-yl)methyl phenyl carbonate with aminopropylmethyl aniline (see **Scheme 13**). Pasquier *et al.* ⁽¹⁴⁹⁾ showed that this type of dicarbonate reacts chemo-selectively with primary amines. At low temperatures (0-25°C) the phenyl carbonate reacts in a substitution reaction, while the cyclic carbonate ring is opened only at higher temperatures (25-60°C).

Based on these results in the first step of dyestuff preparation the reactive cyclic dicarbonate was reacted with aminopropylmethyl aniline as presented in **Scheme 13**. After removal the by-product (phenol), the chromophore moiety was introduced to the benzene ring using azo-coupling to give the reactive dyestuff.

The resulting reactive azo-dye (RD) was a red powder soluble in organic solvents like DMF, THF or chloroform but insoluble in water. A UV-VIS spectrum shown in **Figure 56**; it has an absorption band in the range 400 – 600 nm with a peak at 505 nm, typical for red dyestuffs ⁽¹⁵¹⁾.

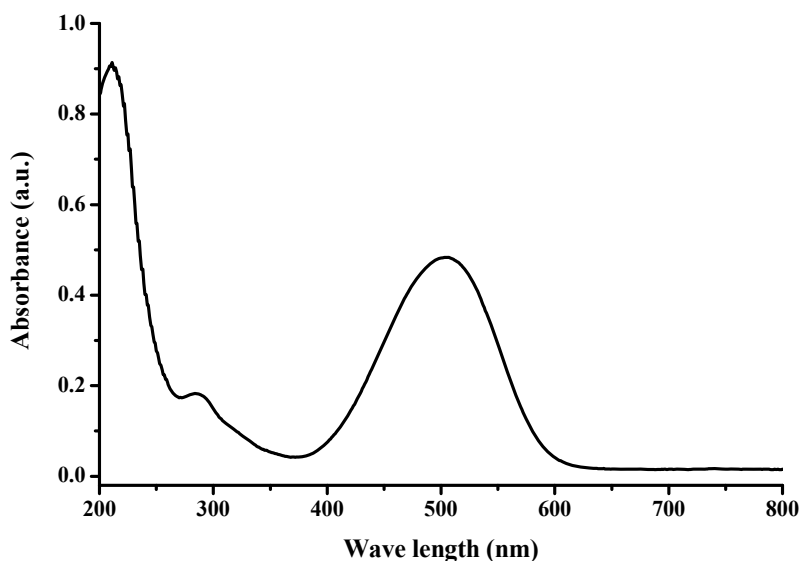


Figure 56: UV-VIS absorption spectra of reactive dyestuff in THF (c = 0.02 g/L)

6.3.2. Synthesis of Modified Poly(ethyleneimine)s

Poly(ethyleneimine) (PEI) of Mwt=25 000 g/mol was chosen as polymer-carrier. It is a commercially available branched polymer bearing about 25 mol-% of primary amine groups, 50 mol-% of secondary amine groups and 25 mol-% of tertiary amine groups. The presence of high amount of amine groups enables its modification and introduction of different

functionalities⁽¹⁴⁹⁾. However, since the carbonate ring attached to the dyestuff reacts only with primary amines we were able to modify only 25 mol-% of repeating units of PEI.

The structure of the obtained polymer-dye complex was investigated by ^1H NMR and UV-vis microscopy. The coupling of PEI with the functional carbonates is supported by the appearance of new signals, which can be assigned to formed urethane bonds. Additionally, the characteristic signals of the functional cyclic carbonates disappeared as shown in **Figure 57**.

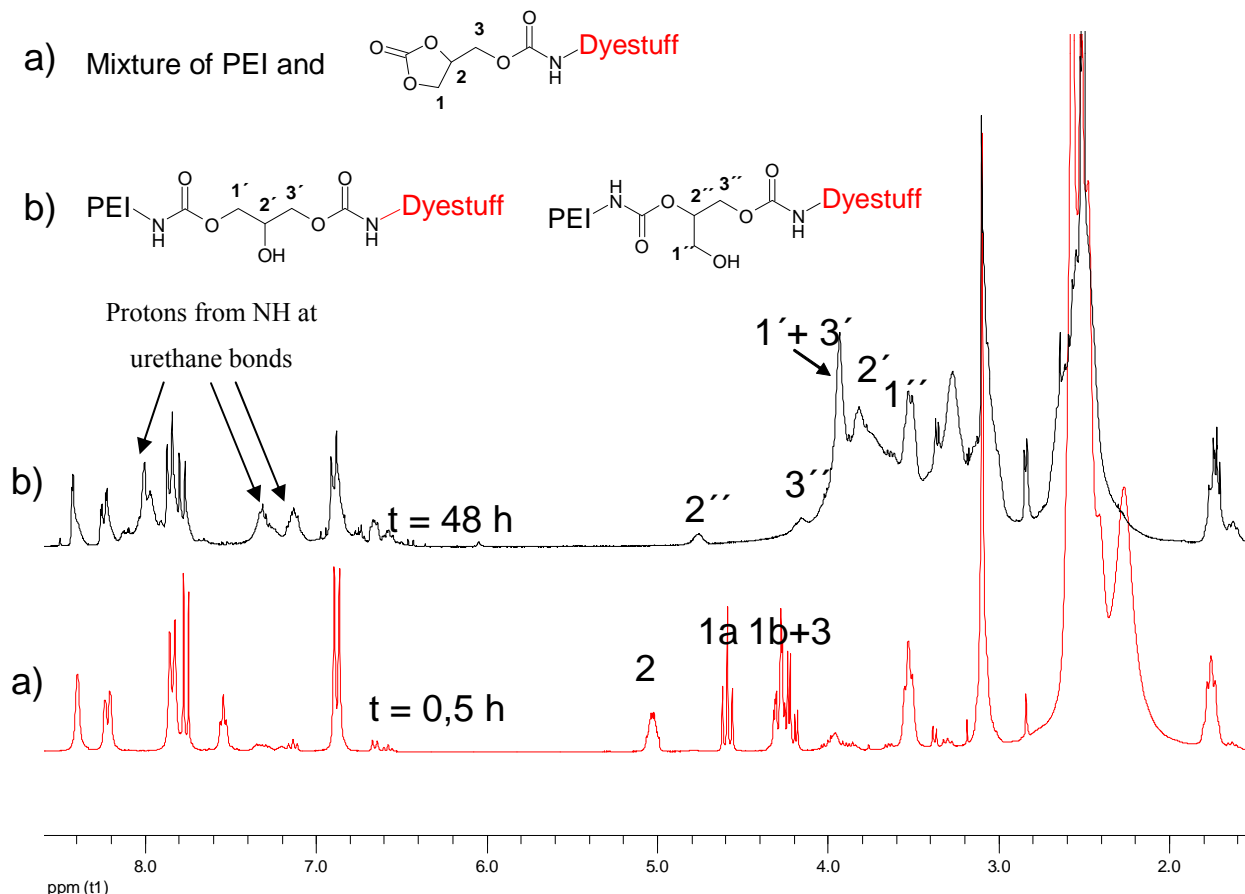


Figure 57: ^1H NMR spectrum of modified PEI in $\text{DMSO-}d_6$ (FPEI_1)

The composition of the resulting products could not be determined from the spectra due to overlapping of signals from dyestuff and cationic groups. However, as full conversion of reactive moieties was obtained the composition of the resulting modified poly(ethylene imine)s (FPEI) should be equal to the theoretical one. It is important for further experiments that the synthesised polymer-dyes are soluble in water. As it can be seen in **Figure 58** the intensity of the red colour of aqueous solutions of the polymer-dye increases as expected with increasing amount of dyestuff in the polymer structure (at the same concentration of the polymer-dye in solution). Additionally it confirms the formation of urethane bonds the linkage of amine groups of the polymer and to the carbonate ring of the dyestuff.

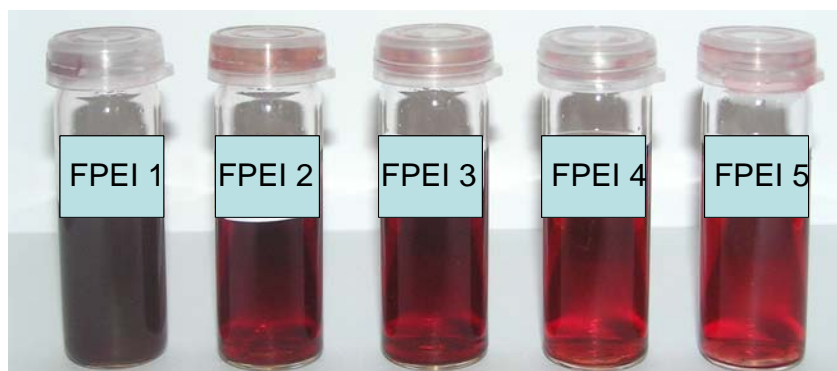


Figure 58: Water solutions of FPEIs at 0.2 g/L

The UV-VIS spectra (**Figure 59**) of the investigated FPEI compounds indicate a hypsochromic shift of the band characteristic for dyestuff from 505 nm to 435 nm. This phenomenon was more pronounced for samples with a higher content of the dyestuff. As a result the colour of sample solutions with a high content of dyestuff is purple-red, while that of samples with lower content of dye (40 mol% and less) is red. It should be noted that the samples contain the same amount of active dyestuff in the solution (the concentration of the polymer-dye was varied). Nevertheless, the intensity of the peak deriving from dyestuff is much lower for samples with high amount of dyestuff in its structure (FPEI 1 and FPEI 2).

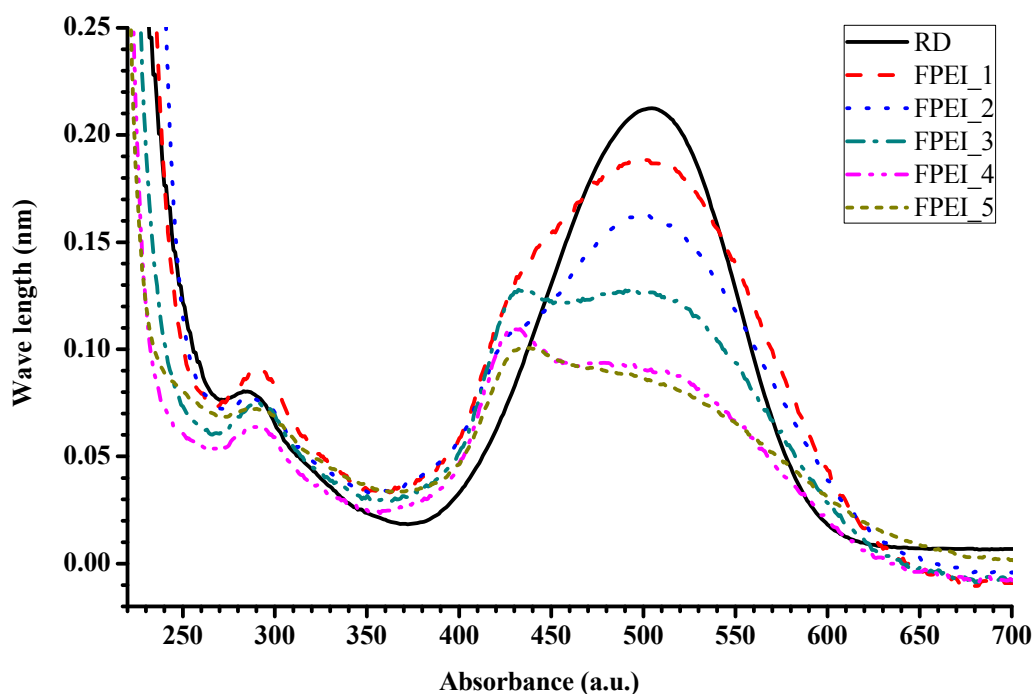


Figure 59: UV-VIS spectra of FPEIs in water at concentration of dyestuff 0.02 g/L

6.3.3. Adsorption of FPEI Compounds onto Fibres

The results of treatment were examined both for exhaustion with UV vis. spectrophotometer (in solution), and for colour intensity ΔE (spectrophotometer with reflection and visual, on fibre). Three kind of polymer-dye complex FPEI_1, FPEI_3 and FPEI_5, soluble in water, were used for dyeing of cotton and wool fibres at different pH.

6.3.3.1. Effect of pH

The effect of initial pH on the adsorption of FPEI compounds onto cotton and wool fibres were studied at a pH of 5 and 7 for wool and of 5, 7 and 9 for cotton, for an initial concentration of 0.2 mg dye/mL.

We observed that the maximum adsorption occurs at pH 7 for wool and pH 9 for cotton respectively, as shown in **Figure 60**. At high pH, a significantly high electrostatic attraction exists between the negatively charged surface of the adsorbent and positively charged cationic dye. As the pH of the solution decreases, the number of negatively charged sites increases and the number of positively charged sites decreases and this appears more with wool than with cotton fibre.

After washing, the amount of FPEIs decreases in all cases, but the final amount onto treated fibre is maximum for the coating from pH 9 for cotton and pH 7 for wool respectively.

6.3.3.2. Effect of Salt

The effect of salt added to the adsorption of FPEIs compounds onto cotton and wool was studied at pH 7 for wool and pH 9 for cotton respectively, for an initial concentration of 0.2 mg dye/mL.

Figure 61 shows the effect of adding salt on the adsorbed amount of FPEI onto cotton and wool fibres. One observes that in absence of salt the amount of FPEI on cotton and wool after washing is higher than in case of using salt. This may be understood as a result of competition for the same sites between the two electrolytes, salt and FPEI.

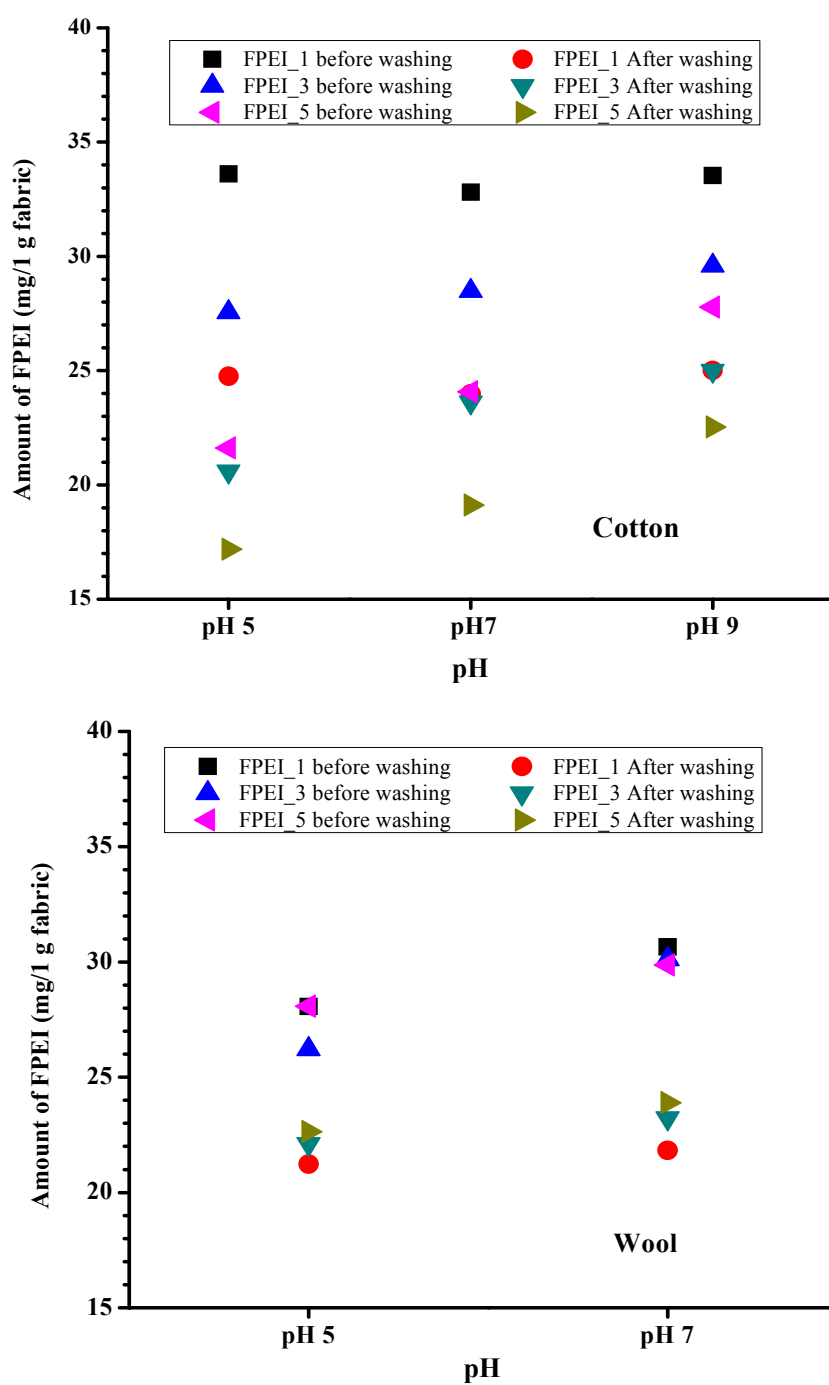


Figure 60: The amount of FPEI before and after washing adsorbed onto cotton and wool fibres at $\lambda = 498$ at different pH treatment medium

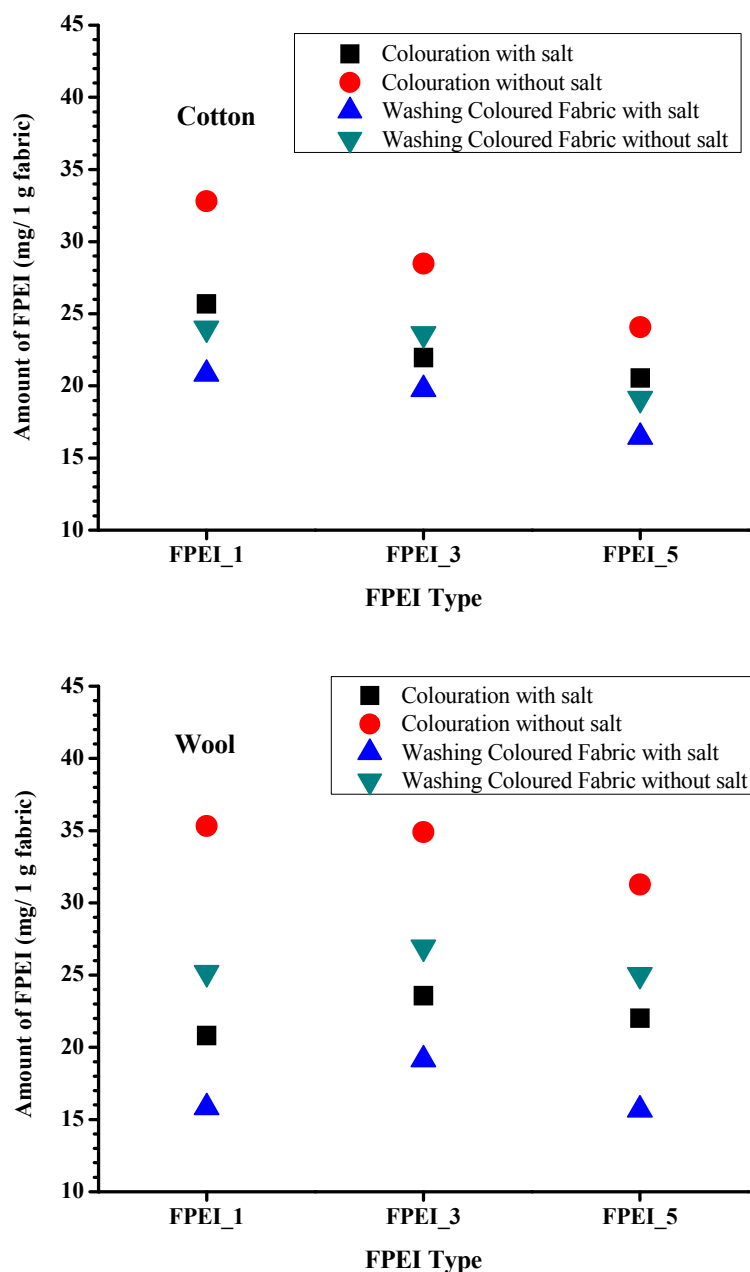


Figure 61: The amount of FPEI before and after washing adsorbed onto cotton and wool fibres at $\lambda = 498$ with and without salt added to treatment medium

6.3.4. Isothermal Studies

The colour intensity for treated fibres at different concentrations is measured by Data Colour. The values of ΔE are represented in colour intensity vs. concentration curve (**Figure 62**) and show that, for both fibres the colour intensity for the treated fibre decreases with increasing the amount of RD in the FPEI molecules. Also for the same FPEI compound we found that wool has a more intense colour than those achieved on cotton.

The colour intensity–concentration curve may be also used to describe the adsorption isotherm, for modelling how FPEI interacts with cotton and wool ⁽¹⁵²⁾.

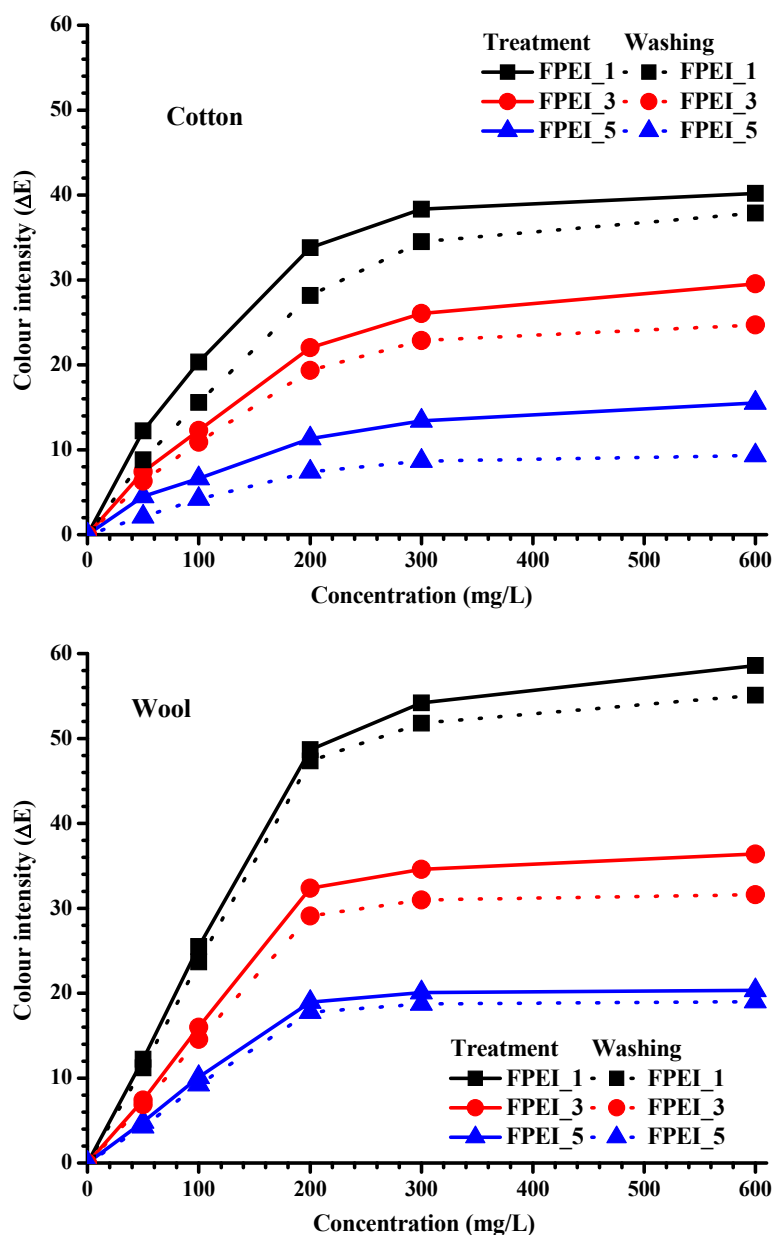


Figure 62: Colour intensity (ΔE) for cotton and wool fibres before and after washing without salt in the treatment medium

$$(\Delta E = E_{\text{sample}} - E_{\text{reference}})$$

Adsorption isotherms are described by many models, among most used for textile fibres being those of Langmuir, and Freundlich ⁽¹⁵²⁻¹⁵⁴⁾.

The Langmuir isotherm is widely used to describe single-solute systems. ^(53, 153-155) This isotherm assumes that intermolecular forces decrease rapidly with distance and consequently it predicts monolayer coverage of the FPEI on the outer surface of the fibre. Further assumption

is that adsorption occurs at specific homogeneous sites of the fibre surface and there is no significant interaction among adsorbed species. The Langmuir isotherm is given by the equation:

$$q_e = \frac{q_m C_e K_L}{1 + C_e K_L} \quad \text{Equation 10}$$

where q_e is the equilibrium FPEI concentration on the fibre (mg/g) (represent as ΔE in this study), C_e is the equilibrium FPEI concentration in solution (mg/L), q_m is the maximum capacity of the fibre (mg/g) (represent as ΔE_{\max} in this study), and K_L is the Langmuir adsorption constant (L/mg). Rearranging the terms in **Equation 10** one obtains a linearization of the Langmuir isotherm, as shown in **Equation 11**. The plot of $1/q_e$ versus $1/C_e$ gives a straight line with a slope of $1/q_e K_L$ and an intercept of $1/q_m$.

$$\frac{1}{q_e} = \frac{1}{q_m} + \left(\frac{1}{q_m K_L} \right) \left(\frac{1}{C_e} \right) \quad \text{Equation 11}$$

Freundlich isotherm may be also used for studying the adsorption of FPEI compounds on cotton and wool fibres. This empirical expression is good for describing heterogeneous systems. ⁽¹⁵⁵⁻¹⁵⁷⁾ The Freundlich isotherm equation is given below:

$$q_e = K_F C_e^{1/n} \quad \text{Equation 12}$$

where q_e is the equilibrium FPEI concentration on the fibre (mg/g) (represent as ΔE in this study), C_e is the equilibrium FPEI concentration in solution (mg/L), K_F is the Freundlich adsorption constant (L/mg), and n is the heterogeneity factor. The linear expression for the Freundlich isotherm is shown in **Equation 13**. The plot of $\ln(q_e)$ versus $\ln(C_e)$ gives a straight line with the slope of $1/n$ and an intercept of $\ln(K_F)$.

$$\ln q_e = \ln K_F + \frac{1}{n} \ln C_e \quad \text{Equation 13}$$

The two models were used for fitting the colour intensity data from treatment processes (**Figure 62**). **Table 20** lists the results of curve fittings with the above two adsorption isotherms. As one may notice, for both fibres the Langmuir model fits better the experimental data than the Freundlich model does (as evident from correlation coefficients R^2).

The fit to Langmuir model suggests that FPEI adsorbs on active sites of the fibre surface and form a monolayer.

Table 20: Comparison between the parameters of adsorption isotherm models

Fibre Type	FPEI Type	Langmuir Isotherm			Freundlich Isotherm		
		K_L	ΔE_{\max}	R^2	K_F	n	R^2
Coton	FPEI_1	0.004	71.02	0.9969	0.96	1.52	0.97916
	FPEI_3	0.003	53.39	0.99356	0.44	1.38	0.98734
	FPEI_5	0.003	20.46	0.97207	0.38	1.59	0.98784
Wool	FPEI_1	0.0018	187.62	0.99804	0.455	1.16	0.95892
	FPEI_3	0.0008	135.66	0.99786	0.239	1.11	0.94695
	FPEI_5	0.0008	122.34	0.99751	0.209	1.21	0.94174

6.3.5. Kinetic Study

The kinetics of the adsorption processes provides useful information regarding the efficiency of adsorption and feasibility of scale-up operations. The concentration time curves (**Figure 63**) of the adsorption of FPEI compounds on the surface of cotton and wool suggest that wool adsorbs higher amounts than cotton fibre. However, after washing the final amount on the surface of both fibres is almost the same for all FPEI compounds. FPEI_1 adsorbs on both fibres very well, exhausting 90% from bath content, but about 30% from the 90% desorbs by washing. One may also observe that by increasing the amount of QI in FPEI the amount of desorbed FPEI decreases (about 14 %) for both fibres. This shows that the amount of QI helps better binding of the compound to the fibre surface.. The data are listed in **Table 21**.

Table 21: FPEI concentration desorbed from the fibres after 1800 sec treatment

Fibre Type	FPEI	Concentration of FPEIs on the Fibre (mg/g fibre)		Loss Concentration by Washing
		Before washing	After washing	
Cotton	FPEI_1	35.81 (89.53 %)	23.99 (59.98 %)	11.82 (29.55 %)
	FPEI_3	29.19 (72.98 %)	23.61 (59.03 %)	5.58 (13.95 %)
	FPEI_5	24.07 (60.18 %)	19.12 (47.80 %)	4.95 (12.38 %)
Wool	FPEI_1	37.33 (93.33 %)	23.93 (59.83 %)	13.40 (33.50 %)
	FPEI_3	30.11 (75.28 %)	23.73 (59.33 %)	6.38 (15.95 %)
	FPEI_5	29.87 (74.68 %)	23.62 (59.05 %)	6.25 (15.63 %)

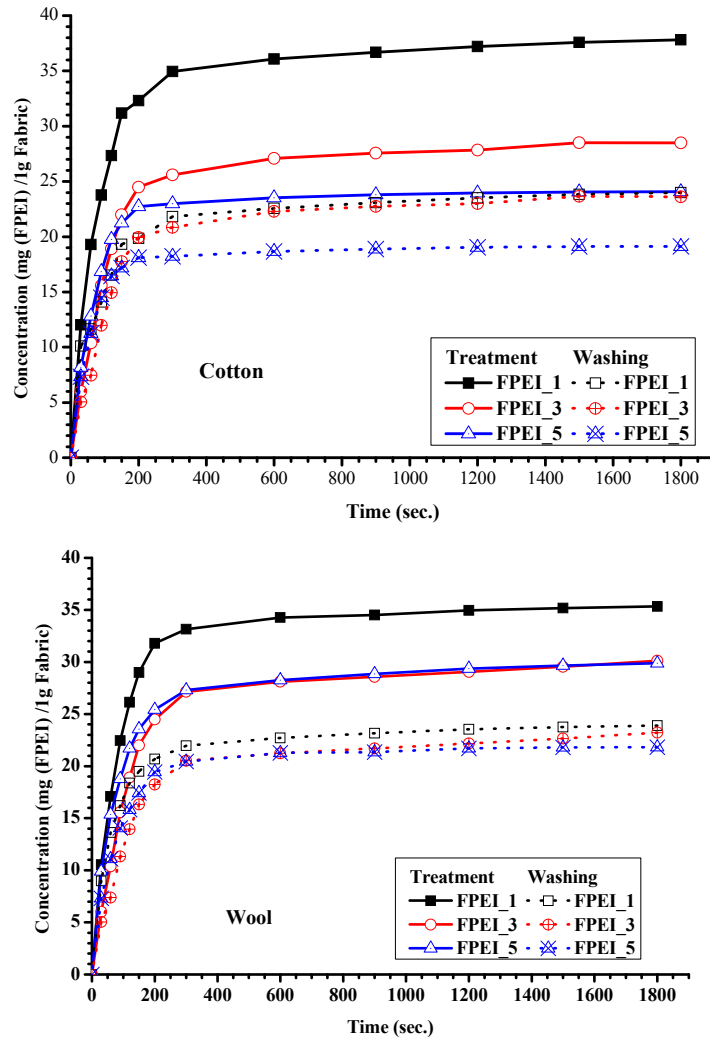


Figure 63: Concentration-time curve for cotton and wool fibres before and after washing without salt in the treatment medium

Two kinetic models were tested to find out the appropriate expression for the adsorption rate, viz.: the pseudo-first-order, ⁽¹⁵⁸⁾ and the pseudo-second-order model respectively ⁽¹⁵⁹⁾. The pseudo-first-order rate equation is given below:

$$\frac{dq}{dt} = k_1(q_e - q_t)^n \quad \text{Equation 14}$$

where q_t is the amount of dye adsorbed (mg/g) at time t , q_e is the maximum adsorption capacity (mg/g), k is the rate constant (min) and n is the reaction order. On integration the linear form can be written:

$$\ln(q_e - q_t) = \ln(q_e) - k_1 t \quad \text{for } n=1 \text{ (first order reaction)} \quad \text{Equation 15}$$

Or

$$q_e^{1-n} - (q_e - q_t)^{1-n} / (1-n) = k_1 t \quad \text{for } n \neq 1 \quad \text{Equation 16}$$

The values of adsorption rate constant (k for FPEI adsorption on cotton and wool were determined from the plot of the left-member of **Equation 14 and 16** versus t . The value of reaction order, n , was varied and the correlation coefficient was calculated for each plot. The value of reaction order was chosen for which the best linear correlation is achieved (the highest value for R^2). The corresponding values of rate-constant, k , and correlation coefficients R^2 are given in **Table 22**.

Table 22 indicates that the best fit is given by first-order kinetics for the data of adsorption of FPEI by cotton or wool fibres. The first order kinetic model suggests also that the mechanism of adsorption is a diffusional one.

Table 22: The values of the kinetic parameters as obtained from the experimental data

Fibre Type	FPEI Type	Pseudo-first- order	
		k_1	R^2
Cotton	FPEI_1	0.01812	0.9932
	FPEI_3	0.01432	0.9973
	FPEI_5	0.00981	0.9961
Wool	FPEI_1	0.02088	0.9999
	FPEI_3	0.00969	0.9958
	FPEI_5	0.00697	0.9937

6.3.6. Colour Strength

In order to evaluate the efficiency of FPEI compounds the colour strength of the coated fibre was measured and compared with fibres coloured with CI Basic Red 51. A perusal of data in **Table 23** reveals that:

- The colour strength of all treated fibres with FPEIs is generally higher than that of treated fibres with C.I. Basic Red 51,
- The colour strength of all treated fibres with FPEIs without salt is slightly higher than that of treated fibres with salt, and
- The colour strength of all treated fibres with FPEIs decreases by increasing the amount of QI in FPEI molecules; for a small amount of RD (FPEI_5) the colour strength is close to those of treated fibre with the commercial dyestuff (before and after washing),

Table 23: Colour strength of cotton and wool fibre treated with FPEIs compounds before and after washing with and without salt adding during the treatment at pH 7

FPEI Compounds	Wool Fibres		Cotton Fibres		
	After treatment	After washing	After treatment	After washing	
Blank	0.10729		0.042400		
CI Basic Red 51	0.70521	0.4838	0.254232	0.123831	
FPEI_1	With salt	4.222101	3.528172	0.678925	0.457679
	Without salt	4.508409	4.005851	1.141656	0.736235
FPEI_3	With salt	1.468749	1.262423	0.411119	0.275549
	Without salt	1.492475	1.272889	0.515364	0.413282
FPEI_5	With salt	0.531645	0.425299	0.183860	0.117254
	Without salt	0.612963	0.495531	0.186292	0.117577

6.4. Conclusions

Quaternary ammonium salt and new reactive dye were prepared, characterised and linked to polyethylenimine for producing cationic functionalized polyethylenimine dyes (FPEIs). These compounds were applied on wool and cotton. The used polymers have a strong cationic charge, responsible for a good adsorption to the fibre surface via electrostatic attraction to the negative charges of the fibres surface result from the -OH groups for cotton and -OH and -COOH groups for wool. The FPEI compounds adsorb onto the fibre surfaces and the washing does not change significantly the deposited amounts probably because of the high molecules of functional groups in the FPEI molecules like secondary and tertiary amines which contribute to the binding force.

Isothermal studies show that the adsorption follows the Langmuir model, indicating a binding on sites of the compound. The kinetic studies show that the adsorptions of FPEIs compound follow a pseudo-first-order kinetics suggesting that the diffusion is the step-determining process.

Compared to dyeing with CI Basic Red 51, a commercially available dyestuff, the coating leads to higher colour strength than the reference. The colour is uniform on the whole surface of fibres, and is fast to washing, supporting the assumption of bonds created between secondary, tertiary amine and quaternary ammonium groups (QI) of the polymer and functional groups of the wool and cotton surface.

7. Summary

This study was done for functionalizing the surface of cotton and wool fibres with different polymeric materials in order to impart and manage properties like thermoregulation, lustre or colour. Thermoregulation property was achieved on the fibre surface by depositing phase change materials (organic, or inorganic). The lustre of the fibres was managed by depositing micro-gels onto the surfaces. The fibre colour was handled by depositing functionalized polyethelene imine with quaternary ammonium salt group onto these surfaces.

All the polymeric materials were deposit onto the surfaces at room temperature under environmentally friendly conditions.

PHASE CHANGE MATERIALS FOR THERMOREGULATION

Three different groups of PCM/Polymer composites are prepared. Two of them are based on organic PCMs and one uses the inorganic PCM.

One of the organic groups was prepared by encapsulating one of the following six different paraffin waxes, namely *n*-decane, *n*-dodecane, *n*-tetradecane, *n*-hexadecane, *n*-octadecane and *n*-nonadecane. Various polymer structures, viz.: Hexamethylene diisocyanate uretdione derivatives (HDI_1 and HDI_2), poly lauryl acrylate (PLA), poly decyl ethylene glycol (PDEG) and poly dodecyl ethylene glycol (PDDEG) were used as complex coacervates. The thermal behaviour of these PCM/polymer composites was evaluated with DSC measurements at 10 K min⁻¹.

Hexadecane and HDI derivatives as support polymer show the best results of all studied paraffin-polymer compounds. Due to capillary forces existing between branches of polymer and the melted paraffin the PCM composites are held up well by the polymer matrix after heating. Finally, the PCM/polymer composites based on HDI uretdione are applied onto cotton and wool fabrics. The fabrics exhibit good temperature control properties, with coated wool behaving better than coated cotton fabric.

The second organic group of PCM-polymers was prepared by using poly(alkyl acrylate). The PCM/polymer composites are characterized extensively, and found that both the *n*-octadecanol/polybehenyl acrylate composite, and the methyl octadecanoate/polybehenyl acrylate composite can be successfully used for storing heat.

The composite polybehenyl acrylate/*n*-octadecanol (PBA/C₁₇H₃₅COOCH₃) was chosen for applying onto the fabric. The heat transfer through the coated fabric was measured and it

shows the good thermal insulation effect of the material. The system does not separate by storing, as indicated by evaluation of the behaviour of composites over three weeks. Watching the heating and cooling of the composite of polybehenyl acrylate and methyl-octadecanoate under microscope allows seeing that the PCM are hosted in the loops of the polymeric network. The homo polymerizing of the behenyl acrylate, followed by the mixture with PCM, allows controlling better the end product properties.

The third group of materials is based on inorganic phase change materials which have been studied for their application in textiles. During this part of work I evaluated six different hydrated inorganic salts to be used as inorganic phase change materials (namely: calcium nitrate tetrahydrate ($\text{Ca}(\text{NO}_3)_2 \cdot 4\text{H}_2\text{O}$), calcium chloride hexahydrate ($\text{CaCl}_2 \cdot 6\text{H}_2\text{O}$), sodium sulphate decahydrate ($\text{Na}_2\text{SO}_4 \cdot 10\text{H}_2\text{O}$), disodium hydrogen phosphate dodecahydrate ($\text{Na}_2\text{HPO}_4 \cdot 12\text{H}_2\text{O}$), ferric nitrate nonahydrate ($\text{Fe}(\text{NO}_3)_3 \cdot 9\text{H}_2\text{O}$), and manganese (II) nitrate hexahydrate ($\text{Mn}(\text{NO}_3)_2 \cdot 6\text{H}_2\text{O}$)) in silica-based micro-capsules. Pure inorganic silica capsules were prepared using PAOS as a cross-linker, and the capsules contain inorganic hydrated salt inside. The best results are achieved for sodium sulphate decahydrate, and disodium hydrogen phosphate dodecahydrate, respectively. The microcapsules, which show good phase change property, were embedded in a film of the polypropylene at the extruding stage. The basic mechanical properties of the new material do not differ from those of the pure polypropylene.

THERMO-SENSITIVE MICROGELS TO IMPROVING TEXTILE GLOSS

Three different thermo-sensitive microgels obtained by copolymerisation of vinylcaprolactam (VCL) and various monomers (vinylimidazole (VIm), acetoacetoxyethyl methacrylate (AAEM) and itaconic acid dimethyl ester (IADME)) were used to coat onto different fibre surfaces. The structures of the prepared microgel were confirmed with ^1H -NMR and ^{13}C -NMR. Scanning electron microscopy indicates that the diameter of the particles ranges from 200 to 300 nm for all microgels.

Two different pH and two different temperatures, (25°C and 50°C, respectively), are chosen for the deposition of the microgels. Scanning electron microscopy of the treated fibre shows good distribution of the particles onto the fibre especially at increasing temperature.

The chemistry of the microgel affects the deposition of the particles on the fibre surface, the microgel behaving differently at the same pH on different fibres. The gloss index was measured for the treated fibre, and it shows that it may be controlled for all the fibres with the treatment parameters (pH and temperature) and microgel structure.

The increasing of the gloss index is given by a special distribution of the microgel particles on the investigated surface. The arrangement of particles in dots randomizes the reflected light which helps increasing the gloss index.

The washing process of the treated cotton fibre does not affect the gloss index property, meaning that the microgel is kept well on the fibre surface. On the other side, the gloss index values of treated wool decreases after washing, indicating that the treatment is temporary for keratin fibres.

FUNCTIONALISED PEI (POLYETHYLENE IMINE) TO IMPROVING TEXTILE SURFACE

Functionalized polyethylenimine–dye complexes (FPEI) were prepared by mixing branched polyethyleneimine (PEI), whose primary amine groups were modified at different ratio with synthesised quaternary ammonium coupler (QI), and synthesised new reactive dyestuff (RD) (QI/RD = 0/100, 20/80, 40/60, 60/40 and 80/20 mole/mole %). The FPEI compounds, which have a strong cationic charge, are deposit from aqueous solution on the surface of cotton and wool fibres via electrostatic attraction.

The adsorption of charged FPEI from external aqueous media by cotton and wool fibres is investigated at different pH, and the uptake of colour on fibres measured by data colour and UV-VIS. The washing do not change significantly the deposited amounts probably because of the high amount of functional groups in the FPEI molecules (secondary and tertiary amines) which contribute to the binding force.

The study of the kinetics of adsorption shows that the first-order kinetics provides the best correlation of the experimental data and the diffusion is the step-determining process. Equilibrium data shows that the deposition process onto both cotton and wool follows the Langmuir isotherm indicating a binding on sites of the compound.

In terms of colour strength (K/S value) the coated fibres compare well with those dyed with commercial C.I. Basic Red 51 dyestuff, suggesting that the coating is a good alternative to a classical dyeing. The colour is uniform on the whole surface of fibres, and is fast to washing, supporting the assumption of bonds created between secondary, tertiary amine and quaternary ammonium groups (QI) of the polymer and functional groups of the wool and cotton surface.

8. Zusammenfassung

Der Gegenstand der aktuellen Arbeit ist die Funktionalisierung von Baumwoll- und Wollfaser Oberflächen mit verschiedenen Polymerwerkstoffen um Eigenschaften wie Wärmeregulation, Glanz oder Farbe zu gewähren und zu steuern. Thermoregulierende Eigenschaften wurden auf der Faseroberfläche geschaffen durch Hinterlegung von Phasenänderungsmaterialien (organisch oder anorganisch). Der Glanz wurde durch Hinterlegung von Mikrogelen auf der Faseroberfläche gesteuert. Die Farbe der Faser wurde durch die Oberflächenbehandlung mit quaternärem Ammoniumsalz funktionalisierten Polyethylenimin erhalten.

Alle Polymere wurden auf den Oberflächen bei Raumtemperatur unter Ausschluss störender äußerer Einflüsse aufgebracht.

PHASENÄNDERUNGSMATERIALIEN ZUR THERMOREGULIERUNG

Es wurden drei verschiedene Gruppen von PCM/Polymer-Kompositen hergestellt. Zwei davon sind auf Basis von organischen PCM und eines auf Basis von anorganischem PCM hergestellt worden.

Eine der organischen Gruppen wurde durch Verkapselung eines der folgenden sechs verschiedenen Paraffinen, nämlich n-Decan, n-Dodecan, n-Tetradecan, n-Hexadecan, n-Octadecan und n-Nonadecan vorbereitet. Verschiedene Polymer-Strukturen, nämlich: Hexamethylendiisocyanat Uretidion Derivate (HDI_1 und HDI_2), Polylaurylacrylat (PLA), Polydecylethylenglykol (PDEG) und Polydodecylethylenglykol (PDDEG) wurden als Komplexkoazervate verwendet. Das thermische Verhalten dieser PCM/Polymer-Verbunde wurde durch DSC-Messungen bei 10 K min^{-1} evaluiert.

Hexadecan und HDI-Derivate als Unterstützende Polymer zeigten die besten Ergebnisse von allen untersuchten Paraffin-Polymer-Verbindungen. Durch die bestehenden Kapillarkräfte zwischen Polymerzweigen und dem geschmolzenen Paraffin, sind die PCM/ Polymer Komposite nach der Erhitzung von der Polymermatrix gut abgestützt. Schließlich werden die PCM/Polymer-Verbundwerkstoffe auf Basis von HDI-Uretidion auf die Baumwoll- bzw. Wollfasern aufgetragen. Die Stoffe weisen gute Temperaturregelungs-Eigenschaften, wobei die beschichtete Wolle ein besseres Verhalten als das beschichtete Baumwollgewebe aufweist.

Die zweite Gruppe von organischen PCM-Polymeren wurde auf Basis von Poly(Alkylacrylat) hergestellt. Nach einer ausführlichen Charakterisierung der PCM-Polymer-Verbundwerkstoffe wurde festgestellt, dass sowohl die n-Octadecanol/Polybehenylacrylat verbünde, als auch die

Methyl-octadecanoate/Polybehenylacrylat-Komposite erfolgreich für die Wärmespeicherung verwendet werden können.

Polybehenylacrylat/n-Octadecanol der Verbund (PBA/C₁₇H₃₅COOCH₃) wurde für die Anwendung auf den Stoff gewählt. Die Wärmeübertragung durch das beschichtete Gewebe wurde gemessen und es zeigt eine gute wärmedämmende Wirkung des Materialien. Die Auswertung des Verhaltens von Verbundwerkstoffen über drei Wochen zeigt, dass das System während der Lagerung stabil bleibt. Betrachtet man die Aufheizung und Abkühlung des Verbundes aus Polybehenylacrylat und Methyloctadecanoate unter dem Mikroskop, ist es möglich zu sehen, dass das PCM in den Schlaufen des Polymernetzwerkes enthalten ist. Die Homopolymerisation des Behenylacrylat, gefolgt durch die Mischung mit PCM, ermöglicht eine bessere Kontrolle der Eigenschaften des Endproduktes.

Die dritte Gruppe von Werkstoffen, die für ihre Anwendung in Textilien untersucht wurden, sind auf Basis anorganischer Phasenänderungsmaterialien hergestellt worden. In diesem Teil der Arbeit wurden sechs verschiedene hydratisierte anorganische Salze (nämlich: Calciumnitrat Tetrahydrat (Ca(NO₃)₂·4H₂O), Calciumchlorid Hexahydrat (CaCl₂·6H₂O), Natriumsulfat Decahydrat (Na₂SO₄·10H₂O), Hydrogendinatriumphosphat Dodecahydrat (Na₂HPO₄·12H₂O), Eisennitrate Nonahydrat (Fe(NO₃)₃·9H₂O) und Mangan(II)nitrate Hexahydrat (Mn(NO₃)₂·6H₂O)) zur Verwendung als anorganische Phasenänderungsmaterialien in Mikro-Kapseln auf Basis von Siliciumdioxid evaluiert. Rein anorganische Siliciumdioxid Kapseln mit einem Kern aus anorganischem hergestellt hydratisiertem Salz wurden durch Verwendung von PAOS als Vernetzer. Die besten Ergebnisse wurden mit Natriumsulfat Decahydrat bzw. Hydrogendinatriumphosphat Dodecahydrat erzielt. Die Mikro kapseln, die gute Phasenänderungs-Eigenschaften zeigten, wurden über Extrusion in einer Polypropylen Film eingebettet. Die elementaren mechanischen Eigenschaften der neuen Materialien weichen von denen des reinen Polypropylens nicht ab.

WÄRMEEMPFINDLICHE MIKROGELE ZUR VERBESSERUNG VOR TEXTIL-GLANZ

Drei verschiedene wärmeempfindliche Mikrogele, die durch Copolymerisation von Vinylcaprolactam (VCL) mit verschiedenen Monomeren (Vinylimidazol (VIM), Acetoacetoxyethylmethacrylat (AAEM) und Itaconsäuredimethylester (IADME)) hergestellt wurden, wurden zur Beschichtung von Faseroberflächen verwendet. Die Strukturen der hergestellten Mikrogele wurden durch ¹H- und ¹³C-NMR bestätigt

Rasterelektronenmikroskopische Untersuchungen zeigten einen Durchmesser der Mikrogelteilchen im Bereich von 200 bis 300 nm für alle verwendeten Mikrogele.

Zwei unterschiedliche pH-Werte und Temperaturen, (25°C und 50°C) wurden jeweils für die Abscheidung der Mikrogele gewählt. Rasterelektronenmikroskopie der behandelten Faser zeigte eine gute Verteilung der Partikel auf Faser vor allem bei hohen Temperaturen. Die chemische Struktur des Mikrogels bestimmt die Abscheidung der Teilchen auf der Faseroberfläche. Es wurde festgestellt, dass sich das Mikrogel bei gleichem pH auf verschiedenen Fasern unterschiedlich verhält. Glanzindex-Werte wurden für die behandelten Fasern gemessen und die Ergebnisse zeigen, dass er für alle Fasern durch Behandlung (pH-Wert und Temperatur) und über die Mikrogelstruktur gesteuert werden kann.

Die Erhöhung des Glanzgrades wird durch eine spezielle Verteilung der Mikrogelpartikel auf der Oberfläche erreicht. Die Anordnung der Partikel in Punkten randomisiert das reflektierte Licht, was zur Erhöhung des Glanzgrades führt.

Der Waschvorgang der behandelten Baumwollfasern beeinflusst nicht die Glanzeigenschaften, da das Mikrogel festgehalten wird auf der Faseroberfläche. Andererseits nimmt der Glanzindexwert der behandelten Wolle nach dem Waschen ab einen Hinweis darauf, dass die Behandlung für Keratinfasern vorübergehend ist.

FUNKTIONALISIERTE PEI (POLYETHYLENIMIN) ZUR VERBESSERUNG DER TEXTIL

Funktionalisierte Polyethylenimin-Farbstoff-Komplexe (FPEI) wurden hergestellt durch Mischung von verzweigten Polyethylenimin (PEI) (dessen primäre Aminogruppen modifiziert wurden durch synthetisierte quartäre Ammonium-Koppler (QI) zu unterschiedlichen Verhältnissen geändert) mit neu hergestellten Reaktivfarbstoffen (RD) (QI/RD = 0/100, 20/80, 40/60, 60/40 und 80/20 mol/mol%). Die FPEI Mischungen, die eine starke kationische Ladung enthalten, sind auf den Baumwoll- und Wolloberflächen aus wässriger Lösung angelagert durch elektrostatische Anziehung.

Die Adsorption von geladenen FPEI aus externen wässrigen Medien auf Baumwolle und Wolle wurde bei verschiedenen pH-Werten untersucht, und die Aufnahme von Farbe auf den Fasern durch Farbdaten und UV-VIS gemessen. Das Waschen änderte nicht wesentlich die abgesetzten Mengen wahrscheinlich wegen dem hohen Maß an funktionellen Gruppen in den FPEI Molekülen (sekundäre und tertiäre Amine), welche zu der bindenden Kraft beitragen.

Die Untersuchung der Adsorptionskinetik zeigt, dass die Kinetik erster Ordnung liefert die beste Korrelation der experimentellen Daten liefert und die Diffusion der entscheidenden Prozess ist. Gleichgewicht Daten zeigen, dass die Abscheidung sowohl auf Baumwolle als auch auf Wolle der Langmuir-Isotherme folgt, was auf eine Bindung der Präparate auf den Seiten hindeutet.

Im Hinblick auf die Farbstärke, (K/S-Wert) sind die beschichteten Fasern wohl vergleichbar mit denen die mit kommerziellen CI Basic Red 51 Farbstoff gefärbt wurden. was darauf hindeutet, dass die Beschichtung eine gute Alternative zu einer klassischen Färbung ist. Die Farbe ist einheitlich auf der gesamten Oberfläche der Fasern verteilt, und ist schnell ab zu waschen. Diese Tatsache unterstützt die Theorie. Der Annahme von Bindungen zwischen sekundären- und tertiären Aminen, sowie quartären Ammoniumgruppen (QI) des Polymers und den funktionellen Gruppen der Woll-und Baumwoll-oberflächen.

9. Reference

1. Epa/625/R-96/004; "Best Management Practices for Pollution Prevention in the Textile Industry"; U.S. Environmental Protection Agency, Office of Research and Development, National Risk Management Research Laboratory, Center for Environmental Research Information: Cincinnati, Ohio, September, (1996); p 443
2. J. Lindberg; "Relationship between Various Surface Properties of Wool Fibers: Part I: Methods for Estimating Wool Fiber Modification", *Text. Res. J.*, **23**, 2 (1953) 67-76
3. G. Lagermalm, J. Lindberg and L. Weissbein; "Relation between Dyeing Properties of Wool and Modifications of the Fiber", *Text. Res. J.*, **23**, 6 (1953) 398-400
4. J. English, H. G. Cassidy and R. I. Baird; "Principles of Organic Chemistry", McGraw Hill. Ltd., London, 4th Edition, (1971) 475 - 501
5. V. M. Potapov and S. N. Tatarinchik; "Organic Chemistry. English Translation", Mir Publishers, Moscow, (1979) 147–157
6. F. W. Billmeyer, in "Textbook of Polymers Science", New York, John. Wiley & Sons, Inc., (1984). pp.
7. N. M. Blkaes and L. Segal; "Cellulose and Cellulose Derivatives", Wiley Interscience, New York, Part V, Vol. V, (1976)
8. A. Hebeish and J. T. Guthrie; "The Chemistry and Technology of Cellulose Copolymers", Springer Verlag, Berlin, (1981)
9. R. N. Hans and K. Rouette, "Encyclopedia of Textile Finishing"; Springer, (2001), Vol 1, p 255-257, 439-445, 456-463, 846-852, 907-909
10. A. Hebeish; "Development in Textile Chemistry and Chemical Technology", Academy of Scientific Research and Technology, 2nd Edition, (1994) 25-55, 78-83, 95
11. K. Ekman, V. Ekland, J. Fors, J. Huttunen, J. Fredrik and O. Turunen; "Cellulose, Structure, Modification and Hydrolysis", Wiley Interscience, New York, (1986) 277-298
12. Cottoninc; "Cotton Nonwoven Technical Guide", <http://www.cottoninc.com/Cotton-Nonwoven-Technical-Guide/>
13. J. W. S. Hearle and W. E. Morton; "Physical Properties of Textile Fibres ", Woodhead Publishing Series in Textiles No. 68, The Textile Institute, London, 4th Edition, (2008) 796
14. D. F. Durso; "Wood and Agricultural Residues: Research on Use for Feed and Chemicals", Academic Press, New York, (1980) 89 – 102

15. R. Molina, J. P. Espinós, F. Yubero, P. Erra and A. R. González-Elipe; "Xps Analysis of Down Stream Plasma Treated Wool: Influence of the Nature of the Gas on the Surface Modification of Wool", *Appl. Surf. Sci.*, **252**, 5 (2005) 1417-1429
16. W. Xu, G. Ke, J. Wu and X. Wang; "Modification of Wool Fiber Using Steam Explosion", *Eur. Polym. J.*, **42**, 9 (2006) 2168-2173
17. T. Wakida, S. Cho, S. Choi, S. Tokino and M. Lee; "Effect of Low Temperature Plasma Treatment on Color of Wool and Nylon 6 Fabrics Dyed with Natural Dyes", *Text. Res. J.*, **68**, 11 (1998) 848-853
18. S. Shahidi, M. Ghoranneviss, B. Moazzenchi, A. Rashidi and D. Dorrani; "Study of Surface Modification of Wool Fabrics Using Low Temperature Plasma", Paper Presented at the '*Proceedings of the 3rd International Conference on the Frontiers of Plasma Physics and Technology (PC/5099)*', Bangkok, Thailand, 05 March.(2007), P-8
19. C. J. S. M. Silva; "Enzymatic Treatment of Wool with Modified Proteases", PhD. Thesis in Textile Engineering, *University of Minho*, Portugal, (2005)
20. J. A. Rippon; "The Structure of Wool; Chapter 1", in "Wool Dyeing" in: Lewis, D. M. (Ed.), England, Bradford (UK): Society of Dyers and Colourists, (1992). pp. 384
21. J. Pearson, F. Lu and K. Gandhi; "Disposal of Wool Scouring Sludge by Composting", *AUTEX Res. J.*, **4**, 3 (2004) 147 - 156
22. L. J. Hogg, H. G. M. Edwards, D. W. Farwell and A. T. Peters; "Ft Raman Spectroscopic Studies of Wool", *J. Soc. Dyer. Colour.*, **110**, 5-6 (1994) 196-199
23. V. L. Hughes, G. Nelson and G. East; "Surface Modification of Cashmere Fibers by Reverse Proteolysis", *AATCC Review*, (2001)
24. E. Heine and H. Höcker; "Enzyme Treatments for Wool and Cotton", *Rev. Prog. Color. Related Topics*, **25**, 1 (1995) 57-70
25. L. Ammayappan and J. J. Moses; "Study on Improvement in Handle Properties of Wool/Cotton Union Fabric by Enzyme Treatment and Subsequent Polysiloxane-Based Combination Finishing", *Asian J. Text.*, **1**, (2011) 1-13
26. Csiro Division: Textile and Fibre Technology; "The Structure of a Merino Wool Fibre", <http://www.scienceimage.csiro.au/index.cfm?event=site.image.detail&id=7830>
27. M. Feughelman; "Natural Protein Fibers", *J. Appl. Polym. Sci.*, **83**, 3 (2002) 489-507
28. M. Feughelman; "Introduction to the Physical Properties of Wool, Hair & Other A-Keratin Fibres. In: Mechanical Properties and Structure of Alpha-Keratin Fibres: Wool, Human Hair and Related Fibres", UNSW Press, (1997) 1-14

29. K. R. Makinson; "Shrinkproofing of Wool", Marcel Dekker Inc., New York, Basel, (1979) 373
30. A. P. Negri, H. J. Cornell and D. E. Rivett; "A Model for the Surface of Keratin Fibers", *Text. Res. J.*, **63**, 2 (1993) 109 - 115
31. J. E. Plowman; "Proteomic Database of Wool Components", *J. Chromatog. B*, **787**, 1 (2003) 63-76
32. F. J. Wortmann; "The Viscoelastic Properties of Wool and the Influence of Some Specific Plasticizers", *Colloid Polym. Sci.*, **265**, 2 (1987) 126-133
33. Y. Shin, D. I. Yoo and K. Son; "Development of Thermoregulating Textile Materials with Microencapsulated Phase Change Materials (Pcm). Ii. Preparation and Application of Pcm Microcapsules", *J. Appl. Polym. Sci.*, **96**, 6 (2005) 2005-2010
34. W. Bendkowska, J. Tysiak, L. Grabowski and A. Blejzyk; "Determining Temperature Regulating Factor for Apparel Fabrics Containing Phase Change Material", *Int. J. Cloth. Sci. Technol.*, **17** 3/4 (2005) 209 - 214
35. J. W. S. Hearle and W. E. Morton; "Physical Properties of Textile Fibres", Crc. Press, (2008)
36. J. W. S. Hearle; "The Structural Mechanics of Fibers", *J. Polym. Sci. Part C: Polym. Symp.*, **20**, 1 (1967) 215-251
37. Y.-L. Hsieh; Gordon, S. and Hsieh, Y.-L. E., "Chemical Structure and Properties of Cotton", Cotton: Science and Technology. Woodhead Publishing, UK, (2007)
38. Chemistry.Msu.Edu; "Proteins", <http://www2.chemistry.msu.edu/faculty/reusch/VirtTxtJml/proteins.htm>
39. A. M. Sookne and M. Harris; "Electrophoretic Studies of Wool", *Text. Res. J.*, **9**, 12 (1939) 437-443
40. V. A. Wilkerson; "The Chemistry of Human Epidermis: Ii. The Isoelectric Points of the Stratum Corneum, Hair, and Nails as Determined by Electrophoresis", *J. Biol. Chem.*, **112**, 1 (1935) 329-335
41. K. El-Nagar, S. M. Saleh and A. R. Ramadan; "Utilization of Feather Waste to Improve the Properties of the Egyptian Cotton Fabrics", *JTATM*, **5**, 2 (2006) 1 - 12
42. J. Steinhardt and M. Harris; "Combination of Wool Protein with Acid and Base: Hydrochloric Acid and Potassium Hydroxide", *Text. Res. J.*, **10**, 6 (1940) 229-252
43. F. W. Sears and G. L. Salinger; "Thermodynamics, Kinetic Theory and Statistical Thermodynamics", Addison-Wesley, 3rd Edition, (1975)

44. S. Sarge, W. Hemminger, E. Gmelin, G. Höhne, H. Cammenga and W. Eysel; "Metrologically Based Procedures for the Temperature, Heat and Heat Flow Rate Calibration of Dsc", *J. Therm. Anal. Calorim.*, **49**, 2 (1997) 1125-1134
45. B. Mottinger; "Space Hardware Design Final Project, Asen 4512"; University of Colorad: USA, (1999);
46. D. F. Doerr; "Heat Stress Assessment and a Countermeasure"; Biomedical Laboratory Kennedy Space Center: West Melbourne, FL 32912-0642, November, (1997); p 2
47. H. Shim, E. A. Mccullough and B. W. Jones; "Using Phase Change Materials in Clothing", *Text. Res. J.*, **71**, 6 (2001) 495-502
48. X.-Z. Lan, Z.-C. Tan, Q. Shi and Z.-H. Gao; "Gelled $\text{Na}_2\text{hpo}_4 \cdot 12\text{h}_2\text{o}$ with Amylose-G-Sodium Acrylate: Heat Storage Performance, Heat Capacity and Heat of Fusion", *J. Therm. Anal. Calorim.*, **96**, 3 (2009) 1035-1040
49. X. Zhu, M. Jaumann, K. Peter, M. Möller, C. Melian, A. Adams-Buda, D. E. Demco and B. Blümich; "One-Pot Synthesis of Hyperbranched Polyethoxysiloxanes", *Macromolecules*, **39**, 5 (2006) 1701-1708
50. M. Jaumann, E. A. Rebrov, V. V. Kazakova, A. M. Muzafarov, W. A. Goedel and M. Möller; "Hyperbranched Polyalkoxysiloxanes Via Ab3-Type Monomers", *Macromolecular Chem. Phys.*, **204**, 7 (2003) 1014-1026
51. M. Möller and C. Popescu; "Chapter 9.6: Natural Fibres", in "Sustainable Solutions for Modern Economies" in: Höfer, R. (Ed.), UK, The Royal Society of Chemistry (2009). pp. 364 - 389
52. Y. Morimoto, M. Tanaka, R. Tsuruno and K. Tomimatsu; "Visualization of Dyeing Based on Diffusion and Adsorption Theories", Paper Presented at the '*Proceedings of the 15th Pacific Conference on Computer Graphics and Applications*' (2007), 57 - 64
53. P. P. Selvam, S. Preethi, P. Basakaralingam, N. Thinakaran, A. Sivasamy and S. Sivanesan; "Removal of Rhodarrine B from Aqueous Solution by Adsorption onto Sodium Montmorillonite", *J. Hazard. Mater.*, **55**, (2008) 39 - 44
54. M. M. Ramos-Tejada, A. Ontiveros-Ortega, E. Gimenez-Martin, M. Espinosa-Jimenez and A. Molina Diaz; "Effect of Polyethyleneimine Ion on the Sorption of a Reactive Dye onto Leacril Fabric: Electrokinetic Properties and Surface Free Energy of the System", *J. Colloid Interf. Sci.*, **297**, 1 (2006) 317-321

55. M. E. Jiménez and A. C. Suárez; "The Effect of Ethyl Xanthogenate on Both the Electrokinetic Properties and Sorption of a Cationic Dye onto Polyester Fibers", *Colloid. Surface. A.*, **97**, 3 (1995) 227-234
56. H.-J. Flath and N. Saleh; "Zur Bedeutung Des Zetapotentials Von Faserstoffen Für Den Färbeprozess", *Acta Polym.*, **31**, 8 (1980) 510-517
57. F. González-Caballero, M. Espinosa-Jiménez and C. F. González-Fernández; "The Uptake of a Reactive Dye by Bleached Cotton and Its Effect on the Electrical Properties of the Interface : I. Electrokinetic Properties", *J. Colloid Interf. Sci.*, **123**, 2 (1988) 537-543
58. J. A. Faucher and E. D. Goddard; "Influence of Surfactants on the Sorption of a Cationic Polymer by Keratinous Substrates", *J. Colloid Inter. Sci.*, **55**, 2 (1976) 313-319
59. L. Wågberg; "Polyelectrolyte Adsorption on Cellulose Fibres"; R-00-7; Mid Sweden University, Fibre Science and Communication Network: Sweden, Jan, (2001); pp 1-30
60. L. Wågberg and R. Hagglund; "Kinetics of Polyelectrolyte Adsorption on Cellulosic Fibers", *Langmuir*, **17**, 4 (2001) 1096-1103
61. M. Hadjianfar, D. Semnani and M. Sheikhzadeh; "A New Method for Measuring Luster Index Based on Image Processing", *Text. Res. J.*, **80**, 8 (2010) 726-733
62. Astm, "Standard Definitions of Terms Relating to Appearance of Materials", in "Annual Book"; ASTM Standards Philadelphia, USA, (1996),
63. Astm, "Standard Guide for Selection of Geometric Conditions for Measurement of Reflection and Transmission Properties of Materials", in "Annual Book"; ASTM Standards Philadelphia, USA, (1996),
64. Cie Technical Report; "Colorimetry"; 15 (3rd edition): CIE Central Bureau, Vienna, (2004);
65. S. R. Beech, P. Whorton and J. A. Wilkins; "Textile Terms and Definitions", The Textile Institute, London, 8th Edition, (1986) 148
66. M. P. Gashti and A. Peyravi; "Colorimetric Properties of Direct Dyed Cotton Fabrics after Treatment with Softeners", Paper Presented at the '10th Congress of the International Colour Association', Granada.(2005), 721 - 724
67. Z. Cao, B. Du, T. Chen, J. Nie, J. Xu and Z. Fan; "Preparation and Properties of Thermo-Sensitive Organic/Inorganic Hybrid Microgels", *Langmuir*, **24**, 22 (2008) 12771-12778

68. M. Shibayama; "Spatial Inhomogeneity and Dynamic Fluctuations of Polymer Gels", *Macromol. Chem. Phys.*, **199**, 1 (1998) 1-30
69. P. Sutar, R. Mishra, K. Pal and A. Banthia; "Development of Ph Sensitive Polyacrylamide Grafted Pectin Hydrogel for Controlled Drug Delivery System", *J. Mater. Sci.: Mater. Med.*, **19**, 6 (2008) 2247-2253
70. A. Suzuki, M. Yamazaki and Y. Kobiki; "Direct Observation of Polymer Gel Surfaces by Atomic Force Microscopy", *J. Chem. Phys.*, **104**, 4 (1996) 1751-1757
71. G. D. Nicodemus and S. J. Bryant; "Cell Encapsulation in Biodegradable Hydrogels for Tissue Engineering Applications", *Tissue Eng.: Part B Rev.*, **14**, 2 (2008) 149-165
72. N. Ranjha, J. Mudassir and N. Akhtar; "Methyl Methacrylate-Co-Itaconic Acid (Mma-Co-Ia) Hydrogels for Controlled Drug Delivery", *J. Sol.-Gel Sci. Technol.*, **47**, 1 (2008) 23-30
73. G. Rathna; "Gelatin Hydrogels: Enhanced Biocompatibility, Drug Release and Cell Viability", *J. Mater. Sci.: Mater. Med.*, **19**, 6 (2008) 2351-2358
74. W. I. Choi, M. Kim, G. Tae and Y. H. Kim; "Sustained Release of Human Growth Hormone from Heparin-Based Hydrogel", *Biomacromolecules*, **9**, 6 (2008) 1698-1704
75. J. Kim, N. Singh and L. A. Lyon; "Label-Free Biosensing with Hydrogel Microlenses", *Angew. Chem., Int. Ed.*, **45**, 9 (2006) 1446-1449
76. M. R. Romero, F. Garay and A. M. Baruzzi; "Design and Optimization of a Lactate Amperometric Biosensor Based on Lactate Oxidase Cross-Linked with Polymeric Matrixes", *Sens. Actuators, B: Chem.*, **131**, 2 (2008) 590-595
77. T. Tanaka and D. J. Fillmore; "Kinetics of Swelling of Gels", *J. Chem. Phys.*, **70**, 3 (1979) 1214-1218
78. M. M. Ali, S. Su, C. D. M. Filipe, R. Pelton and Y. Li; "Enzymatic Manipulations of DNA Oligonucleotides on Microgel: Towards Development of DNA-Microgel Bioassays", *Chemical Communication*, 43 (2007) 4459-4461
79. T. Hoare and R. Pelton; "Highly Ph and Temperature Responsive Microgels Functionalized with Vinylacetic Acid", *Macromolecules*, **37**, 7 (2004) 2544-2550
80. T. Hoare and R. Pelton; "Impact of Microgel Morphology on Functionalized Microgel-Drug Interactions", *Langmuir*, **24**, 3 (2008) 1005-1012
81. T. Hoare and R. Pelton; "Charge-Switching, Amphoteric Glucose-Responsive Microgels with Physiological Swelling Activity", **9**, 2 (2008) 733-740

82. R. H. Pelton and P. Chibante; "Preparation of Aqueous Latices with N-Isopropylacrylamide", *Colloids Surf., A*, **20**, 3 (1986) 247-256
83. G. L. Madan and S. K. Shrivastava; "Electro-Kinetic Studies of Cotton Part II: Measurement of Surface Potential at the Interface between Cellulose and Solution of Cross-Linking Agents", *Colloid Polym. Sci.*, **253**, 11 (1975) 969-973
84. W. A. Kindler and J. W. Swanson; "Adsorption Kinetics in the Polyethylenimine-Cellulose Fiber System", *J. Polym. Sci.A-2: Polym. Phys.*, **9**, 5 (1971) 853-865
85. M. P. Nedelcheva and G. V. Stoilkov; "Polyethylenimine Adsorption by Cellulose", *J. Appl. Polym. Sci.*, **20**, 8 (1976) 2131-2141
86. L. Pille, J. S. Church and R. G. Gilbert; "Adsorption of Amino-Functional Polymer Particles onto Keratin Fibres", *J. Colloid Interf. Sci.*, **198**, 2 (1998) 368-377
87. B. Alince; "The Role of Porosity in Polyethylenimine Adsorption onto Cellulosic Fibers", *J. Appl. Polym. Sci.*, **39**, 2 (1990) 355-362
88. T. Lindström and C. Söremark; "Adsorption of Cationic Polyacrylamides on Cellulose", *J. Colloid Interf. Sci.*, **55**, 2 (1976) 305-312
89. H. Tanaka, L. Ödberg, L. Wågberg and T. Lindström; "Adsorption of Cationic Polyacrylamides onto Monodisperse Polystyrene Latices and Cellulose Fiber: Effect of Molecular Weight and Charge Density of Cationic Polyacrylamides", *J. Colloid Interf. Sci.*, **134**, 1 (1990) 219-228
90. G. Nelson; "Application of Microencapsulation in Textiles", *Int. J. Pharm.*, **242**, 1 (2002) 55-62
91. N. S. Zubkova; "Thermal Insulation", *Knit. Int.*, **102** 1216 (1995) 50
92. N. S. Zubkova; "Phase Change Technology Outlasts Lofted Fabrics", *Tech. Text. Int.*, **4**, 7 (1995) 28-29
93. D. P. Colvin and G. Y. Bryant; "Protective Clothing Containing Encapsulated Phase Change Materials, Advances in Heat and Mass Transfer in Biotechnology", (*HTD*) *New York: ASME*, **362**, (1998) 123 -132
94. B. Pause; "Measuring the Thermal Barrier Function of Phase Change Materials in Textiles", *Tech. Text. Int.*, **9**, 3 (2000) 20 - 21
95. X. X. Zhang, Y. F. Fan, X. M. Tao and K. L. Yick; "Crystallization and Prevention of Super-Cooling of Microencapsulated N-Alkanes", *J. Colloid Interf. Sci.*, **281**, (2005) 299 - 306

96. S. Himran, A. Suwono and G. A. Mansoori; "Characterization of Alkanes and Paraffin Waxes for Application as Phase Change Energy Storage Medium", *Energ. Source., Part A: Recov.Utiliz. Environ. Effects*, **16**, 1 (1994) 117 - 128
97. A. J. Fossett, M. T. Maguire, A. A. Kudirka, F. E. Mills and D. A. Brown; "Avionics Passive Cooling with Microencapsulated Phase Change Material", *J. Electron. Packag.*, **120**, 3 (1998) 238 - 242
98. J. C. Mulligan, D. P. Colvin and Y. G. Bryant; "Microencapsulated Phase-Change Material Suspensions for Heat Transfer in Spacecraft Thermal Systems", *J. Spacecraft Rockets*, **33**, 2 (1996) 278 - 284
99. Y. Yamagishi, H. Takeuchi, A. T. Pyatenko and N. Kayukawa; "Characteristics of Microencapsulated Pcm Slurry as a Heat-Transfer Fluid", *AIChE J.*, **45**, 4 (1999) 696
100. P. B. L. Chaurasia; "Solar Energy Thermal Storage System Based on Encapsulated Phase-Charge Material", *Res. Ind.*, **26**, 3 (1981) 159 - 161
101. M. N. A. Hawlader, M. S. Uddin and H. J. Zhu; "Encapsulated Phase Change Materials for Thermal Energy Storage: Experiments and Simulation", *Int. J. Energ. Res.*, **26**, 2 (2002) 159-171
102. Y. G. Bryant; "Melt Spun Fibers Containing Microencapsulated Phase Change Material", *HTD. Adv. Heat Mass Transfer Biotechnol. ASME*, **363**, BED-44 (1999) 225-234
103. Y. G. Bryant; "In: 2.0 New Textiles-New Technologies", Paper Presented at the 'Techtextile Symposium', Frankfurt (1992), 1
104. D. C. Hittle and T. L. André; "A New Test Instrument and Procedure for Evaluation of Fabrics Containing Phase-Change Material", *ASHRAE Trans. Res.*, **108**, (2002) 175 - 180
105. Y. Yamagishi, T. Sugeno, T. Ishige, H. Takeuchi and A. T. Pyatenko; "An Evaluation of Microencapsulated Pcm for Use in Cold Energy Transportation Medium", Paper Presented at the 'Proceedings of the Intersociety Energy Conversion Engineering Conference'.(1996), **3**, 2077
106. S. Reemers; "Dendritic Structures for Nanoscience and Nanotechnology", PhD. Thesis in Polymer Chemistry, *RWTH Univ.*, Aachen, Germany, (2007)
107. W. F. Smith and J. Hashemi; "Foundations of Materials Science and Engineering", McGraw-Hill, 4th Edition, (2006) 1032 (326–327)

108. Z.-Y.-. Zhang, M.-. Frenkel, K. N. March and R. C. Wilhoit; Marsh, K. N., "Landolt-Börnstein - Index of Organic Compounds", "Thermodynamic Properties of Organic Compounds and Their Mixtures, Subvolume A: Enthalpies of Fusion and Transition of Organic Compounds", Landolt-Börnstein: Numerical Data and Functional Relationships in Science and Technology, The Texas A&M University, USA, IV/8, VIII, (1995) 588
109. E. Onder, N. Sarier and E. Cimen; "Encapsulation of Phase Change Materials by Complex Coacervation to Improve Thermal Performances of Woven Fabrics", *Thermochimic. Acta* **467**, (2008) 63 – 72
110. N. Sarier and E. Onder; "The Manufacture of Microencapsulated Phase Change Materials Suitable for the Design of Thermally Enhanced Fabrics", *Thermochimic. Acta*, **452**, 2 (2007) 149 – 160
111. N. Sarier and E. Onder; "Thermal Characteristics of Polyurethane Foams Incorporated with Phase Change Materials", *Thermochimic. Acta*, **454**, 2 (2007) 90 – 98
112. S. Mondal; "Phase Change Materials for Smart Textiles - an Overview", *Appl. Therm. Eng.*, **28**, 11-12 (2008) 1536-1550
113. U. Beginn; "Applicability of Frozen Gels from Ultra High Molecular Weight Polyethylene and Paraffin Waxes as Shape Persistent Solid/Liquid Phase Change Materials", *Macromol. Mater. Eng.*, **288**, 3 (2003) 245-251
114. S. D. Baruah, N. C. Laskar and B. Subrahmanyam; "Experimental Investigation on High Conversion Free-Radical Polymerization of Behenyl Acrylate", *J. Appl. Polym. Sci.*, **51**, 10 (1994) 1701-1707
115. K. Ito; "Initiator Concentration Dependence of the Autoacceleration of Polymerization Rate", *J. Polym. Sci.: Polym. Chem. Edn.*, **13**, 2 (1975) 401-413
116. J. N. Cardenas and K. F. O'driscoll; "High-Conversion Polymerization. Ii. Influence of Chain Transfer on the Gel Effect", *J. Polym. Sci.: Polym. Chem. Edn.*, **15**, 8 (1977) 1883-1888
117. C. A. Angell and J. C. Tucker; "Heat Capacities and Fusion Entropies of the Tetrahydrates of Calcium Nitrate, Cadmium Nitrate, and Magnesium Acetate. Concordance of Calorimetric and Relaxational Ideal Glass Transition Temperatures", *J. Phys. Chem.*, **78**, 3 (1974) 278-281
118. D. Vargas-Florencia, O. Petrov and I. Furó; "Inorganic Salt Hydrates as Cryoporometric Probe Materials to Obtain Pore Size Distribution", *J. Phys. Chem. B*, **110**, 9 (2006) 3867-3870

119. J. Guion, J. D. Sauzade and M. Laügt; "Critical Examination and Experimental Determination of Melting Enthalpies and Entropies of Salt Hydrates", *Thermochimic. Acta*, **67**, 2-3 (1983) 167-179
120. C. H. Shomate and F. E. Young; "Heats of Formation of Solid and Liquid $\text{Mn}(\text{NO}_3)_2 \cdot 6\text{H}_2\text{O}$ ", *J. Am. Chem. Soc.*, **66**, 5 (1944) 771-773
121. S. U. Pickering; "Pickering: Emulsions, Cxcvi", *J. Chem. Soc., Trans.*, **91**, (1907) 2001 - 2021
122. W. Ramsden; "Separation of Solids in the Surface-Layers of Solutions and 'Suspensions' (Observations on Surface-Membranes, Bubbles, Emulsions, and Mechanical Coagulation", Paper Presented at the '*Proceedings of the Royal Society of London*', London.(1903), **72**, 156 - 164
123. H. Wang, X. Zhu, L. Tsarkova, A. Pich and M. Möller; "All-Silica Colloidosomes with a Particle-Bilayer Shell", *ACS Nano*, **doi:10.1021/nn200436s**, null-null
124. K. Kratz, T. Hellweg and W. Eimer; "Structural Changes in Pnipam Microgel Particles as Seen by SANS, DLS, and EM Techniques", *Polymer*, **42**, 15 (2001) 6631-6639
125. Y. Hirokawa and T. Tanaka; "Volume Phase Transition in a Nonionic Gel", *J. Chem. Phys.*, **81**, 12 (1984) 6379 - 6381
126. M. Shibayama, T. Tanaka and C. C. Han; "Small Angle Neutron Scattering Study on Poly(N-Isopropyl Acrylamide) Gels near Their Volume-Phase Transition Temperature", *J. Chem. Phys.*, **97**, 9 (1992) 6829 - 6841
127. L. Fourn and H. J. Elliott; "The Improvement of Luster of Cotton: Part X: Special Swelling Treatments and Nonthermosetting Additives", *Text. Res. J.*, **25**, 1 (1955) 11-19
128. L. Fourn, R. M. Howorth and M. B. Rutherford; "Improvement of Luster of Cotton: Part III: Correlation of Visual and Physical Aspects of Luster", *Text. Res. J.*, **24**, 1 (1954) 61-66
129. L. Fourn and M. B. Rutherford; "Improvement of Luster of Cotton: Part IV: Effect of Weaving Pattern on Luster in a Series of Bleached Cotton Fabrics", *Text. Res. J.*, **24**, 1 (1954) 67-72
130. J. J. Kim, K. In Shin, H. S. Ryu, E. A. Kim, M. Lee and K. Wha Oh; "Luster Properties of Polyester Filament Yarn Woven Fabrics", *Text. Res. J.*, **74**, 1 (2004) 72-77
131. L. Fourn, R. M. Howorth, M. B. Rutherford and P. Streicher; "Improvement of Luster of Cotton: Part V: Fiber Shape in Relation to Luster", *Text. Res. J.*, **24**, 2 (1954) 156-163

132. L. Fourt, R. M. Howorth, M. B. Rutherford and P. Streicher; "Improvement of Luster of Cotton: Part Vi: Yarn Structure in Relation to Luster", *Text. Res. J.*, **24**, 2 (1954) 163-172
133. L. Fourt, R. M. Howorth, M. B. Rutherford and P. Streicher; "The Improvement of Luster of Cotton: Part Vii: Fiber Properties and Variety Characteristics in Relation to Luster", *Text. Res. J.*, **24**, 3 (1954) 279-291
134. L. Fourt and A. M. Sookne; "The Improvement of Luster of Cotton: Part I: Measurement of Reflectance Characteristics Related to Luster", *Text. Res. J.*, **21**, 7 (1951) 469-479
135. L. Fourt, R. M. Howorth, M. B. Rutherford and P. Streicher; "The Improvement of Luster of Cotton: Part Viii: Selection within Commercial Varieties on the Basis of Fiber Properties", *Text. Res. J.*, **24**, 7 (1954) 685-694
136. L. Fourt and H. J. Elliott; "The Improvement of Luster of Cotton: Part Ix: Thermosetting Resins", *Text. Res. J.*, **24**, 8 (1954) 779-784
137. L. Fourt; "Improvement of Luster of Wool Fabrics", *Text. Res. J.*, **36**, 10 (1966) 915-924
138. V. Boyko, A. Pich, Y. Lu, S. Richter, K.-F. Arndt and H.-J. P. Adler; "Thermo-Sensitive Poly(N-Vinylcaprolactam-Co-Acetoacetoxyethyl Methacrylate) Microgels: 1-Synthesis and Characterization", *Polymer*, **44**, 26 (2003) 7821-7827
139. A. Pich, A. Tessier, V. Boyko, Y. Lu and H.-J. P. Adler; "Synthesis and Characterization of Poly(Vinylcaprolactam)-Based Microgels Exhibiting Temperature and Ph-Sensitive Properties", *Macromolecules*, **39**, 22 (2006) 7701-7707
140. S. Schachschal, A. Balaceanu, C. Melian, D. E. Demco, T. Eckert, W. Richtering and A. Pich; "Polyampholyte Microgels with Anionic Core and Cationic Shell", *Macromolecules*, **43**, 9 (2010) 4331-4339
141. A. Pich, Y. Lu, V. Boyko, K.-F. Arndt and H.-J. P. Adler; "Thermo-Sensitive Poly(N-Vinylcaprolactam-Co-Acetoacetoxyethyl Methacrylate) Microgels: 2. Incorporation of Polypyrrole", *Polymer*, **44**, 25 (2003) 7651-7659
142. A. Pich, Y. Lu, V. Boyko, S. Richter, K.-F. Arndt and H.-J. P. Adler; "Thermo-Sensitive Poly(N-Vinylcaprolactam-Co-Acetoacetoxyethyl Methacrylate) Microgels. 3. Incorporation of Polypyrrole by Selective Microgel Swelling in Ethanol-Water Mixtures", *Polymer*, **45**, 4 (2004) 1079-1087

143. A. Pich, S. Bhattacharya, Y. Lu, V. Boyko and H.-J. P. Adler; "Temperature-Sensitive Hybrid Microgels with Magnetic Properties", *Langmuir*, **20**, 24 (2004) 10706-10711
144. A. Pich, J. Hain, Y. Lu, V. Boyko, Y. Prots and H.-J. Adler; "Hybrid Microgels with Zns Inclusions", *Macromolecules*, **38**, 15 (2005) 6610-6619
145. A. Pich, A. Karak, Y. Lu, A. K. Ghosh and H.-J. P. Adler; "Preparation of Hybrid Microgels Functionalized by Silver Nanoparticles", *Macromol. Rapid. Commun.*, **27**, 5 (2006) 344-350
146. F.-J. Wortmann, E. S. Z. Wiesche and A. Bierbaum; "Analyzing the Laser-Light Reflection from Human Hair Fibers. I. Light Components Underlying the Goniophotometric Curves and Fiber Cuticle Angles", *J. Cosmet. Sci.*, **54**, 5 (2003) 301 - 316
147. H. Petersen, P. M. Fechner, D. Fischer and T. Kissel; "Synthesis, Characterization, and Biocompatibility of Polyethylenimine-Graft-Poly(Ethylene Glycol) Block Copolymers", *Macromolecules*, **35**, (2002) 6867 - 6874
148. T. G. M. Van De Ven; "Kinetic Aspects of Polymer and Polyelectrolyte Adsorption on Surfaces", *Adv. Colloid Interf. Sci.*, **48**, (1994) 121-140
149. N. Pasquier, H. Keul and M. Möller; "Polymers with Specific Adhesion Properties for Surface Modification: Synthesis, Characterization and Applications", *Des. Monomers Polym.*, **8**, 6 (2005) 679 - 703
150. Y. Cai, M. T. Pailthroe and S. K. David; "A New Method for Improving the Dyeability of Cotton with Reactive Dyes", *Text. Res. J.*, **69**, 6 (1999) 440 - 446
151. H. Zollinger; "Color Chemistry", Basel, Cambridge, Weinheim, New York, Second, Revised Edition, (1991)
152. V. Gökmen and A. Serpen; "Equilibrium and Kinetic Studies on the Adsorption of Dark Colored Compounds from Apple Juice Using Adsorbent Resin", *J. Food. Eng.*, **53**, 3 (2002) 221-227
153. S. Chakraborty, S. De, S. Dasgupta and J. K. Basu; "Adsorption Study for the Removal of a Basic Dye: Experimental and Modeling", *Chemosphere*, **58**, 8 (2005) 1079-1086
154. O. Nitzsche and H. Vereecken; "Modeling Sorption and Exchange Processes in Column Experiments and Large Scale Field Studies", *Mine Water Environ.*, **21**, 1 (2002) 15-23
155. S. Wang, Y. Boyjoo, A. Choueib and Z. H. Zhu; "Removal of Dyes from Aqueous Solution Using Fly Ash and Red Mud", *Water Res.*, **39**, 1 (2005) 129-138

156. R. Malarvizhi and N. Sulochana; "Sorption Isotherm and Kinetic Studies of Methylene Blue Uptake onto Activated Carbon Prepared from Wood Apple Shell", *J. Environ. Protect. Sci.*, **2**, 1 (2008) 40-46
157. M. T. Uddin, M. S. Islam and M. Z. Abedin; "Adsorption of Phenol from Aqueous Solution by Water Hyacinth Ash", *ARPJ. Eng. Appl. Sci.*, **2**, 2 (2007) 11-17
158. N. Kannan and M. M. Sundaram; "Kinetics and Mechanism of Removal of Methylene Blue by Adsorption on Various Carbons--a Comparative Study", *Dyes & Pigments*, **51**, 1 (2001) 25-40
159. Y. S. Ho, D. A. J. Wase and C. F. Forster; "Kinetic Studies of Competitive Heavy Metal Adsorption by Sphagnum Moss Peat", *Environ. Technol.*, **17**, 1 (1996) 71-77

CURRICULUM VITA

Personal Data

Name Ahmed Gomaa Abd Allah Hassabo
Date of birth 10.03.1979
Place of birth Demmita Governorate, Egypt
Marital state Married
Nationality Egyptian
E-mail aga.hassboo@yahoo.com
hassabo@dw.rwth-aachen.de



Mail Address	Assistant Researcher Textile Research Department (TRD) National Research Centre (NRC) El-Behooth St., Dokki, 12311 Cairo, Egypt	PhD Student DWI an der RWTH–Aachen Pauwelsstr. 8, D-52056 Aachen Germany
---------------------	---	--

Professional experience

March 2007-May. 2011 **PhD. Scholarship,**
 DWI an der RWTH-Aachen, department of chemistry,
 Aachen, Germany.

May 2005-March 2007 **Assistant Researcher,**
 National Research Centre, Textile Research Division, Cairo, Egypt

Sept. 2002-May. 2005 **Research Assistant,**
 National Research Centre, Textile Research Division, Cairo, Egypt

Educational background

Sep. 1992-Jun. 1996 Secondary education, Azhar Institute of Seal of the Prophets Boys
 (Prepartory - Secondary), Giza, Egypt.

Sep. 1989-May 1992 Preparatory education, Azhar Institute of Seal of the Prophets Boys
 (Prepartory - Secondary), Giza, Egypt.

Sep. 1984-May 1989 Primary education, El-Fadael Private Islamic School, Giza, Egypt

Sep. 1996-May 2001 **B.Sc. in Chemistry,**
 Faculty of Science, Chemistry Department, Al Azhar University,
 Cairo, Egypt "Very Good with Honour Degree"
 Theses: "Raman Spectroscopy as an Analytical Technique"

- Sep. 2001-May 2002 **Pre-stage Master**, Organic Chemistry, Faculty of Science, Chemistry Department, Al Azhar University, Cairo, Egypt "Very Good"
- Sept. 2002-May. 2005 **M.Sc. in Organic Chemistry**,
National Research Centre, Textile Research Division, Cairo, Egypt
M.Sc. in Organic Chemistry (16 April 2005), Faculty of Science, Chemistry Department, Al Azhar University, Cairo, Egypt.
Thesis: (*Preparation, Characterization and Utilization of Some Textile Auxileries*)
Adviser: Prof. Dr. Mohamed H. Abo-Shosha
- March 2007-May. 2011 **PhD. in Material Science**,
DWI an der RWTH-Aachen, department of chemistry,
Aachen, Germany.
Dissertation: Synthesis and Deposition of Functional Nano-Materials on Natural Fibres
Supervised by: Univ. Prof. Dr. rer. nat. Martin Möller
Univ. Prof. Dr. rer. nat. Andrij Pich

Profile

Mr. Hassabo has integrated background in Organic chemistry with comprehensive research experience in polymers science; preparation, characterization and their applications in many fields. Mr. Hassabo participated in a research project in Egypt to develop the textile surfactants, which is entitled "Road Map". In addition, he was one of the committee to control the textile waste pollution in Egyptian Textile Company, and to improve the small project for dyeing textiles (SEAM project, Denmark Governmental). Furthermore, Mr. Hassabo participated in many research projects during his work in Textile Research Division, National Research Centre. Furthermore, Mr. Hassabo participated in DWI an der RWTH Aachen Projects for "Preparation New Phase Change Materials for Different Applications", Exploratory project of "Polyethyleneimine and its modification" and Exploratory project of "Application of Microgel Compounds".

LIST OF PUBLICATIONS

A - PUBLICATIONS ARISING FROM THIS THESIS

1. **A. G. Hassabo**, R. Vinokur, C. Popescu and M. Möller, "Controlling the Temperature of Textiles with Organic PCMs Material Retained in Poly Acrylate", (In press)
2. **A. G. Hassabo**, U. Beginn, C. Popescu and M. Möller, "Controlling the Temperature of Textiles with Organic PCMs Material based on Paraffin Compounds", (In press)
3. **A. G. Hassabo**, A. Mendrek, H. Keul, C. Popescu and M. Möller, "Deposition of Functionalized Polyethylenimine-Dye onto Cotton and Wool Fibres", RJTA (In press)
4. **A. G. Hassabo**, X. Zhu, C. Popescu and M. Möller, "Inorganic Encapsulation of Inorganic PCM for Polymer Composites", RJTA, (In press)
5. **A. G. Hassabo**, S. Schachschal, C. Cheng, A. Pich, C. Popescu and M. Möller, "Polyvinylcaprolactam Based Microgels to Improve Gloss Properties of Different Natural Fibres", RJTA, (In press)
6. C. Popescu, R. Vinokur, **A. Hassabo**, U. Beginn and M. Möller; "Phase Change Materials (PCM) for Textiles", Poster Presented at the '4th Aachen Dresden International Textile Conference', Dresden, Germany (2010)

B - OTHER PUBLICATIONS

1. **A. G. Hassabo**, M. Salama, C. Popescu and M. Möller; "Polyvinyl Alcohol Composite Films with Cotton or Wool Micro-Particles and Its Application as Absorbance Membrane", (In Press)
2. M. Salama, **A. G. Hassabo**, C. Popescu and M. Möller; "Composite Materials Based on Natural Fibres and Synthetic Polymers", (In Press)
3. **A. G. Hassabo**, M. Salama and C. Popescu; "Preparation and Characterization of Wool and Cotton Nano-Powder", (In Press)
4. M. H. Abo-Shosha, F. A. Nassar, Z. El-Sayed and **A. G. Hassabo**; "Preparation and Characterizations of Some Fatty Acid/Polyethylene Glycol Condensates and Utilization as Softeners for Cotton Fabric", RJTA, 13, 2 (2009) 46-60
5. M. H. Abo-Shosha, F. A. Nassar, K. Hagag, Z. El-Sayed and **A. G. Hassabo**; "Utilization of Some Fatty Acid/PEG Condensates as Emulsifiers in Kerosene Paste Pigment Printing", RJTA, 13, 1 (2009) 65-77

6. M. H. Abo-Shosha, F. A. Nassar, Z. El-Sayed and **A. G. Hassabo**; "Utilization of Fatty Acid/PEG Condensates as Textile Softeners", Paper Presented at the '3rd International Conference of Textile Research Division, NRC; Textile Processing: State of the Art & Future Developments', Cairo, Egypt, 2 – 4 April (2006), 3, 369
7. N. A. Ibrahim, Z. M. El-Sayed, H. M. Fahmy, **A. G. Hassabo** and M. H. Abo-Shosha; "Perfume Finishing of Cotton/Polyester Fabric Crosslinked with DMDHEU in Presence of Some Softeners", Paper Presented at the '1st International Conference of Textile Research Division, NRC; Textile Processing: State of the Art & Future Developments', Cairo, Egypt, 2 - 4 March (2004), 1, 422 – 425

C - ORAL LECTURES

1. N. A. Ibrahim, Z. M. El-Sayed, H. M. Fahmy, **A. G. Hassabo** and M. H. Abo-Shosha; "Perfume Finishing of Cotton/Polyester Fabric Crosslinked with DMDHEU in Presence of Some Softeners", Paper Presented at the '1st International Conference of Textile Research Division, NRC; Textile Processing: State of the Art & Future Developments', Cairo, Egypt, 2 - 4 March (2004), 1, 422 – 425
2. M. H. Abo-Shosha, F. A. Nassar, Z. El-Sayed and **A. G. Hassabo**; "Utilization of Fatty Acid/PEG Condensates as Textile Softeners", Paper Presented at the '3rd International Conference of Textile Research Division, NRC; Textile Processing: State of the Art & Future Developments', Cairo, Egypt, 2 – 4 April (2006), 3, 369
3. M. H. Abo-Shosha, F. A. Nassar, K. Hagag, Z. El-Sayed and **A. G. Hassabo**; "Utilization of Some Fatty Acid/PEG Condensates as Emulsifiers in Kerosene Paste Pigment Printing", Paper Presented at the '3rd International Conference of Textile Research Division, NRC; Textile Processing: State of the Art & Future Developments', Cairo, Egypt, 2 – 4 April (2006)

D - POSTERS

1. C. Popescu, R. Vinokur, **A. Hassabo**, U. Beginn and M. Möller; "Phase Change Materials (PCM) for Textiles", Poster Presented at the '4th Aachen Dresden International Textile Conference', Dresden, Germany (2010)